AD-A122 926 TRANSIENT HEAT FLOW ALONG UNI-DIRECTIONAL FIBERS IN COMPOSITES(U) OHIO STATE UNIV RESEARCH FOUNDATION COLUMBUS L S HAN DEC 82 AFWAL-TR-82-3061 AFOSR-78-3640 1/2

UNCLASSIFIED F/G 11/4 NL

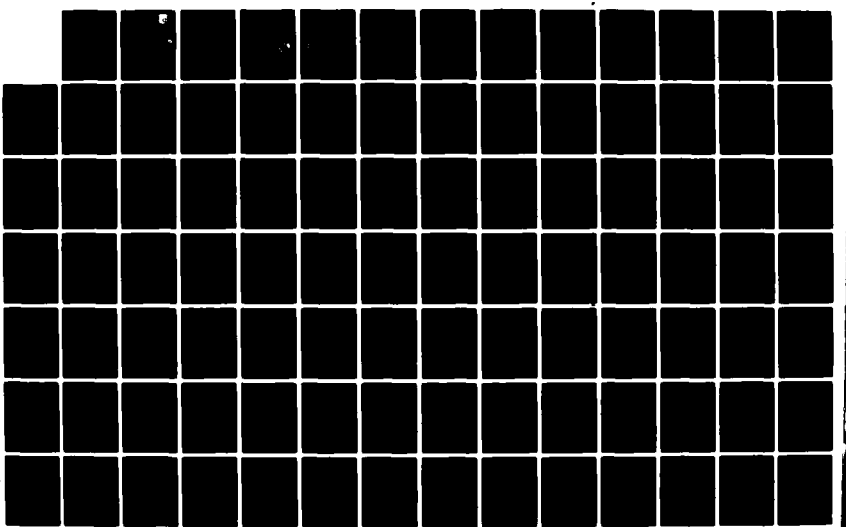

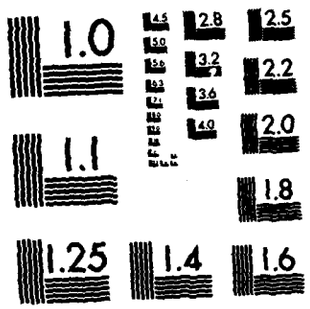

AFWAL-TR-82-3061

(2)

AD A122926

TRANSIENT HEAT FLOW ALONG UNI-DIRECTIONAL FIBERS IN COMPOSITES

LIT S. HAN

THE OHIO STATE UNIVERSITY
RESEARCH FOUNDATION
1314 KINNEAR ROAD
COLUMBUS, OH 43212

December 1982

Final Report for period July 1978 - December 1982

Approved for public release; distribution unlimited.

FLIGHT DYNAMICS LABORATORY
AIR FORCE WRIGHT AERONAUTICAL LABORATORIES
AIR FORCE SYSTEMS COMMAND
WRIGHT-PATTERSON AIR FORCE BASE, OHIO 45433

DTIC FILE COPY

NOTICE

When Government drawings, specifications, or other data are used for any purpose other than in connection with a definitely related Government procurement operation, the United States Government thereby incurs no responsibility nor any obligation whatsoever; and the fact that the government may have formulated, furnished, or in any way supplied the said drawings, specifications, or other data, is not to be regarded by implication or otherwise as in any manner licensing the holder or any other person or corporation, or conveying any rights or permission to manufacture use, or sell any patented invention that may in any way be related thereto.

This report has been reviewed by the Office of Public Affairs (ASD/PA) and is releasable to the National Technical Information Service (NTIS). At NTIS, it will be available to the general public, including foreign nations.

This technical report has been reviewed and is approved for publication.

Sheryl K. Bryan

SHERYL K. BRYAN, 1 Lt, USAF
Project Engineer
Design & Analysis Methods Group

Fred A. Picchioni

FREDERICK A. PICCHIONI, Lt Col, USAF
Chf, Analysis & Optimization Branch

FOR THE COMMANDER

Ralph L. Kuster

RALPH L. KUSTER, JR., Col, USAF
Chief, Structures & Dynamics Div.

"If your address has changed, if you wish to be removed from our mailing list, or if the addressee is no longer employed by your organization please notify AFWAL/FIBR, W-PAFB, OH 45433 to help us maintain a current mailing list".

Copies of this report should not be returned unless return is required by security considerations, contractual obligations, or notice on a specific document.

Unclassified

SECURITY CLASSIFICATION OF THIS PAGE (When Data Entered)

REPORT DOCUMENTATION PAGE		READ INSTRUCTIONS BEFORE COMPLETING FORM
1. REPORT NUMBER AFWAL-TR-82-3061	2. GOVT ACCESSION NO. AD-A122 926	3. RECIPIENT'S CATALOG NUMBER
4. TITLE (and Subtitle) TRANSIENT HEAT FLOW ALONG UNI-DIRECTIONAL FIBERS IN COMPOSITES		5. TYPE OF REPORT & PERIOD COVERED Final Report 7/1/78-12/31/81
		6. PERFORMING ORG. REPORT NUMBER 761108/711129
7. AUTHOR(s) Lit S. Han		8. CONTRACT OR GRANT NUMBER(s) Grant No. AFOSR-78-3640
9. PERFORMING ORGANIZATION NAME AND ADDRESS The Ohio State University Research Foundation, 1314 Kinnear Road Columbus, Ohio 43212		10. PROGRAM ELEMENT, PROJECT, TASK AREA & WORK UNIT NUMBERS 2307/N1 12
11. CONTROLLING OFFICE NAME AND ADDRESS AIR FORCE OFFICE OF SCIENTIFIC RESEARCH Building 410 Bolling Air Force Base, D.C. 20332		12. REPORT DATE December 1982 13. NUMBER OF PAGES 147
14. MONITORING AGENCY NAME & ADDRESS(if different from Controlling Office) Flight Dynamics Laboratory (AFWAL/FIBRA) Air Force Wright Aeronautical Laboratories (AFSC) Wright Patterson Air Force Base, Ohio 45433		15. SECURITY CLASS. (of this report) Unclassified 15a. DECLASSIFICATION/DOWNGRADING SCHEDULE

16. DISTRIBUTION STATEMENT (of this Report)

Approved for public release; distribution unlimited.

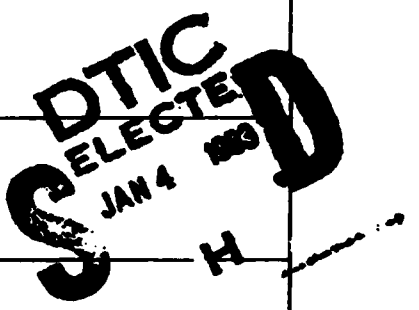

17. DISTRIBUTION STATEMENT (of the abstract entered in Block 20, if different from Report)

18. SUPPLEMENTARY NOTES

19. KEY WORDS (Continue on reverse side if necessary and identify by block number)

Conduction
Composites
Transient
Heat-Flow

20. ABSTRACT (Continue on reverse side if necessary and identify by block number)

For uni-directional fibrous composites and laminated composites, a heat-balance integral method has been developed for the analysis of transient heat flow along the fibers or in the plane of laminates. The method is based on the construction of, for the two constituent media, temperature profiles which not only satisfy the necessary boundary conditions but also fulfill the asymptotic error function properties when inter-region conduction is vanishingly small or at very early times of the heat transient.

(continued on back)

DD FORM 1 JAN 73 1473 EDITION OF 1 NOV 65 IS OBSOLETE

Unclassified

SECURITY CLASSIFICATION OF THIS PAGE (When Data Entered)

Block 20 (Abstract) - Continued

By comparing with the results of exact solutions, accuracy of the method has been established to be dependent on a number of factors expecially the inter-face conduction coefficient and thermal capacity ratio.

For the case of a constant surface heat flux, a relevant engineering problem, surface temperature rises of the two regions may be quite different from each other. Temperature differences, however, diminish quite rapidly toward the interior and are only confined to a depth equal to a few fiber radii or laminate thicknesses.

FOREWORD

As a sequel to the first two reports, which are concerned with the steady-state effective transverse thermal conductivities in fibrous composites, the present investigation deals with transient heat flow in composite materials. This effort, being a first phase in the transient analyses, considers composite materials with uni-directional fibers or those composed of alternate layers of two different materials. Heat flow in the direction of the fibers or in the stacking plane of the laminations is analyzed.

The study of heat flow phenomena in composites was financially supported by the Air Force Office of Scientific Research through a grant (AFOSR-78-3640), and was technically monitored by Mr. Nelson Wolf and Lt Kay Bryan of AFFDL/FIBRA, Flight Dynamics Laboratory, WPAFB, Dayton, Ohio. The author of this report gratefully acknowledges their assistance.

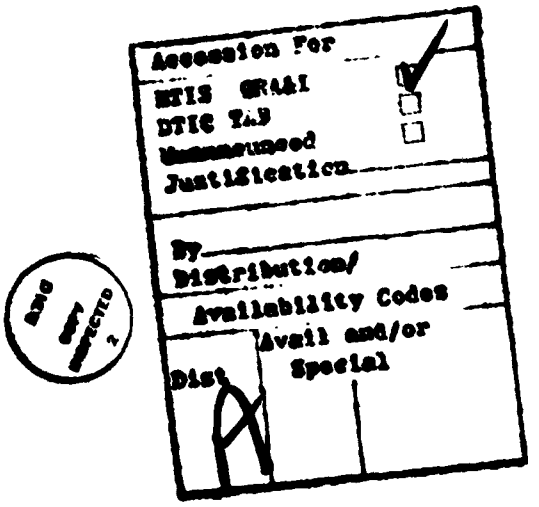

TABLE OF CONTENTS

TABLE OF CONTENTS (Cont.)

LIST OF ILLUSTRATIONS

LIST OF ILLUSTRATIONS (Cont.)

LIST OF ILLUSTRATIONS (CONCLUDED)

NOMENCLATURE

a	half-thickness of a laminate; radius of a fiber or two
$\bar{a}$	non-dimensional, (a/L)
A	generalized Fourier coefficient, Appendix C
b	half-thickness of a laminate-section; radius of a matrix cell
$\bar{b}$	non-dimensional, (b/L)
c	specific heat
B	generalized Fourier coefficient, Appendix C
E	generalized Fourier coefficient, Appendix C
g	intermediate function as defined
G	generalized Fourier coefficient, Appendix C
H	intermediate function of β, see Equations III-13 and IV-13; also generalized Fourier coefficient, Appendix C
i, j	integer indexes, Appendix C
k	thermal conductivity
L	transverse conductance parameter, see Equations III-18 or IV-18; also length of fiber, Appendix C
m, n	integer indexes, Appendix C
P	intermediate parameter, see Equation II-22
Q	surface heat flux
R	thero capacity ration, see Equation III-17
s	intermediate function
S	generalized Fourier coefficient, Appendix C

NOMENCLATURE (CONCLUDED)

T	temperature rise
$\bar{T}$	transverse average temperature
x	axial coordinate along laminate or fiber
$\bar{x}$	(x/a); (x/L) in Appendix C
$\bar{y}$	(y/a); (y/L) in Appendix C
$\bar{Y}$	function of $\bar{y}$, Appendix C

Greek Letters

α	thermal diffusivity, $(k/\rho c)$
Δ	heat penetration depth
β	transverse time-parameter; also eigenvalue, Appendix C
ϕ	intermediate function
γ	axial time-parameter
λ	intermediate function; thermal conductivity ratio (transverse/axial), Appendix C
θ	time
$\overline{\theta}$	non-dimensional time $(\alpha_1\theta/a^2)$; $(\alpha_1\theta/L^2)$, Appendix C
η	similarity variable, $\eta = x/2\sqrt{\alpha\theta}$
ρ	density

Subscripts

1	refers to fiber material
2	refers to matrix material
∞	refers to infinity, or a reference condition $(\overline{\theta} \rightarrow \infty)$
i	refers to interface
0	refers to small times

I. INTRODUCTION

In this grant study of heat conduction in composite materials, several phases of investigation were started in different stages of the grant period. These phases are individually self-contained from a technical viewpoint, but are related to one another in an overall sense. They are either sequential or proceed in parallel paths leading to a common objective.

For steady-state applications and for the purpose of acquiring a basic data bank, a methodology to analyze the effective transverse thermal conductivities of composites consisting of uni-directional fibers was developed in Phase I (AFWAL-TR-80-3012, Han and Cosner). Extensive calculations were performed to obtain accurate values for the transverse conductivities of composites with various packing densities, dispersion patterns and tow-matrix conductivity ratios. The large amount of data-heretofore unavailable, but generated in Phase I - was used subsequently by Zimmerman in a Phase II report (AFWAL-TR-80-3155, R. H. Zimmerman) in which the then-existing predictive schemes were examined in detail. Using the accurate data from Phase I as a base, prior simplified predictive equations were modified to extend their ranges of validity. Above all, a unified approach to predict the effective transverse (to fibers) conductivities was achieved with accuracy of 5 to 10 per cent. Zimmerman's work was significant in its comprehensiveness and definitiveness of its conclusions.

As thermal transients are a crucial concern in the analysis of thermal stresses and strains - such as delamination - investigations on thermal transients were initiated in this grant study, and they were pursued in several tasks. One task is concerned with the experimental determination of directional thermal conductivities and thermal diffusivities of fibrous materials. The purposes of this task are two-fold: (1) to evolve a simple and reliable experimental technique, and (2) to acquire basic data for graphite/epoxy composites, with future extensions to other (metallic) composites. This phase of work will be documented in a separate report shortly.

A second task is concerned with the development of a simplified method of calculating transient temperature distributions in composites with problems involving heat flows along the uni-directional fiber as a starting point. This task is motivated by the fact that rigorous solutions of the governing diffusion equations for different media in composites are conceptually speaking possible, but practically speaking prohibitive. The methodology developed is that of a heat-balance integral method - a concept whose origin lies in the work of von Karman on the analysis of boundary layer flows.

Transient heat flow analyses in composite bodies are not new; they date back to one hundred years. The early work and the majority of current efforts are largely patterned after classical methods of analysis for simplified geometries. Even for simplified geometries, the mathematical complexities are quite forbidding. For example, the use of the Laplace transform method to two-phase problems often results

in solving a non-linear algebraic equation for the transform parameter. Numerical implementation of its solution necessitates various kinds of perturbation analyses, and the amount of labor required renders these conceptually elegant and exact method much less elegant and less exact, when translated into a practical level. Hence, a need exists for a more pragmatic approach which is more accessible to design engineers confronted with thermal problems of composites. The contents of this report are a first step to achieve the goal.

Presented in this phase III report is the development of a heat-balance integral method for the analysis of thermal transients in composites with two different media. As an initial attempt, the integral-method is applied to heat flow problems in composites comprised of two different laminated materials, and in composites with uni-directional fibers dispersed evenly in a binding matrix. Heat flow takes place along the fiber axial direction or in the plane of laminations due to a step-rise in the surface temperature or a step-rise of the surface heat flux. The latter is the most commonly encountered boundary condition and is the most practical one to consider. Problems with more involved boundary conditions can be constructed on the basis of a combination of these two fundamental solutions.

It is, of course, recognized that the heat-balance integral method is intrinsically approximate but with increasing accuracy as the trial functions - to be explained later in this report - satisfy more secondary boundary conditions. Therefore, in order to establish and

confirm its usefulness, it is necessary to compare with available exact solutions for the problems considered. Consequently, exact solutions of the types of problems described earlier form the core objective of another task of the grant study. The rigorous solution is either in the form of analytical developments or in the form of numerical solutions with both approaches revealing the micro-structural temperature distributions. It is to be emphasized that the detailed computations of micro-structure temperature-time histories are not an end by itself. They serve a purpose of identifying where the heat-balance integral-method may be deficient and therefore requires further refinements. A report outlining this particular phase of work should be completed soon after this report is available.

II. TWO QUARTER-INFINITE REGIONS

As an introductory illustration of approximate analyses of heat flow in composites, consider the problem of two quarter-infinite regions of two different materials, 1 and 2, occupying the right-hand side of the y-axis in a x-y space (See Figure II-1). In the first quadrant, material 1 has physical properties designated by k_1, ρ_1, and c_1 and in the fourth quadrant material 2 has properties of k_2, ρ_2, and c_2.

With both regions initially at a uniform temperature (considered zero), it is desired to determine the temperature responses in these two regions when the temperature on the surface $x = 0$ is impulsively raised to a finite value or is given an impulsive heat flux. The key feature of the problem is of course the interface at $y = 0$ across which inter-region heat conduction affects the respective temperature distributions in the vicinity of the interface. Although this particular heat conduction problem has been elegantly studied by Grimado (Quarterly of Applied Mathematics p.379, Jan. 1954), the results obtained by him are not readily usable from an engineering viewpoint. With a minimum of complications, this example problem serves to illustrate the essential features of the heat-balance integral method, which are applied to problems with more practical interest in Sections III and IV.

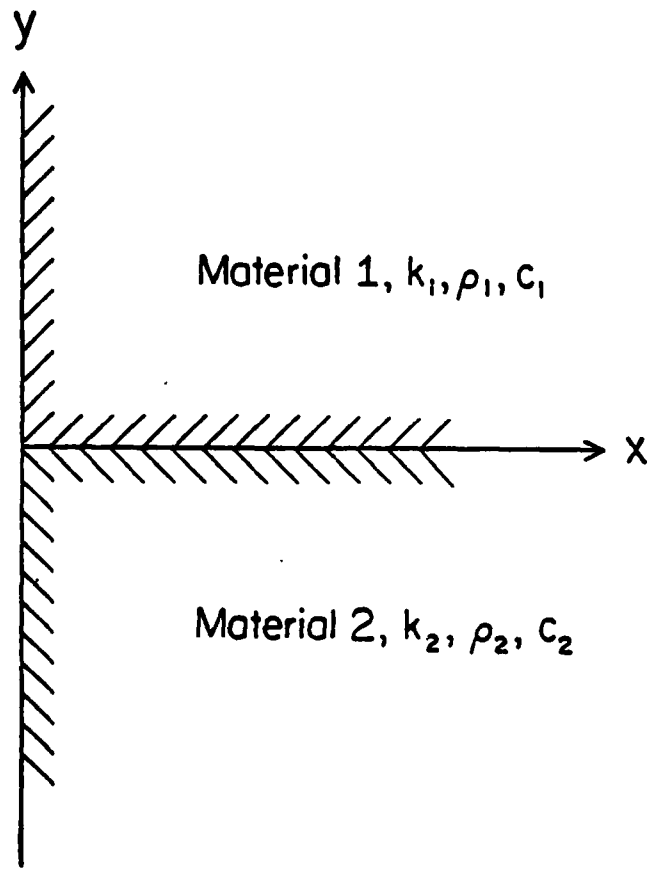

Figure II.1. Schematic of Two Quarter-infinite Regions

II.1 CONSTANT SURFACE-TEMPERATURE SOLUTIONS

In each region away from the interface, the temperature response is asymptotically identical to that in a semi-infinite region. These asymptotic solutions, valid for $|y| \to \infty$, are:

$$T_{1-\infty} = \frac{2}{\sqrt{\pi}} \int_{\frac{x}{2\sqrt{\alpha_1 \theta}}}^{\infty} e^{-n^2} dn \qquad \text{(II-1)}$$

$$T_{2-\infty} = \frac{2}{\sqrt{\pi}} \int_{\frac{x}{2\sqrt{\alpha_2 \theta}}}^{\infty} e^{-n^2} dn \qquad \text{(II-2)}$$

It is of interest to note that it is possible to have two materials with equal diffusivity ($\alpha_1 = \alpha_2$) such that Equations II-1 and II-2 are identical. In this case, no interface distortion would result. Our interest is of course the general case when $\alpha_1 \neq \alpha_2$.

When $\alpha_1 \neq \alpha_2$, the temperature responses given by Equations II-1 and II-2 cannot be valid in a region near the interface $y = 0$. The temperature distribution is in a transition stage from $T_{1-\infty}$ at $y = \infty$ through the interface and then to $T_{2-\infty}$ at $y = -\infty$. Figure II.2a illustrates such a distribution. The purpose of an approximate analysis is to determine the transitional temperature distribution.

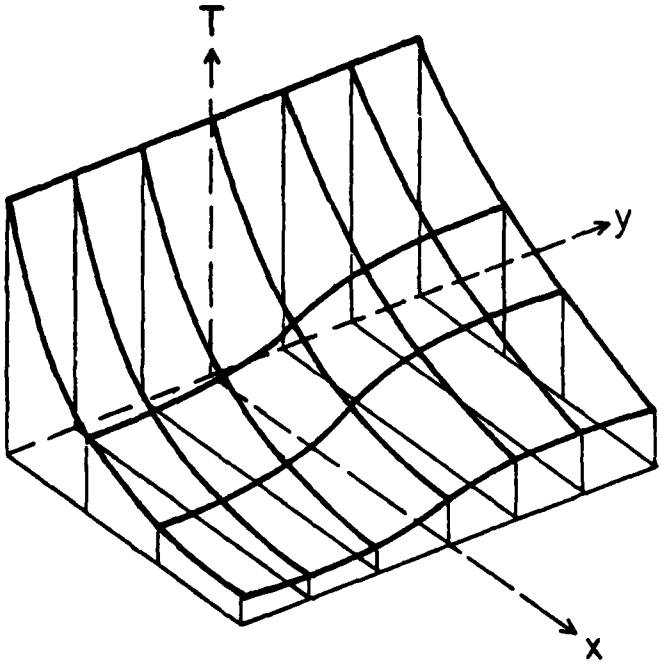

Figure II.2a. Temperature Distributions in Two Quarter-infinite Regions.

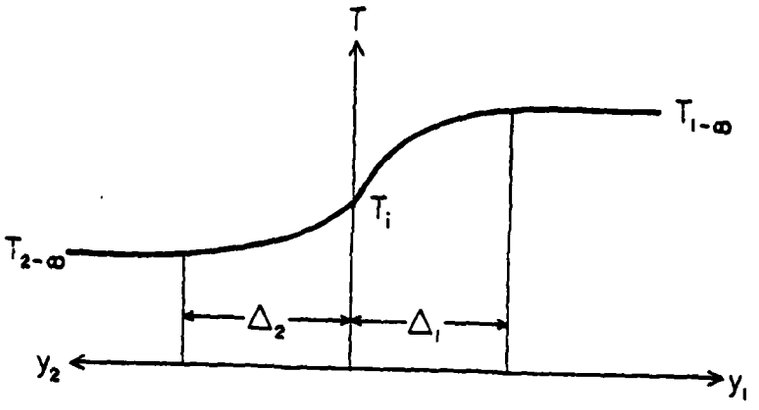

Figure II.2b. Temperature Profile Cross-section

Shown in Figure II.2b is a cross-sectional view of the temperature surface in Figure II.2a. The temperature distribution in each region is conceptualized into two zones: (i) a boundary zone of width Δ and (ii) the rest of the region. In the boundary zone, temperature varies from an interface temperature T_i to the fully established value corresponding to either one of Equations II-1 and II-2. In other words, the distribution is simplified by the discretized quantity Δ_1 or Δ_2 such that only near the interface does the temperature undergo a transition from one established value to another.

Suggested in Figure II.2b are therefore two boundary zones Δ_1 and Δ_2, and within them, the temperature distributions for materials 1 and 2 are given by the following:

$$T_1 = T_i + (T_{1-\infty} - T_i)F(y_1/\Delta_1) \qquad \text{(II-3)}$$

$$T_2 = T_i + (T_{2-\infty} - T_i)F(y_2/\Delta_2) \qquad \text{(II-4)}$$

Note that the same functional combination is used on either side of the interface. Equations II-3 and II-4 are of course limited to the boundary zones; outside, the temperatures T_1 and T_2 are equal to $T_{1-\infty}$ and $T_{2-\infty}$ directly. The latter requirement leads to the boundary condition on F at $y_1 = \Delta_1$ or $y_2 = \Delta_2$:

$$F(1) = 1 \qquad \text{(II-5)}$$

In Equations II-3 and II-4, the common interface temperature is denoted by T_i, which both T_1 and T_2 must assume when $y_1 = y_2 = 0$. This then requires:

$$F(0) = 0 \tag{II-6}$$

Finally of course is the equality of the heat flux at the interface, expressed by:

$$k_1(\partial T_1/\partial y_1) + k_2(\partial T_2/\partial y_2) = 0$$

Differentiating Equations II-3 and II-4 and putting $y_1 = y_2 = 0$, there results:

$$T_i = [(k_1/\Delta_1)T_{1-\infty} + (k_2/\Delta_2)T_{2-\infty}]/[(k_1/\Delta_1) + (k_2/\Delta_2)] \tag{II-7}$$

II-2 THE HEAT-BALANCE INTEGRAL-METHOD

The governing differential equations for both regions are of course the diffusion equations:

$$(\partial T_1/\partial\theta) = \alpha_1 \nabla^2 T_1 \qquad \text{(II-8)}$$

$$(\partial T_2/\partial\theta) = \alpha_2 \nabla^2 T_2 \qquad \text{(II-9)}$$

Since the above equations are satisfied by $T_{1-\infty}$ and $T_{2-\infty}$ defined by Equations II-1 and II-2 for these two separate regions (each in a semi-infinite domain), Equations II-8 and II-9 can also be written in terms of the respective differences $(T_1 - T_{1-\infty})$ and $(T_2 - T_{2-\infty})$, thus resulting in:

$$\frac{\partial}{\partial\theta}[T_{1-\infty} - T_1] = \alpha_1 \nabla^2 [T_{1-\infty} - T_1] \qquad \text{(II-10)}$$

$$\frac{\partial}{\partial\theta}[T_{2-\infty} - T_2] = \alpha_2 \nabla^2 [T_{2-\infty} - T_2] \qquad \text{(II-11)}$$

As the central idea of the heat-balance integral-method is that a differential equation is satisfied on the average while the boundary conditions are fulfilled through appropriate functional forms. Hence, by integrating Equation II-10 from $y_1 = 0$ to $y_1 = \infty_1$ the result is:

$$\frac{\partial}{\partial\theta}\int_0^\infty (T_{1-\infty} - T_1)dy_1 = \alpha_1\frac{\partial^2}{\partial x^2}\int_0^\infty (T_{1-\infty} - T_1)dy_1 -$$

$$- \frac{\partial}{\partial y_1}[T_{1-\infty} - T_1]_{y_1=0} \qquad \text{(II-12)}$$

A similar equation is obtained starting from Equation II-11; the resulting equation is obtainable from Equation II-12 by changing the subscript 1 to 2.

Now, the distribution function F can be chosen to conform with the requirements enumerated before. A popular choice in viscous boundary layer analyses is the following:

$$F(y_1/\Delta_1) = \frac{3}{2}\left(\frac{y_1}{\Delta_1}\right) - \frac{1}{2}\left(\frac{y_1}{\Delta_1}\right)^3 \qquad \text{(II-13)}$$

In the preceding expression, the heat penetration depth Δ_1 is considered a function of time only and so is Δ_2. From Equations II-3 and II-7, the temperature difference is given as:

$$T_{1-\infty} - T_1 = [T_{1-\infty} - T_{2-\infty}][1 - F(y_1/\Delta_1)]/[1 + (k_1/k_2)(\Delta_2/\Delta_1)] \qquad \text{(II-14)}$$

Equation II-12 then becomes:

$$\frac{(3\Delta_1/8)}{[1 + (k_1/k_2)(\Delta_2/\Delta_1)]} \frac{\partial}{\partial\theta}[T_{1-\infty} - T_{2-\infty}]$$

$$+ [T_{1-\infty} - T_{2-\infty}]\frac{\partial}{\partial\theta}\left[\frac{3\Delta_1/8}{1 + (k_1/k_2)(\Delta_2/\Delta_1)}\right]$$

$$= \alpha_1 \frac{3\Delta_1/8}{[1 + (k_1/k_2)(\Delta_2/\Delta_1)]} \frac{\partial^2}{\partial x^2}[T_{1-\infty} - T_{2-\infty}]$$

$$+ \alpha_1 \frac{3/(2\Delta_1)}{[1 + (k_1/k_2)(\Delta_2/\Delta_1)]}[T_{1-\infty} - T_{2-\infty}] \qquad \text{(II-15)}$$

With $T_{1-\infty}$ and $T_{2-\infty}$ given by Equations II-1 and II-2, the heat-balance Equation II-15 is integrated once again from $x = 0$ to $x = \infty$, producing:

$$\frac{3\Delta_1/8}{[1 + (k_1/k_2)(\Delta_2/\Delta_1)]} \frac{(\sqrt{\alpha_1} - \sqrt{\alpha_2})}{\sqrt{\theta}} + 2\sqrt{\theta}(\sqrt{\alpha_1} - \sqrt{\alpha_2})\frac{\partial}{\partial\theta}\left[\frac{3\Delta_1/8}{1 + (k_1/k_2)(\Delta_2/\Delta_1)}\right]$$

$$= \alpha_1 \frac{3\Delta_1/8}{[1 + (k_1/k_2)(\Delta_2/\Delta_1)]} \frac{(\sqrt{\alpha_2} - \sqrt{\alpha_1})}{\sqrt{\alpha_1\alpha_2\theta}}$$

$$+ \alpha_1 \frac{3/(2\Delta_1)}{[1 + (k_1/k_2)(\Delta_2/\Delta_1)]} 2\sqrt{\theta}(\sqrt{\alpha_1} - \sqrt{\alpha_2}) \qquad \text{(II-16)}$$

There is another equation, similar to Equation II-16, obtained by interchanging the indexes 1 and 2 in Equation II-16.

To solve for Δ_1 and Δ_2 as to how they change with time θ, let:

$$\Delta_1 = S_1\sqrt{\alpha_1\theta} \tag{II-17}$$

$$\Delta_2 = S_2\sqrt{\alpha_2\theta} \tag{II-18}$$

where S_1 and S_2 are coefficients to be determined. Implicit in the preceding relations is the fact that (Δ_2/Δ_1) is a constant, independent of time. The numerical coefficients S_1 and S_2 can then be immediately obtained as:

$$S_1^2 = 8/[2 + \sqrt{\alpha_2/\alpha_1}] \tag{II-19}$$

$$S_2^2 = 8/[2 + \sqrt{\alpha_2/\alpha_1}] \tag{II-20}$$

which define the extents of the two boundary zones on either side of the interface. At the interface, the temperature is given by Equation II-7 which can be written as:

$$T_i = [T_{1-\infty} + PT_{2-\infty}]/[1 + P] \tag{II-21}$$

where:

$$P = (k_2/k_1)(\Delta_1/\Delta_2)$$

$$= (k_2/k_1)\sqrt{\alpha_1/\alpha_2}\left\{(2 + \sqrt{\alpha_2/\alpha_1})/(2 + \sqrt{\alpha_1/\alpha_2})\right\}^{1/2} \qquad \text{(II-22)}$$

The ratio of these two penetration depths (Δ_1/Δ_2) is given by:

$$\frac{\Delta_1}{\Delta_2} = \sqrt{\alpha_1/\alpha_2}\left[\frac{2 + \sqrt{\alpha_2/\alpha_1}}{2 + \sqrt{\alpha_1/\alpha_2}}\right]^{1/2} \qquad \text{(II-23)}$$

II.3 THE COMPLETE TEMPERATURE REPRESENTATION

The temperature distributions in the two quarter-infinite regions, 1 and 2, are now defined by:

(i) Equations II-1 and II-2 remote from the interface. They are of course the well-known error functions in terms of the similarity variables $x/2\sqrt{\alpha_1\theta}$ and $x/2\sqrt{\alpha_2\theta}$.

(ii) Equations II-3 and II-4 near the interface within finite distances Δ_1 and Δ_2 from the interface. The functional form $F(y_1/\Delta_1)$ or $F(y_2/\Delta_2)$ is that of Equation II-13, and the time-dependent zone depths Δ_1 and Δ_2 are given by Equations II-17 through II-20.

(iii) Equation II-21 for the interface temperature T_i. The parameter P is indicated in Equation II-22.

In order to bring all equations to a common basis, a similarity variable η, is defined as:

$$\eta_1 = \frac{x}{2\sqrt{\alpha_1 \theta}}$$

and the fully-established temperatures $T_{1-\infty}$ and $T_{2-\infty}$ are expressed by:

$$T_{1-\infty} = \text{erfc}(\eta_1) \tag{II-24}$$

$$T_{2-\infty} = \text{erfc}\left(\eta_1 \sqrt{\frac{\alpha_1}{\alpha_2}}\right) \tag{II-25}$$

With the above definitions and unifications, numerical results are illustrated for the following combinations of the physical properties:

$$k_1/k_2 = 5, \qquad \alpha_2/\alpha_1 = 0.3$$

for which the parameter P becomes 0.298, and $(\Delta_1/\Delta_2) = 1.48$.

In Figure II.3 are shown the established temperature distributions away from the interface and the interface temperature T_i calculated from Equation II-21 for the parametric values specified above. The interface zones have their respective temperature variations indicated in Figure II.4 with the ordinate values i.e. $T_{1-\infty}$, T_i, and $T_{2-\infty}$ chosen

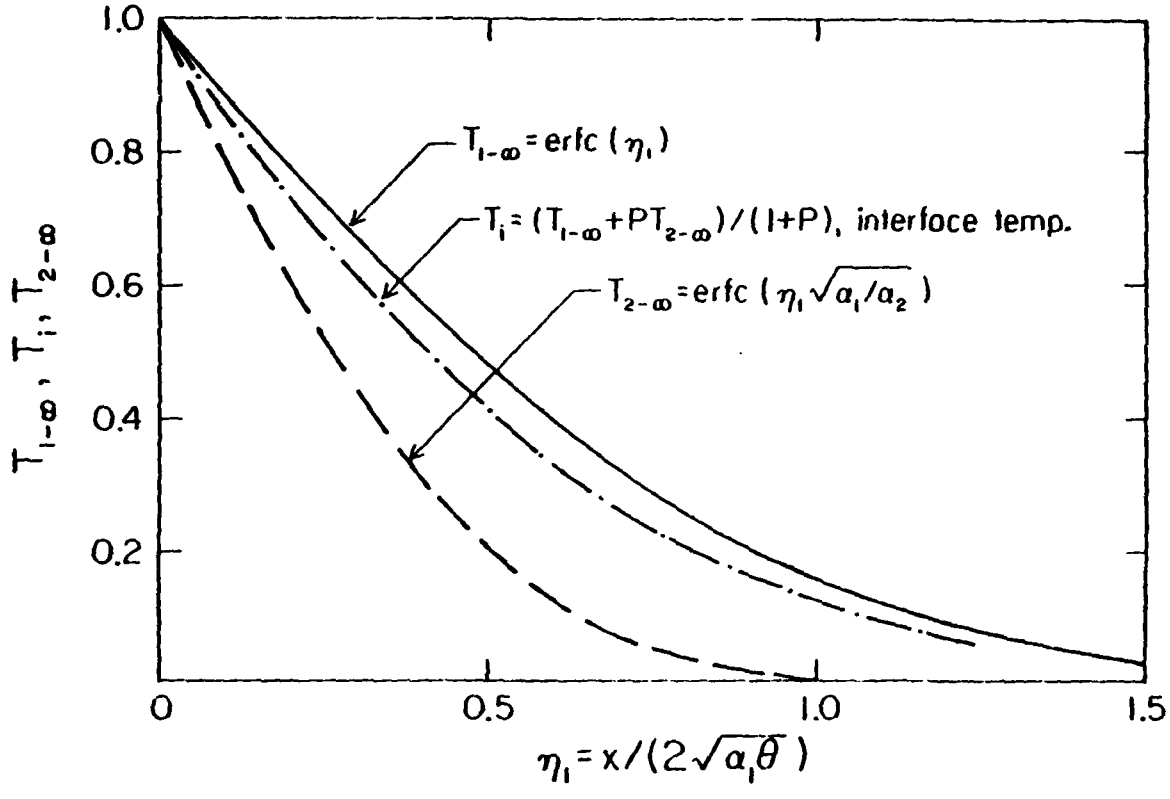

Figure II.3. Temperature Distributions in Semi-Infinite Region with Two Different Media. ($k_1/k_2 = 5$, $\alpha_2/\alpha_1 = 0.3$, Constant Surface Temperature).

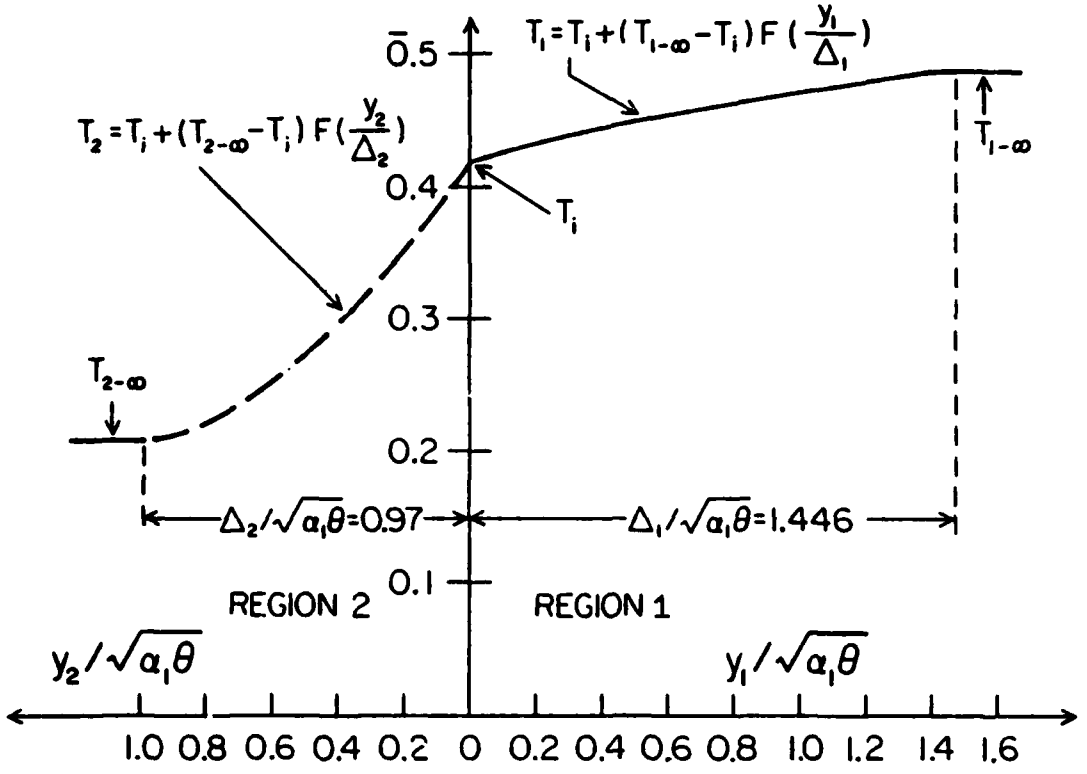

Figure II.4. Cross-sectional Temperature Distribution in Interface Region. Ordinate values for η_1 = .5 (k_1/k_2 = 5, α_2/α_1 = 0.3, Constant Surface Temperature)

for $X/2\sqrt{\alpha_1\theta} = 0.5$, while the abscissa is universally valid for the parameters so chosen. The discontinuity of the temperature gradient at the interface y = 0 is clearly defined.

II.4 CONSTANT HEAT-FLUX SOLUTION

For the case in which a constant (equal in both regions) heat flux is imparted to the exposed surface x = 0, the solution method is quite similar, but with the exception that the fully-established solutions, instead of Equations II-1 and II-2, are now given by:

$$T_{1-\infty} = \frac{2Q}{k_1}\sqrt{\alpha_1\theta}\ \text{ierfc}\left(\frac{x}{2\sqrt{\alpha_1\theta}}\right) \qquad \text{(II-26)}$$

$$T_{2-\infty} = \frac{2Q}{k_2}\sqrt{\alpha_2\theta}\ \text{ierfc}\left(\frac{x}{2\sqrt{\alpha_2\theta}}\right) \qquad \text{(II-27)}$$

where Q denotes the surface heat flux, which in this illustrative case is the same for both regions (this is not necessary for the method to work).

Subsequent developments are identical up to and including Equation II-15 which upon integration from x = 0 to x = ∞ yields the following equation:

$$(3\Delta_1/16)[(\alpha_1/k_1) - (\alpha_2/k_2)]/[1 + (k_1/k_2)(\Delta_2/\Delta_1)]$$

$$+ \sqrt{\theta}(3/16)[(\alpha_1/k_1) - (\alpha_2/k_2)]\frac{d}{d\theta}\{\Delta_1/[1 + (k_1/k_2)(\Delta_2/\Delta_1)]\}$$

$$= \alpha_1(3\Delta_1/16)[(1/k_1) - (1/k_2)]/[1 + (k_1/k_2)(\Delta_2/\Delta_1)]$$

$$+ \alpha_1(3/4\Delta_1)\theta[(\alpha_1/k_1) - (\alpha_2/k_2)]/[1 + (k_1/k_2)(\Delta_2/\Delta_1)] \qquad \text{(II-28)}$$

There is another equation obtained by starting with Equation II-11 in region 2. Integrating Equation II-11 from $y_2 = 0$ to $y_2 = \infty$, an equation similar to Equation II-15 is obtained. Further integration from $x = 0$ to $x = \infty$ results in an equation which is a companion to Equation II-28 and can be obtained from Equation II-28 by interchanging the indexes 1 and 2.

It is of importance to note that inter-region conduction is manifested in the last term of equation II-15 in the form of $(T_{1-\infty} - T_{2-\infty})$. The inter-region conduction influence, which modifies the temperature distribution near the interface, has now been summed up from $x = 0$ to $x = \infty$ and is identified in Equation II-28 as being proportional to $(\alpha_1/k_1 - \alpha_2/k_2)$. There could be cases depending on the thermo-physical properties of the media so that the integrated sum of the inter-facial heat conduction becomes zero. This occurs when $\rho_1 c_1 = \rho_2 c_2$. Figure II.5 illustrates this particular combination which is due to a reversal of the transverse heat conduction. At or

near this condition, the analysis of axial heat-balance integral would be quite inaccurate and a modification of the method is necessary.

The cause of trouble as revealed in Figure II.5 leads to an obvious remedy. Instead of integrating Equation II-15 and its companion (obtained by interchanging the indexes 1 and 2 in Equation II-15) from $x = 0$ to $x = \infty$, two heat-balance integrals are obtained from each of these two equations. One is obtained from $x = 0$ to $x = x_0$, the cross-over point in Figure II.5 and the other is obtained from $x = x_0$ to $x = \infty$. In this way, cancellation of the transverse conductance is prevented, and the conduction effect is duly accounted for in each range. In each range then, variations of Δ_1 and Δ_2 with time are determined. It is to be noted that the time-variation of Δ_1 or Δ_2 in the first range ($x = 0$ to $x = x_0$) may be at variance with the time-variation in the second range ($x > x_0$). The discrepancy between the values on either side of the cross-over point is not detrimental to a smooth transition of the temperature at the cross-over point, since at the latter there is no inter-region temperature difference or in other words the heat penetration depths Δ_1 and Δ_2 are moot at this location.

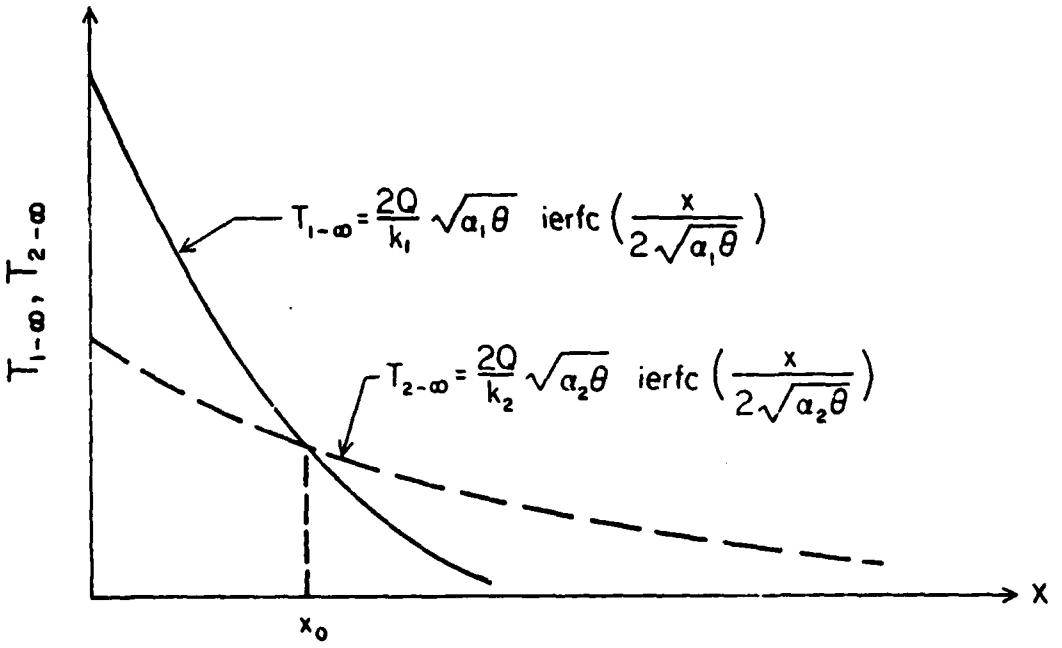

Figure II.5. Cross-over of Fully-established Temperature Profiles. ($\alpha_2 > \alpha_1$, $k_2 > k_1$)

III. PARALLEL HEAT FLOW IN LAMINATED COMPOSITES

Consider a laminated composite consisting of two alternate layers of two different materials and occupying a half-space $x \geq 0$. For heat flow along the x-direction, a unit-cell can be isolated from the assembly and the cell consists of a half-lamination of material 1 adjoint to a half-lamination of material 2. Figure III.1 depicts such an arrangement.

The boundary conditions on the symmetry surfaces, $y = 0$ and $y = b$, are of course zero heat-conduction. The interface boundary conditions are equal temperature and equal heat flux. The boundary condition at the exposed surface $x = 0$ will be taken as (i) that of a constant heat flux, or (ii) that of a constant surface temperature. The composite body is initially at zero temperature.

Before proceeding with various approximate methods, exact analytical solutions were first obtained for laminated composites with a finite length in the principal heat flow direction. Instead of extending to infinity along the x-direction in Figure II.1, the composite terminates at $x = L$.

Two boundary conditions at $x = L$ were used alternately in that analytical study, namely (i) a perfect insulation and (ii) constant temperature (equal to its initial value). Hence, all together four analytical solutions expressed by infinite series were developed and presented in Appendix C.

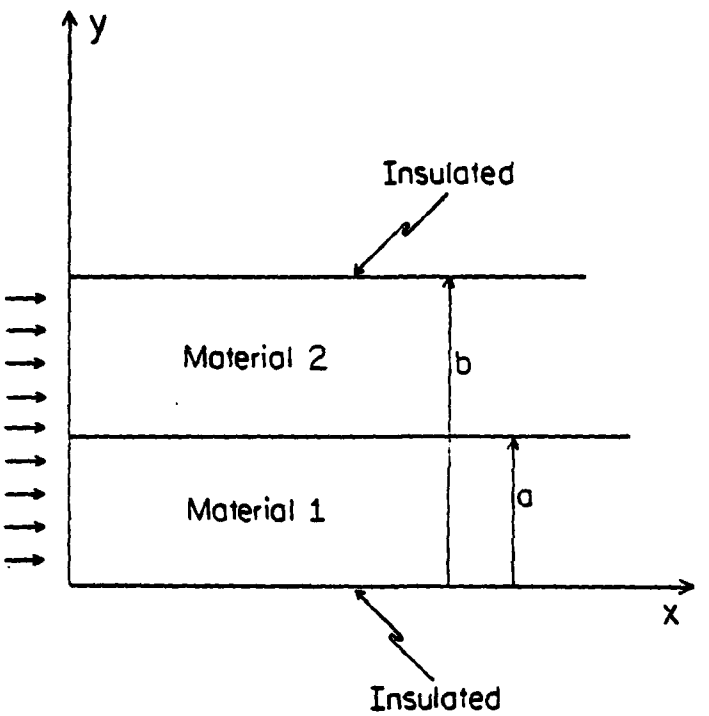

Figure III.1. Schematic of a Laminated Composite

The reasons for that effort are two-fold. First, exact solutions for composite configurations of practical interest are sparse, and secondly the availability of solutions for the geometry described would establish a standard with which approximate methods can be compared from the viewpoint of labor-vs.-accuracy trade-off. Even though no numerical results have come forth from that effort, because of the resulting complexity, they are presented in Appendix C for completeness and possible future uses.

Turning now to the approximate methods of analysis, the geometry depicted in Figure III.1 is taken up next. Conceptually, the temperature variations in both regions are expected to be, at small times, very much like those in a semi-infinite domain occupied by each constituent with the other absent in the half-space. As an example, the temperature responses for the case of a step-rise in their surface temperature at $x = 0$ are given by:

$$T_1 = \text{erfc}(x/2\sqrt{\alpha_1\theta})$$

$$T_2 = \text{erfc}(x/2\sqrt{\alpha_2\theta})$$

for small times.

As time proceeds, inter-region heat transfer takes place which is manifested by transverse temperature variations which result in a significant deviation from the solutions just described.

The preceding description of how the temperature varies qualitatively can be replicated by adopting the concept that in each region the

temperature distribution is comprised of two parts: a first part which is dependent on the axial distance x and time θ only, and a second part which is a product of two functions, one dependent on (x, θ) and the other on (y, θ).

Obviously at the interface $y = a$ (Figure II.1), these two regions must have a common temperature T_i. Such a temperature picture is given by the following:

$$T_1 = t_1 + (t_i - t_1)F(y, \theta) \qquad (y < a)$$

$$T_2 = t_2 + (t_i - t_2)\phi(y, \theta) \qquad (a < y < b)$$

where t_1, t_2, t_i are functions of (x, θ).

Two crucial roles are to be fulfilled by $F(y, \theta)$ and $\phi(y, \theta)$. First, at the interface $y = a$, these two functions must assume a value of unity so that $T_1 = T_2 = t_i$. Secondly, at time zero, both functions must vanish. These two requirements produce a singularity at $\theta = 0$ and $y = a$, and are therefore met by the following functional form for F:

$$F(y, \theta) = \cosh\beta_1 y / \cosh\beta_1 a$$

where β_1 is an implicit function of time θ, such that the singular behavior of $\beta_1 \to \infty$ at $\theta \to 0$ yields the desired characteristics of $F(y, \theta)$ as discussed before. Of course, the fact that $\cosh \beta_1 y$ has a zero slope at $y = 0$, the symmetry line, is a built-in feature.

Similarly, the function $\phi(y, \theta)$ is given the form:

$$\phi(y, \theta) = \cosh\beta_2(y - b)/\cosh\beta_2(a - b)$$

which has a zero slope at $y = b$, thus fulfilling the insulated condition at $y = b$.

III.1 FUNCTIONAL REPRESENTATION OF THE TRANSVERSE TEMPERATURE VARIATION

Consider the following functions to denote the temperatures in regions 1 and 2 respectively.

$$T_1 = t_1 + \frac{\lambda}{1 + \lambda}(t_2 - t_1)\frac{\cosh\beta_1 y}{\cosh\beta_1 a} \qquad \text{(III-1)}$$

for region 1, and

$$T_2 = t_2 + \frac{\lambda}{1 + \lambda}(t_1 - t_2)\frac{\cosh\beta_2(y - b)}{\cosh\beta_2(a - b)} \qquad \text{(III-2)}$$

for region 2.

The parameter λ is defined by:

$$\lambda = \left(\frac{k_2}{k_1}\right)\left(\frac{\beta_2}{\beta_1}\right)\frac{\tanh\beta_2(b - a)}{\tanh\beta_1 a} \qquad \text{(III-3)}$$

The second terms of Equations III-1 and III-2 represent the interaction of one region with another through conduction across the interface $y = a$.

If the second terms are zero, then t_1 or t_2 will be the temperature distribution in each region when the other is absent. These temperature distributions in such an extreme case are of course known from previous work and can therefore be used in the construction of these one-dimensional solutions t_1 and t_2.

In these equations, β_1 and β_2 are functions of time and can be thought of roughly as $1/\sqrt{\alpha_1\theta}$ and $1/\sqrt{\alpha_2\theta}$ respectively, although not precisely equal to them. Thus, when at small-time instants, β_1 and β_2 tend to infinity, the second terms of Equations III-1 and III-2 have a vanishingly small influence. In this way, the temperature responses in regions 1 and 2 independent of the other are preserved.

The interface conditions at y = a are fulfilled by their functional formations. These conditions are:

$$T_1 = T_2$$

$$k_1(\partial T_1/\partial y) = k_2(\partial T_2/\partial y)$$

and are satisfied by Equations II-1, II-2 and III-3. Furthermore, the insulated condition at y = a and y = b are also complied with.

In summary, it should be noted that t_1 and t_2 are functions of x and θ, and that T_1 and T_2 give the spatial-time distributions of temperature in these two regions. Undetermined, however, are the time-parameters β_1 and β_2 as well as t_1 and t_2. It is the purpose of the heat-balance integral-approach to obtain these variations.

III.2 THE HEAT-BALANCE EQUATIONS

By averaging the temperature in each region as given by Equations III-1 and III-2, there result:

$$\overline{T}_1 = \frac{1}{a}\int_0^a T_1 dy = t_1 + \frac{\lambda}{1+\lambda}(t_2 - t_1)\left[\frac{\tanh\beta_1 a}{\beta_1 a}\right] \qquad \text{(III-4)}$$

$$\overline{T}_2 = \frac{1}{b-a}\int_a^b T_2 dy = t_2 + \frac{1}{1+\lambda}(t_1 - t_2)\left[\frac{\tanh\beta_2(b-a)}{\beta_2(b-a)}\right] \qquad \text{(III-5)}$$

The equations which govern $\overline{T}_1$ and $\overline{T}_2$ are obtained by averaging the governing differential Equations II-6 and II-7. In carrying out the process of averaging, the insulated (zero conduction) condition at y = 0 and y = b and the equal heat flux condition at y = a are utilized. The governing equations after being averaged then become:

$$\frac{\partial t_1}{\partial\theta} + (t_2 - t_1)\frac{\partial}{\partial\theta}\left[\frac{\lambda}{1+\lambda}\frac{\tanh\beta_1 a}{\beta_1 a}\right] + \frac{\lambda}{1+\lambda}\frac{\tanh\beta_1 a}{\beta_1 a}\frac{\partial}{\partial\theta}[t_2 - t_1]$$

$$= \alpha_1 \frac{\partial^2}{\partial x^2}\left[t_1 + (t_2 - t_1)\frac{\lambda}{1+\lambda}\frac{\tanh\beta_1 a}{\beta_1 a}\right]$$

$$+ \frac{\alpha_1}{a}\left[\frac{\lambda}{1+\lambda}(t_2 - t_1)\beta_1 \tanh\beta_1 a\right] \qquad \text{(III-6)}$$

$$\frac{\partial t_2}{\partial \theta} + (t_1 - t_2)\frac{\partial}{\partial \theta}\left[\frac{1}{1+\lambda}\frac{\tanh\beta_2(b-a)}{\beta_2(b-a)}\right] + \frac{1}{1+\lambda}\frac{\tanh\beta_2(b-a)}{\beta_2(b-a)}\frac{\partial}{\partial \theta}[t_1 - t_2]$$

$$= \alpha_2 \frac{\partial^2}{\partial x^2}\left[t_2 + (t_1 - t_2)\frac{1}{1+\lambda}\frac{\tanh\beta_2(b-a)}{\beta_2(b-a)}\right]$$

$$+ \frac{\alpha_2}{(b-a)}\left[\frac{1}{1+\lambda}(t_1 - t_2)\beta_2\tanh\beta_2(b-a)\right] \qquad \text{(III-7)}$$

In the preceding equations, the second terms on the left-hand sides denote the sensible heat as the temperature profiles in the transverse direction (i.e., the y-direction) change with time. The reason for this identification is that the second terms calculate the time-change of β_1 and β_2 respectively. Thus, the three terms on the left-hand sides can be interpreted as follows: the first terms represent sensible heat change due to a bulk temperature change; and the third terms represent the change, not of the profiles as do the second terms, but of the bulk value $(t_1 - t_2)$.

On the right-hand sides of these equations, it is easy to recognize that the first terms represent the net axial conduction and the second terms, the transverse or interface conduction.

In laminated composites, the transverse dimension a or b is usually much smaller than the axial dimension - the direction which coincides with the principal heat flow path. Thus, a diffusion time for the transverse direction is naturally b^2/α_1 or b^2/α_2, which

characterizes the time scale the transverse temperature-change takes place. There is, of course, a diffusion time for the longitudinal direction indicated by z^2/α_1 or z^2/α_2, which is indicative of the time scale for heat propagation in that direction. In the region where $x >> b$, the temperature change (with time) is much slower in the x-direction than that in the transverse direction, due to interface conduction across a much shorter distance. From this dimensional argument, it is plausible to equate the second term on the left hand side of Equation III-6 with the second term on the right-hand side of it. Of course, the same can be said of Equation III-7. By such isolation from the overall equations, the "transverse-balance" equations are now:

$$\rho_1 c_1 \frac{\partial}{\partial \theta}\left[\frac{\lambda}{1+\lambda}\frac{\tanh\beta_1 a}{\beta_1 a}\right] = \frac{k_1}{a}\left[\frac{\lambda}{1+\lambda}\beta_1 \tanh\beta_1 a\right] \qquad \text{(III-8)}$$

$$\rho_2 c_2 \frac{\partial}{\partial \theta}\left[\frac{1}{1+\lambda}\frac{\tanh\beta_2(b-a)}{\beta_2(b-a)}\right] = \frac{k_2}{(b-a)}\left[\frac{1}{1+\lambda}\beta_2 \tanh\beta_2(b-a)\right] \qquad \text{(III-9)}$$

Because of Equation III-3, which equates the interface heat conduction, the right-hand sides of Equations III-8 and III-9 are equal (except for the factors a and b - a). A few manipulations show that although β_1 and β_2 are both unknowns at this stage, they are related by the following simple relation:

$$(\bar{\beta}_2/\bar{\beta}_1) = \sqrt{\alpha_1/\alpha_2} \qquad \text{(III-10)}$$

and Equation III-3 for λ can be re-cast as:

$$\lambda = (k_2/k_1)\sqrt{\alpha_1/\alpha_2}\,\frac{\tanh\bar{\beta}_1\{[(b/a) - 1]\sqrt{\alpha_1/\alpha_2}\}}{\tanh\bar{\beta}_1} \qquad \text{(III-11)}$$

In both expressions:

$$\bar{\beta}_1 = \beta_1 a, \quad \text{and} \quad \bar{\beta}_2 = \beta_2 a \qquad \text{(III-12)}$$

The above developments serve the purpose that only one of the two equations involving β_1 and β_2 needs to be solved. Thus, Equation III-8 will be sufficient to determine β_1 or $\bar{\beta}_1$ as a function of time θ. The pertinent boundary condition is at $\theta \to 0$, $\bar{\beta}_1 \to \infty$ which is required in the temperature-profile Equations III-1 and III-2. For $\beta_1 \to \infty$, consistant with $\beta_2 \to \infty$, the second terms of Equations III-1 and III-2 both vanish as they should, at $\theta \to 0$.

III.3 THE TRANSVERSE HEAT-BALANCE-INTEGRAL EQUATIONS

Regrouping the pertinent equations into this section, and using the following simplified notations:

$$\left.\begin{aligned} \bar{\beta}_1 &= \beta_1 a \\ \bar{\beta}_2 &= \beta_2 a \\ \bar{\theta} &= (\alpha_1 \theta / a^2), \end{aligned}\right\} \qquad \text{(III-12)}$$

the equation to be solved for $\bar{\beta}_1$ is,

$$\frac{d}{d\bar{\theta}} \left[\frac{\lambda}{1+\lambda} \frac{\tanh\bar{\beta}_1}{\bar{\beta}_1} \right] = \frac{\lambda}{1+\lambda} \bar{\beta}_1 \tanh\bar{\beta}_1 \qquad \text{(III-8)}$$

with the boundary condition $\bar{\theta} \to 0$, $\bar{\beta}_1 \to \infty$. The parameter λ is defined by:

$$\lambda = \sqrt{(k_2\rho_2 c_2 / k_1 \rho_1 c_1)} \tanh\left[\bar{\beta}_1 \sqrt{\frac{\alpha_1}{\alpha_2}} \left(\frac{b}{a} - 1\right) \right] \Big/ \tanh\bar{\beta}_1 \qquad \text{(III-11)}$$

Defining a new symbol H such that:

$$H = \frac{\lambda}{1+\lambda} \frac{\tanh\bar{\beta}_1}{\bar{\beta}_1} \qquad \text{(III-13)}$$

equation III-8 can be put as:

$$\frac{dH}{d\bar{\theta}} = H\bar{\beta}_1^2 \qquad \text{(III-14)}$$

with the boundary condition of $\bar{\beta}_1 = \infty$ at $\bar{\theta} = 0$. Appendix A shows the numerical method developed to solve Equation III-14 as well as the asymptotic continuation at large values of $\bar{\theta}$.

For $k_2/k_1 = 10$, $\alpha_2/\alpha_1 = 3$ and $b/a = 2$, the variation of $\bar{\beta}_1$ with $\bar{\theta}$ is shown in Figure III.2. At small values of $\bar{\theta}$, $\bar{\beta}_1 = 1/\sqrt{2\bar{\theta}}$. Hence for small times, the transverse temperature variation as shown in Equation III-1 has the form of:

$$\frac{\cosh\beta y}{\cosh\beta a} = \frac{\cosh\bar{\beta}_1(y/a)}{\cosh\bar{\beta}_1} = \frac{\cosh(y/a)/\sqrt{2\bar{\theta}}}{\cosh(1/\sqrt{2\bar{\theta}})}$$

for the laminate in region 1, i.e., $y < a$. At a short distance from the interface $y = a$, let $y' = a - y$, the transverse temperature variation as given above can be expressed by the following (for $\bar{\beta}_1 \to \infty$):

$$\frac{\cosh\beta y}{\cosh\beta a} = e^{-\beta(a - y)} = e^{-\beta y'} = e^{-(y'/a)/\sqrt{2\bar{\theta}}}$$

which shows the correct combination of the similarity variable in heat conduction theory.

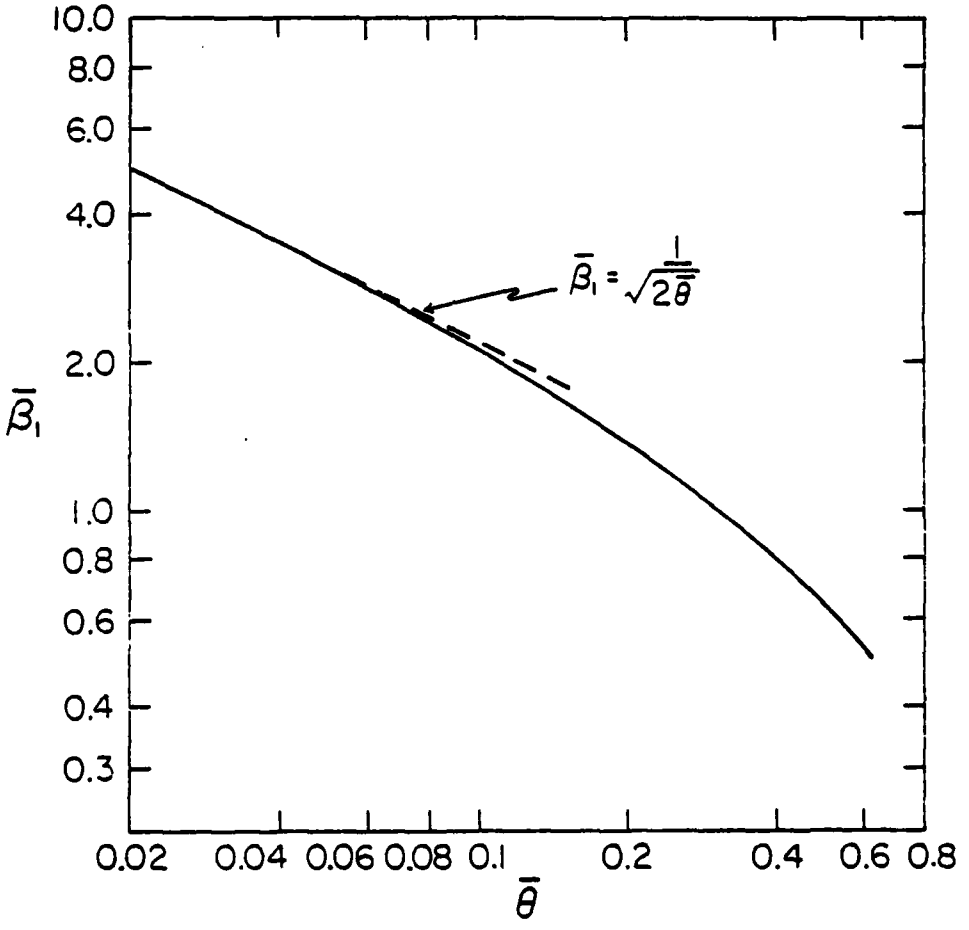

Figure III.2. Variation of Transverse Time-Parameter $\bar{\beta}_1$, vs $\bar{\theta}$ (Laminated Composite). (From Equation III-14, $k_2/k_1 = 10$, $\alpha_2/\alpha_1 = 3$, $b/a = 2$)

III.4 THE AXIAL HEAT DIFFUSION EQUATIONS

In order to solve Equations III-6 and III-7, which are the results of averaging the diffusion equations along the transverse direction over these two regions, the averaged Equations III-6 and III-7 can be expressed, with $\bar{x} = x/a$, as:

$$\frac{\partial \bar{T}_1}{\partial \bar{\theta}} = \frac{\partial^2 \bar{T}_1}{\partial \bar{x}^2} + \frac{H\bar{\beta}_1^2}{1 - H(1 + R)} (\bar{T}_2 - \bar{T}_1) \qquad \text{(III-15)}$$

$$\left(\frac{\alpha_1}{\alpha_2}\right) \frac{\partial \bar{T}_2}{\partial \bar{\theta}} = \frac{\partial^2 T_2}{\partial \bar{x}^2} - \left(\frac{k_1}{k_2}\right) \frac{1}{(b/a - 1)} \frac{H\bar{\beta}_1^2}{1 - H(1 + R)} (\bar{T}_2 - \bar{T}_1) \qquad \text{(III-16)}$$

where H is defined by Equation III-13. The definition for R in the preceding equation is:

$$R = \frac{(\rho c)_1}{(\rho c)_2 (\frac{b}{a} - 1)} \qquad \text{(III-17)}$$

which amounts to the ratio of the thermal capacities in regions 1 and 2.

In these two equations, the coefficients of the second terms on the right-hand side are of course presumed known, as they have been obtained from Equation III-14. Here, the focus is on the average temperatures $\bar{T}_1$ and $\bar{T}_2$ which are the results of axial diffusion and

transverse inter-region heat conduction. The merit of only having to solve Equations III-15 and III-16, in contrast to solving the full diffusion equations for these two regions, lies in the fact that the transverse coordinate y disappears from these two reduced equations by virtue of the transverse time-dependent parameters $\bar{\beta}_1$ and $\bar{\beta}_2$.

This seemingly minor simplification of the equations results in a very significant reduction in labor required to obtain the temperature distributions. The key lies in a proper choice of the profile functions for $F(y, \theta)$ and $\phi(y, \theta)$ in these two regions.

Perturbation approaches. In order to address the various solution techniques available, let the inter-region conduction coefficient be expressed by the following:

$$L = \frac{H\bar{\beta}_1^2}{1 - H(1 + R)} \tag{III-18}$$

and Equations III-15 and III-16 are re-shaped to:

$$\frac{\partial \bar{T}_1}{\partial \bar{\theta}} = \frac{\partial^2 \bar{T}_1}{\partial \bar{x}^2} + L(\bar{T}_2 - \bar{T}_1) \tag{III-19}$$

$$\frac{\partial \bar{T}_2}{\partial \bar{\theta}} = \left(\frac{\alpha_2}{\alpha_1}\right)\frac{\partial^2 T_2}{\partial \bar{x}^2} - RL(\bar{T}_2 - \bar{T}_1) \tag{III-20}$$

The inter-region conductance L has the following characteristics, as deduced from asymptotic analyses (see Appendix A):

$$L \approx 1/\sqrt{\bar{\theta}} \qquad \text{for } \bar{\theta} \to 0$$

$$L \approx \text{constant} \qquad \text{for } \bar{\theta} \to \infty$$

Also of significance is the thermal capacity ratio R, defined by Equation III-17.

Conceptually then, the system of Equations III-19 and III-20 with proper boundary conditions at $\bar{x} = 0$ can be solved by various perturbation techniques (the use of the Laplace transforms does not obviate the use of perturbation, as the transform parameter is not simply obtained). Therefore, one approach is to express the solutions $\bar{T}_1$ and $\bar{T}_2$ in series with time $\bar{\theta}$ as the perturbation parameter, and the scheme is to determine the terms in these two series on a term-wise basis. Thus by writing $\bar{T}_1$ and $\bar{T}_2$ as:

$$\bar{T}_1 = G_0(\bar{x}, \bar{\theta}) + \sqrt{\bar{\theta}}G_1(\bar{x}, \bar{\theta}) + \bar{\theta}G_2(\bar{x}, \bar{\theta}) + \ldots .$$

$$\bar{T}_2 = g_0(\bar{x}, \bar{\theta}) + \sqrt{\bar{\theta}}g_1(\bar{x}, \bar{\theta}) + \bar{\theta}g_2(\bar{x}, \bar{\theta}) + \ldots .$$

where the first term solutions, G_0 and g_0, are the infinite-region solutions without inter-region conduction. This is true, of course, for problems with initial temperature zero in both regions.

A second perturbation approach is through the thermal capacity ratio R. If R is very small, which in a limiting sense may be put to zero, then Equation III-20 can be solved immediately. In other words, the temperature distribution $\overline{T}_2$ will be unaffected by $\overline{T}_1$. Using this solution of $\overline{T}_2$, Equation III-19 can be solved for $\overline{T}_1$, which is used, in turn, to solve for $\overline{T}_2$ from Equation III-18. Such a procedure is equivalent to an iteration approach. Alternately of course, a formal series expansion in terms of R can be used, such as:

$$\overline{T}_1 = S_0(\overline{x},\overline{\theta}) + RS_1(\overline{x}, \overline{\theta}) + \ldots$$

$$\overline{T}_2 = \psi_0(\overline{x}, \overline{\theta}) + R\psi_1(\overline{x}, \overline{\theta}) + \ldots$$

Double Heat-Balance Integral-Method. Equations III-19 and III-20 are the results of using heat-balance integrals in the transverse direction; they are considerably simpler than the full diffusion equations. Under certain conditions, these two equations can be approximately solved by using once more heat-balance integrals in the axial direction. The resulting approximate solutions for the two regions may be termed the double heat-balance integral-method. To demonstrate its efficacy and deficiency, two types of surface heating will be considered: constant surface temperature rise at $x = 0$, and constant surface heat flux. For the former type of boundary condition, the method of double heat-balance integrals shows

a significant advantage, while for the latter type of boundary condition, some limitation of the results must be observed.

Constant-Temperature Case. First, consider the problem of a constant surface temperature rise. Let the surface temperature at $x = 0$ of both regions be impulsively raised to a finite value from their initial temperature of zero. If there is no inter-region conductance, i.e., $L = 0$, then the solution for each region is independent of the other and is given by the following for region 1:

$$\bar{T}_1 = \operatorname{erfc}(\bar{x}/2\sqrt{\bar{\theta}}) \qquad \text{(III-21)}$$

For region 2, the solution is:

$$\bar{T}_2 = \operatorname{erfc}\left(\frac{\bar{x}}{2}\sqrt{\frac{\alpha_1}{\alpha_2\bar{\theta}}}\right) \qquad \text{(III-22)}$$

Essential to the method of heat-balance integral is a proper choice of temperature profiles for these two regions when inter-region conduction is to be accounted for. Accordingly then, the error-functions are chosen to represent the temperature profiles. But in lieu of $\bar{\theta}$, two time-dependent parameters γ_1 and γ_2 are embedded in the preceding expressions; and the chosen profiles are now:

$$\overline{T}_1 = \text{erfc}(\overline{\gamma}_1 \overline{x}) \qquad \text{(III-23)}$$

$$\overline{T}_2 = \text{erfc}(\overline{\gamma}_2 \overline{x})$$

in which the variations of $\overline{\gamma}_1$ and $\overline{\gamma}_2$ versus time $\overline{\theta}$ are to be determined via the heat-balance integral method. At very small times $\overline{\theta}$, Equations III-23 and III-24 must replicate the independent solutions, Equations III-21 and III-22, as the inter-region conductance is initially absent. This requirement establishes the necessary boundary conditions on $\overline{\gamma}_1$ and $\overline{\gamma}_2$, i.e. for $\overline{\theta} \to 0$:

$$\overline{\gamma}_1 = 1/(2\sqrt{\overline{\theta}})$$

$$\overline{\gamma}_2 = \sqrt{\alpha_1/\alpha_2}\,/(2\sqrt{\overline{\theta}}) \qquad \text{(III-24)}$$

In fact, a more appropriate description is:

$$\overline{\gamma}_1 = \infty \qquad \text{at } \overline{\theta} \to 0 \qquad \text{(III-25)}$$

$$\overline{\gamma}_2 = \infty \qquad \text{at } \overline{\theta} \to 0 \qquad \text{(III-26)}$$

and their singular behaviors at $\theta \to 0$ are determined by the heat-balance integrals.

The next step is to integrate Equations III-19 and III-20 from $x = 0$ to $x = \infty$ with the temperature profiles $\bar{T}_1$ and $\bar{T}_2$ given by Equations III-23 and III-24. The result is two equations with $\bar{\gamma}_1$ and $\bar{\gamma}_2$ as the new dependent variables.

$$\frac{d}{\alpha\bar{\theta}}\left[\frac{1}{\bar{\gamma}_1}\right] = 2\bar{\gamma}_1 + L\left(\frac{1}{\bar{\gamma}_2} - \frac{1}{\bar{\gamma}_1}\right) \qquad \text{(III-27)}$$

$$\frac{d}{\alpha\bar{\theta}}\left[\frac{1}{\bar{\gamma}_2}\right] = 2\left(\frac{\alpha_2}{\alpha_1}\right)\bar{\gamma}_2 - RL\left(\frac{1}{\bar{\gamma}_2} - \frac{1}{\bar{\gamma}_1}\right) \qquad \text{(III-28)}$$

The associated boundary conditions are those prescribed by Equations III-25 and III-26. It is to be recalled that the time-dependent transverse conductance, L, having been determined by virtue of solving Equation III-13, is a pre-determined function in Equations III-27 and III-28.

For starting the solution of these two equations, the initial boundary conditions of Equations III-25 and III-26 can be satisfied by taking:

$$\frac{1}{\bar{\gamma}_1} = s_1\sqrt{\bar{\theta}} + \ldots$$

$$\frac{1}{\bar{\gamma}_2} = s_2\sqrt{\bar{\theta}} + \ldots$$

The numerical coefficients s_1 and s_2 are immediately shown to be $s_1 = 2$ and $s_2 = 2\sqrt{\alpha_2/\alpha_1}$ which render the asymptotic solutions (for $\bar{\theta} \to 0$) the same as the independent solutions. As time goes on, the influence of the transverse conductance L starts to modify the solutions. Implementation of the solution can proceed by a simple integration method. Results obtained in this manner are discussed in Section V in comparison with other solution techniques.

Constant Heat-Flux Case. In this case, the temperature profiles in the two regions are guided by their respective independent solutions. Thus, starting with the profiles:

$$\bar{T}_1 = [aQ/k_1\bar{\gamma}_1]\ \text{ierfc}(\bar{\gamma}_1\bar{x}) \qquad \text{(III-29)}$$

$$\bar{T}_2 = [aQ/k_2\bar{\gamma}_2]\ \text{ierfc}(\bar{\gamma}_2\bar{x}) \qquad \text{(III-30)}$$

where $\bar{\gamma}_1$ and $\bar{\gamma}_2$ are, as in the case of constant surface temperature, the time-dependent parameters.

Integrating Equations III-19 and III-20 from $\bar{x} = 0$ to $\bar{x} = \infty$ with $\bar{T}_1$ and $\bar{T}_2$ as the profiles, the resulting equations become:

$$\frac{d}{d\bar{\theta}}\left[\frac{1}{\bar{\gamma}_1^2}\right] = 4 + L\left[\left(\frac{k_1}{k_2}\right)\frac{1}{\bar{\gamma}_2^2} - \frac{1}{\bar{\gamma}_1^2}\right] \qquad \text{(III-31)}$$

$$\frac{d}{d\bar{\theta}}\left[\frac{1}{\bar{\gamma}_1^2}\right] = 4\left(\frac{\alpha_2}{\alpha_1}\right) - R\left(\frac{k_2}{k_1}\right) L\left[\left(\frac{k_1}{k_2}\right)\frac{1}{\bar{\gamma}_2^2} - \frac{1}{\bar{\gamma}_1^2}\right] \qquad \text{(III-32)}$$

The preceding equations can be solved in a closed form for the boundary conditions $\bar{\gamma}_1 \to \infty$, $\bar{\gamma}_2 \to \infty$ at $\bar{\theta} \to 0$:

$$\left[\left(\frac{k_1}{k_2}\right)\frac{1}{\bar{\gamma}_2^2} - \frac{1}{\bar{\gamma}_1^2}\right] = 4\left[\frac{\rho_1 c_1}{\rho_2 c_2} - 1\right]\left[\exp\left(-\int_0^{\bar{\theta}} (1 + R)Ld\bar{\theta}\right)\right] \cdot$$

$$\cdot\left[\int_0^{\bar{\theta}} \exp\left(\int_0^{\bar{\theta}} (1 + R)Ld\bar{\theta}\right)d\bar{\theta}\right] \qquad \text{(III-33)}$$

which, when introduced into Equation III-31 or III-32, gives direct solutions for $\bar{\gamma}_2$ or $\bar{\gamma}_1$. The surface temperature variations (with time) for these two materials are given by:

$$\bar{T}_1 = [aQ/k_1\sqrt{\pi}]/\bar{\gamma}_1 \qquad \text{(III-34)}$$

$$\bar{T}_2 = [aQ/k_1\sqrt{\pi}][k_1/k_2]/\bar{\gamma}_2 \qquad \text{(III-35)}$$

Numerical results obtained from the preceding equations are discussed in Section V in conjunction with results obtained by other methods.

To understand the nature of the double heat-balance integral method, it is necessary to examine Equations III-19 and III-20, which contain the inter-region conductance effect. The inter-region conductance exhibited in these equations is of a local character, i.e., at an axial location, x. When axial heat-balance integrals are applied, the inter-region conductance is therefore summed up. Thus, the local variation of L is thereby lost. This is a source of inaccuracy in the final results. In an extreme case, the inter-region heat conduction may reverse itself, i.e., from $\bar{x} = 0$ to $\bar{x} = \bar{x}_1$ $(\bar{T}_2 - \bar{T}_1) > 0$ and from $\bar{x} = \bar{x}_1$ to $\bar{x} = \infty$, $(\bar{T}_2 - \bar{T}_1) < 0$. The average of the interfacial conduction may be quite influential on the final results.

Finite-Difference Solution. The method of perturbation described in Section III.5.1 is theoretically exact and conceptually elegant. From a practical point of view, the method is tedious, for it requires a number of terms in order to achieve some degree of accuracy. Similarly, the use of the Laplace transform - again conceptually exact - does not render itself to immediate numerical extraction, because the transform parameter does not have simple roots. Consequently, the use of small-time expansion or large-time expansion in the inversion procedure, which constitutes a de facto perturbation process, negates the conceptual advantages the Laplace-transform method possesses.

On the other hand, the double heat-balance method presented in Section III.5.2 reduces the analytical labor to a minimum, but in so doing the local (along the axial position) inter-region conductance effect is averaged out or may be mutually cancelled. Only the total inter-region transverse conduction is recognized, as is pointed out previously in Section II.

Between these two approaches lies the method of solving the axial diffusion Equations III-19 and III-20 by a finite-difference procedure, which in a broader sense belongs to the exact-solution category. The advantage of solving the axial diffusion equations over the full diffusion equations in two spatial coordinates is readily apparent if it is recognized that the labor of the former is about one-tenth of the latter. For this reason, the axial diffusion Equations III-19 and III-20 as well as the corresponding equations for fibrous composites are used extensively in this report.

Appendix B contains a synopsis of the finite-difference formulation, and the results therefrom are presented in Section V together with those from other methods.

IV. PARALLEL HEAT FLOW ALONG UNI-DIRECTIONAL FIBERS

Consider an idealized dispersion pattern of uni-directional fibers* in a matrix material such that the fiber centers form an equilateral triangular pattern as depicted in Figure IV.1, which shows a cross-sectional view of such a composite material. When planar heat flow takes place along the fiber axial direction, it is possible to visualize a repeating cell in which the thermal response is representative of the entire body.

Such a unit cell is a hexagon with a fiber located in its geometrical center as indicated in Figure IV.1. Intuitively, the hexagonal enclosure of the fiber can be replaced by a circular enclosure containing the same amount of the matrix material, and the boundary condition on the circular enclosure is equivalent to that on the hexagonal enclosure, i.e., an insulated condition.

Mathematically speaking, a great simplification has been achieved; both boundaries are now expressed in circular coordinates while preserving almost complete thermal equivalence. Hence, the problem is transformed into two circular cylinders with the matrix material enclosing the fiber as is now illustrated in Figure IV.2.

---

*Here and elsewhere in this report, the terms fiber and tow are used interchangeably.

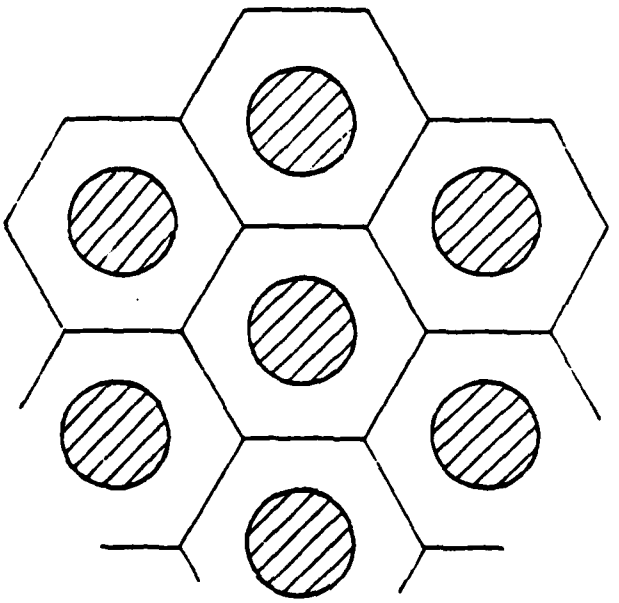

Figure IV.1. Triangular Dispersion Pattern of Uni-directional Fibers in Matrix

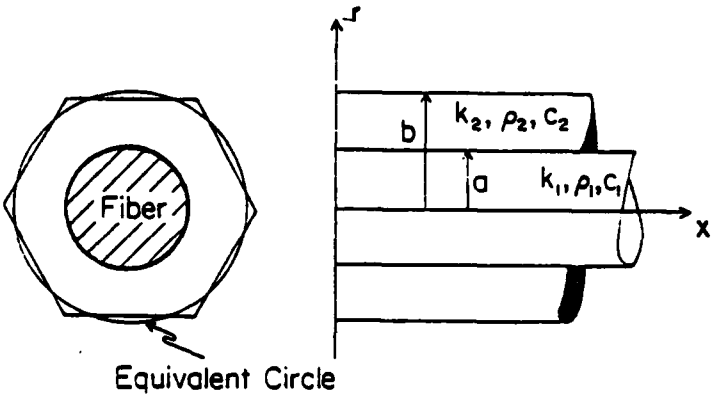

Figure IV.2. Equivalent Two-cylinder Configuration for a Uni-directional Fiber-composite

To preserve parallelism with the case of laminated composites, the radii are named a and b and the principal heat flow is along the axial direction x. For illustrating the heat-balance integral approach, consideration is given to the problem of a uniform initial temperature (zero) and an impulsively applied heat flux Q on the surface, $x = 0$. The material properties are k_1, ρ_1, c_1, for the fiber region and k_2, ρ_2, c_2, for the matrix (annular) region.

With the simplified configuration shown in Figure IV.2, the problem is the same as that treated in Section III except here a circular configuration replaces the planar configuration in Section III.

IV.1 FUNCTIONAL REPRESENTATION OF THE TRANSVERSE VARIATIONS

A mathematical function which reasonably reflects the spacial distribution of the temperature must contain r-variation and x-variation. Expressed in a product-form, the temperatures in regions 1 and 2 can be taken, similar to Equations III-1 and III-2, as:

$$T_1 = t_1 + (t_i - t_1)\left[\frac{\cosh\beta_1 r^2}{\cosh\beta_1 a^2}\right] \qquad \text{(IV-1)}$$

$$T_2 = t_2 + (t_i - t_2)\left[\frac{\cosh\beta_2 (r^2 - b^2)}{\cosh\beta_2 (a^2 - b^2)}\right] \qquad \text{(IV-2)}$$

The radial variation (in space and in time) is expressed through the terms in brackets. It is readily seen that the conditions of zero temperature-gradient at r = 0 and r = b are fulfilled by the form so chosen. Furthermore, at r = a, the interface, T_1, is equal to T_2 as is required. The equal heat-flux conditions:

$$k_1(\partial T_1/\partial r)_a = k_2(\partial T_2/\partial r)_a$$

result in an expression for T_i, the interface temperature, as:

$$t_i = (t_1 + \lambda t_2)/(1 + \lambda) \qquad \text{(IV-3)}$$

and

$$\lambda = \left(\frac{k_2}{k_1}\right)\left(\frac{\beta_2}{\beta_1}\right)\frac{\tanh\beta_2(b^2 - a^2)}{\tanh\beta_1 a^2} \qquad \text{(IV-4)}$$

which is parallel to that for the planar case, see Equation III-3. The profiles, Equations IV-1 and IV-2, can be re-cast as:

$$T_1 = t_1 + (t_2 - t_1)\frac{\lambda}{1 + \lambda}\left[\frac{\cosh\beta_1 r^2}{\cosh\beta_1 a^2}\right] \qquad \text{(IV-1a)}$$

$$T_2 = t_2 + (t_1 - t_2)\frac{1}{1 + \lambda}\left[\frac{\cosh\beta_2(r^2 - b^2)}{\cosh\beta_2(a^2 - b^2)}\right] \qquad \text{(IV-2a)}$$

Temperature variations in x and θ are embedded in t_1 and t_2, whereas temperature variations in r and θ are expressed through β_1, β_2, r, and λ. The time-dependent parameters β_1 and β_2 determine the transverse profiles in both materials.

As in planar case, Section III, it is of importance to note that the boundary conditions on β_1 and β_2 are that as $\theta \to 0$, β_1 and β_2 approach infinity. The latter condition yields a singularity at the interface r = a, while it renders the temperature in the transverse direction uniform in their respective cross-sections.

IV.2 THE HEAT-BALANCE EQUATIONS

First, the temperature profile Equations IV-1a and IV-2a are averaged transversely in each region, resulting in:

$$\bar{T}_1 = t_1 + (t_2 - t_1)\left[\frac{\lambda}{1+\lambda}\frac{\tanh\beta_1 a^2}{\beta_1 a^2}\right] \qquad \text{(IV-5)}$$

$$\bar{T}_2 = t_2 + (t_1 - t_2)\left[\frac{1}{1+\lambda}\frac{\tanh\beta_2(b^2 - a^2)}{\beta_2(b^2 - a^2)}\right] \qquad \text{(IV-6)}$$

Next, the governing heat diffusion equations are averaged in the r-direction for each region. The resulting governing equations are in the following form, similar to those in Section III:

$$\frac{\partial t_1}{\partial \bar{\theta}} + (t_2 - t_1)\frac{\partial}{\partial \bar{\theta}}\left[\frac{\lambda}{1+\lambda}\frac{\tanh\beta_1 a^2}{\beta_1 a^2}\right] + \left[\frac{\lambda}{1+\lambda}\frac{\tanh\beta_1 a^2}{\beta_1 a^2}\right]\frac{\partial}{\partial \bar{\theta}}(t_2 - t_1)$$

$$= \frac{\partial^2 \bar{T}_1}{\partial \bar{X}^2} + (t_2 - t_1)\left[\frac{4\lambda}{1+\lambda}(\beta_1 a^2)\tanh(\beta_1 a^2)\right] \qquad \text{(IV-7)}$$

$$\left(\frac{\alpha_1}{\alpha_2}\right)\left\{\frac{\partial t_2}{\partial \bar{\theta}} + (t_1 - t_2)\frac{\partial}{\partial \bar{\theta}}\left[\frac{1}{1+\lambda}\frac{\tanh\beta_2(b^2 - a^2)}{\beta_2(b^2 - a^2)}\right]\right.$$

$$\left. + \left[\frac{1}{1+\lambda}\frac{\tanh\beta_2(b^2 - a^2)}{\beta_2(b^2 - a^2)}\right]\frac{\partial}{\partial \bar{\theta}}(t_1 - t_2)\right\}$$

$$= \frac{\partial^2 \bar{T}_2}{\partial \bar{X}^2} + (t_1 - t_2)\left[\frac{4}{1+\lambda}\frac{\beta_2 a^2}{((b/a)^2 - 1)}\tanh\beta_2(b^2 - a^2)\right] \qquad \text{(IV-8)}$$

where $\bar{\theta} = \alpha_1\theta/a^2$ and $\bar{x} = x/a$.

IV.3 THE TRANSVERSE HEAT-BALANCE INTEGRAL EQUATIONS

As is explained in Section III, the interface conduction represented by the second term on the right-hand side of Equation IV-7 or IV-8 is associated with the time-rate change of the transverse

temperature-profile represented by the second term on the left-hand side of the equation. These two terms can be isolated from each equation. Such a "transverse equilibrium" gives the following heat-balance integrals:

$$\frac{d}{d\theta}\left[\frac{\lambda}{1+\lambda}\frac{\tanh\beta_1 a^2}{\beta_1 a^2}\right] = 4\,\frac{\lambda}{1+\lambda}\,\beta_1 a^2 \tanh\beta_1 a^2 \qquad \text{(IV-9)}$$

$$\frac{\alpha_1}{\alpha_2}\frac{d}{d\theta}\left[\frac{1}{1+\lambda}\frac{\tanh\beta_2 a^2\left(\left(\frac{b}{a}\right)^2 - 1\right)}{\beta_2 a^2}\right] = 4\,\frac{1}{1+\lambda}\,\beta_2 a^2 \tanh\beta_2 a^2\left(\left(\frac{b}{a}\right)^2 - 1\right)$$

(IV-10)

Because of the definition of λ in Equation IV-4, the right-hand side terms of Equations IV-9 and IV-10 are proportional to each other. This observation leads to a simple ratio for the time-parameters β_1 and β_2 as:

$$\beta_2/\beta_1 = \sqrt{\alpha_1/\alpha_2} \qquad \text{(IV-11)}$$

Consequently, the definition for the interface parameter λ can be written as:

$$\lambda = \sqrt{(k_2\rho_2c_2/k_1\rho_1c_1}\ \tanh\left[\bar{\beta}_1\sqrt{\alpha_1/\alpha_2}\left(\left(\frac{b}{a}\right)^2 - 1\right)\right]/\tanh\bar{\beta}_1 \qquad \text{(IV-12)}$$

where $\bar{\beta}_1 = \beta_1 a^2$.

Thus, only one of the two Equations IV-9 and IV-10 needs to be solved. The boundary condition of $\bar{\beta}_1$ is, as usual,

$$\bar{\beta}_1 \to \infty; \qquad \bar{\theta} \to 0$$

By defining a convenient quantity H as:

$$H = \frac{\lambda}{1+\lambda}\,[\tanh\bar{\beta}_1]/\bar{\beta}_1 \qquad \text{(IV-13)}$$

Equation IV-9 is reduced to:

$$\frac{dH}{d\bar{\theta}} = 4H\bar{\beta}_1^2 \qquad \text{(IV-14)}$$

Its solution with boundary condition IV-13 gives both $\bar{\beta}_1$ and $\bar{\beta}_2$ variations with time. Appendix A details the solution method of Equation IV-14.

Shown in Figure IV-3 is the $\bar{\beta}_1$ distribution curve for $\alpha_2/\alpha_1 = 3$, $k_2/k_1 = 10$ and $b/a = 2$. For the same parametric values, the $\bar{\beta}_1 \sim \bar{\theta}$ curve for a two-dimensional equivalent case is also indicated for comparison.

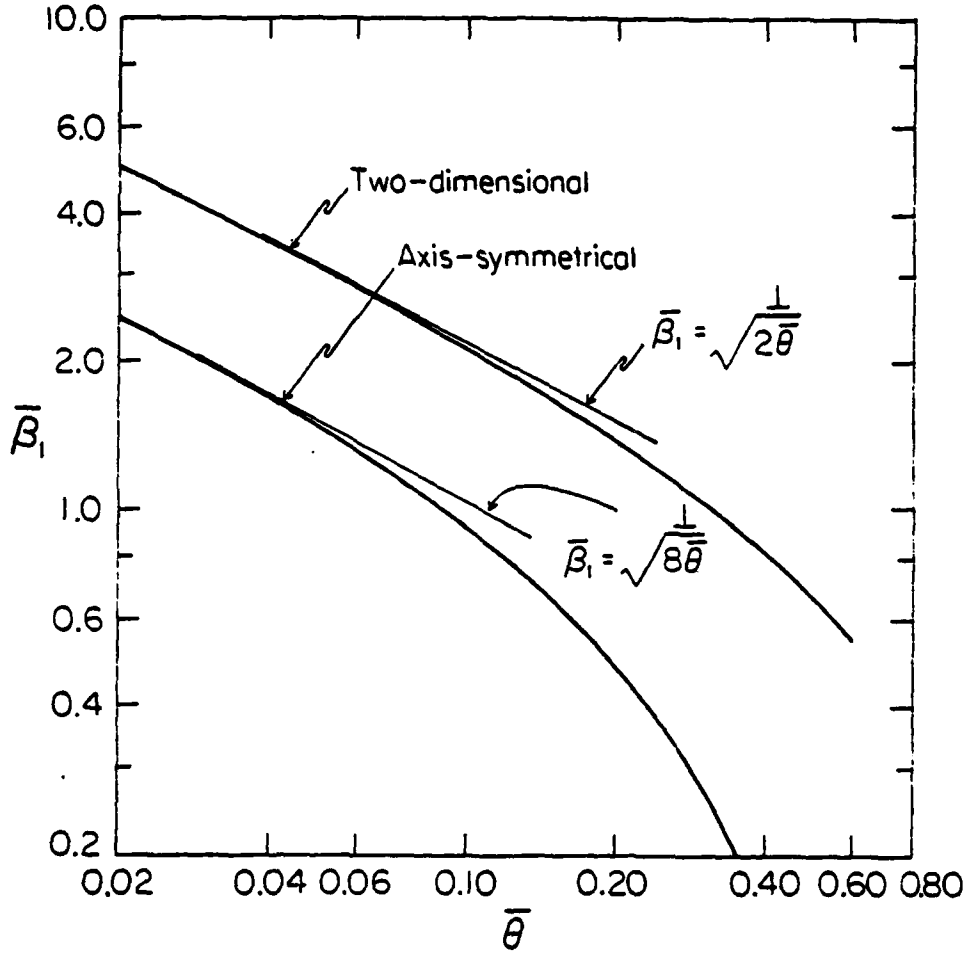

Figure IV.3. Variations of Transverse Time-parameter, $\bar{\beta}_1$, vs. $\bar{\theta}$ (Fiber-Composite)

IV.4 THE AXIAL DIFFUSION EQUATIONS

Re-expressing Equations IV-7 and IV-8 in terms of $\bar{T}_1$ and $\bar{T}_2$, one has the following equations:

$$\frac{\partial \bar{T}_1}{\partial \bar{\theta}} = \frac{\partial^2 \bar{T}_1}{\partial \bar{X}^2} + \frac{4H\bar{\beta}_1^2}{[1 - H(1 + R)]} [\bar{T}_2 - \bar{T}_1] \qquad \text{(IV-15)}$$

$$\frac{\alpha_1}{\alpha_2} \frac{\partial \bar{T}_2}{\partial \bar{\theta}} = \frac{\partial^2 \bar{T}_2}{\partial \bar{X}^2} - \frac{(k_1/k_2)}{[(b/a)^2 - 1]} \frac{4H\bar{\beta}_1^2}{[1 - H(1 + R)]} [\bar{T}_2 - \bar{T}_1] \qquad \text{(IV-16)}$$

where R, the thermal capacity ratio, is defined by

$$R = \frac{\rho_1 c_1}{\rho_2 c_2 [(b/a)^2 - 1]} \qquad \text{(IV-17)}$$

In parallel with the developments for the planar case, let

$$L = \frac{4H\bar{\beta}_1^2}{1 - H(1 + R)} \qquad \text{(IV-18)}$$

and the axial diffusion equations can be represented by the following, which correspond to those in Section III:

$$\frac{\partial \overline{T}_1}{\partial \overline{\theta}} = \frac{\partial^2 \overline{T}_1}{\partial \overline{X}^2} + L(\overline{T}_2 - \overline{T}_1) \qquad \text{(IV-19)}$$

$$\frac{\partial \overline{T}_2}{\partial \overline{\theta}} = \left(\frac{\alpha_2}{\alpha_1}\right)\frac{\partial^2 \overline{T}_2}{\partial \overline{X}^2} - RL(\overline{T}_2 - \overline{T}_1) \qquad \text{(IV-20)}$$

The inter-region conductance L has been pre-determined through the $\overline{\beta}_1$-variation obtained from Equation IV-14. See Appendix A for details.

Because of the close parallel developments with the case of heat flow along laminated composites, the solutions and the methods of obtaining the solutions discussed in Section III are directly applicable to the above equations for heat flow in fibrous composites. In fact, Equations IV-19 and IV-20 are identical to Equations III-19 and III-20, with the only differences in the definitions of L and R (See Equations III-17 and IV-17 for R and Equations III-18 and IV-18 for L). Numerical results obtained for composites with uni-directional fibers are discussed in Section V.

V. PERFORMANCE EVALUATION OF THE METHODS

In order to bring out the essential features of the methods developed in this report as well as significant thermal characteristics in composite bodies, a number of calculations were performed. For simplicity of presentation and discussions, only composites with uni-directional cylindrical fibers were analyzed as conclusions and observations deduced for this configuration are equally applicable to laminated composites.

Principally, two sets of physical parameters were employed in the demonstrative calculations presented in this section. They were

Specification (A) -

$$k_1/k_2 = 5, \quad \alpha_1/\alpha_2 = 3.33, \quad b/a = 2, \quad R = 0.5, \quad L_\infty = 0.75$$

Specification (B) -

$$k_1/k_2 = 0.2, \quad \alpha_1/\alpha_2 = 0.2, \quad b/a = 1.3, \quad R = 1.45, \quad L_\infty = 10.5$$

In Specification (A), the fiber (material 1) is taken to be more conductive than the matrix, indicative of applications to carbon/epoxy composites. The diffusivity ratio of $\alpha_2/\alpha_1 = 0.3$ is to allow for a

temperature cross-over in the interior of the composites in the case of constant heat flux. In Specification (B), reflective of metal matrix applications, the fiber conductivity is less than that of the matrix material. In both sets of the specifications, the thermal capacity ratio, R, is in the order of unity, i.e., the two media have comparable thermal intertias. The asymptotic values of the transverse conductance L are noted to be L_∞ = 0.75 and 10.5 respectively for each material. It turns out through the following analysis that L_∞ is a significant quantity in composite heat transfer analysis.

Analyses were chiefly focused on the case of constant surface heat flux, as it affords a more severe test on the ability of the analytical means, and more importantly it represents a practical need in thermal protection technology.

V.1 THE ANALYTICAL METHODS

For each specification of the physical parameters, several methods of analysis were employed in order to compare their results, and thereby to assess their relative merits from the viewpoints of accuracy and time-consumption. The methods of analysis range from the most elementary approach to full exact solutions of the complete diffusion equations, and consist of the following:

(i) Separate independent solutions which assume that the fibers and the matrix material have no transverse conduction. In this situation, each region behaves

independently of the other, with the temperature responses the same as that for a semi-infinite domain ($x \geq 0$) and given by the following expressions:

$$T_1 = \text{erfc}(x/2\sqrt{\alpha_1 \theta}) \qquad \text{(V-1)}$$

$$T_2 = \text{erfc}(x/2\sqrt{\alpha_2 \theta}) \qquad \text{(V-2)}$$

for the constant surface-temperature boundary condition, and

$$T_1 = 2(Q/k_1)\sqrt{\alpha_1 \theta}\ \ \text{ierfc}(x/2\sqrt{\alpha_1 \theta}) \qquad \text{(V-3)}$$

$$T_2 = 2(Q/k_2)\sqrt{\alpha_2 \theta}\ \ \text{ierfc}(x/2\sqrt{\alpha_2 \theta}) \qquad \text{(V-4)}$$

for the constant heat flux boundary condition.

(ii) Double heat-balance integral-method, which, as discussed in Section III, treats the inter-region transverse heat conduction on an integrated basis. The axial variation of the temperature is characterized by a single parameter γ_1 or γ_2 in each material region. Variations of the characteristic time-dependent parameters are determined by integrating (with respect to θ) Equations III-27 and III-28.

(iii) Semi-finite difference solution which is, in essence, a finite-difference scheme for solving the axial diffusion

Equations III-19 and III-20. Since the transverse temperature variation is expressed through the time-dependent parameter $\bar{\beta}_1$, the use of a finite-difference to account for the axial temperature variation leads to the terminology: semi-finite-difference solution.

(iv) Exact solution or finite-difference solution of the complete diffusion Equations III-8 and III-9, while it is not the objective of the present investigation to analyze heat conduction in composites by exact solutions, results thus obtained serve as a reference by which other methods can be judged. Because of time and storage requirements, only a limited number of computations were made, as will be noted later in this presentation.

V.2 TEMPERATURE DISTRIBUTIONS FOR SPECIFICATION (A)

For the parametric values in Specification (A), the transverse time-dependent parameter $\bar{\beta}_1$ is first determined by the numerical method outlined in Appendix A. Figure V.1 shows how $\bar{\beta}_1$ varies with $\bar{\theta}$, the non-dimensional time. Also included in Figure V.1 is the transverse conductance L, which reaches an asymptotical value of $L_\infty = 0.75$ at large values of θ. In practice, however, the transverse conductance remains virtually unchanged at $L = 0.75$ for $\bar{\theta} = 1$ or larger. Physically, it means that the transverse temperature profiles in the fiber and

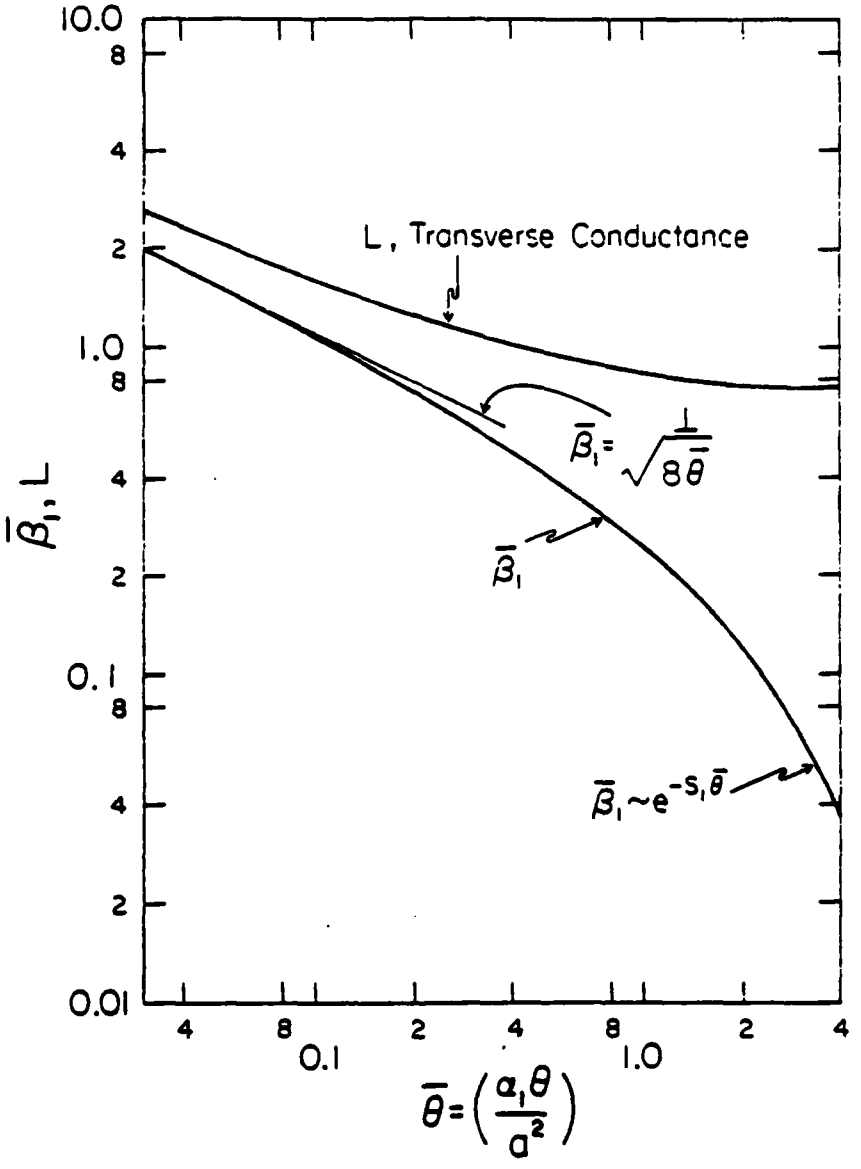

Figure V.1. Variations of Transverse Time-Parameter β_1 and Transverse Conductance L with Time $\bar{\theta}$, Fiber-Composite. ($k_1/k_2 = 5$, $\alpha_2/\alpha_1 = 3$, $b/a = 2$)

matrix regions have reached their equilibrium shapes, though their magnitudes may still be changing owing to axial diffusion. The time for such an event is characterized by $\bar{\theta} = 1$ or the physical time $\theta = a^2/\alpha_1$, the time necessary to diffuse over a distance of the fiber or tow radius of a.

As the boundary condition of constant surface heat flux (equal in both regions) represents a more practical situation encountered, the surface temperature-rise with time, as heating proceeds, is a significant measure of the material capability to diffuse the heat flux away from the surface. Figure V.2 shows the matrix surface and fiber surface temperature variations according to different methods of analysis.

First, Method (i), which assumes that each region responds independently of its adjoint neighbor, produces the extremes of the temperature-time curves. For the physical parameters specified, the matrix surface has a faster-rising temperature than does the fiber surface. Since any mutual conduction in the transverse direction tends to bring these two temperature responses closer together, the calculated temperature responses by Method (i) therefore constitute an outer-limit envelope.

Conversely, the use of full diffusion equations, i.e., Method (iv), produces the exact solutions to the problem, where the inter-region conduction is exactly accounted for, constitutes an inner-limit envelope. Between the inner limit and the outer envelope, there exists a fairly wide latitude in which the results of the other

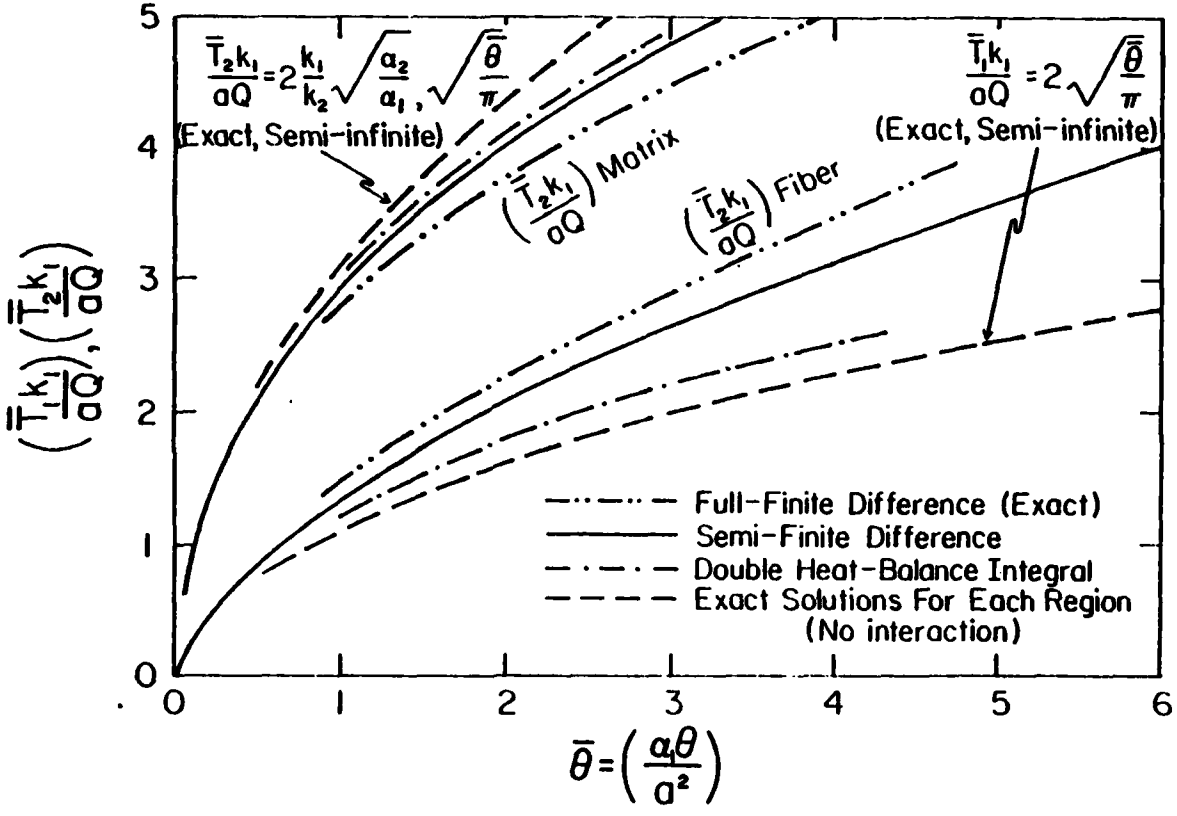

Figure V.2. Comparative Surface Temperature Responses to Impulsive Heat Flux, Fiber Composite ($k_1/k_2 = 5$, $\alpha_2/\alpha_1 = 0.3$, $b/a = 2$)

two methods lie. Results based on the semi-finite-difference method, i.e. Method (iii), are located quite closely to the exact-solution results, whereas results based on the double heat-balance integral-method, i.e. Method (iv), are closer to those from Method (i) than other methods.

Proximity to the exact-solution results appears to lend credence to Method (iii), i.e., the semi-finite-difference solution of Equations III-19 and III-20, although further improvements are desirable and indeed possible through a better representation of the transverse temperature distributions in both regions. Inability of Method (ii) to include transverse conduction effect is attributable to its one-parameter (γ_1 or γ_2) representation of the axial temperature profile, and to the fact that inter-region conduction is only accounted for on an integrated basis. Along the axial direction, cross-over of the temperature profiles, as will be discussed next, indicates reversal of transverse heat conduction from one direction to another. Thus, in summing up the local transverse conduction distribution, mutual cancellation causes significant errors in the final results of analysis.

To further examine the relative merits of the various methods of analysis, the temperature variations along the axial direction are shown in Figure V.3. Only the results from Methods (iii) and (iv) are presented and the closeness between the results from Method (iii) to those from the exact method gives another indication of the usefulness of the semi-finite difference method. Figure V.3 also

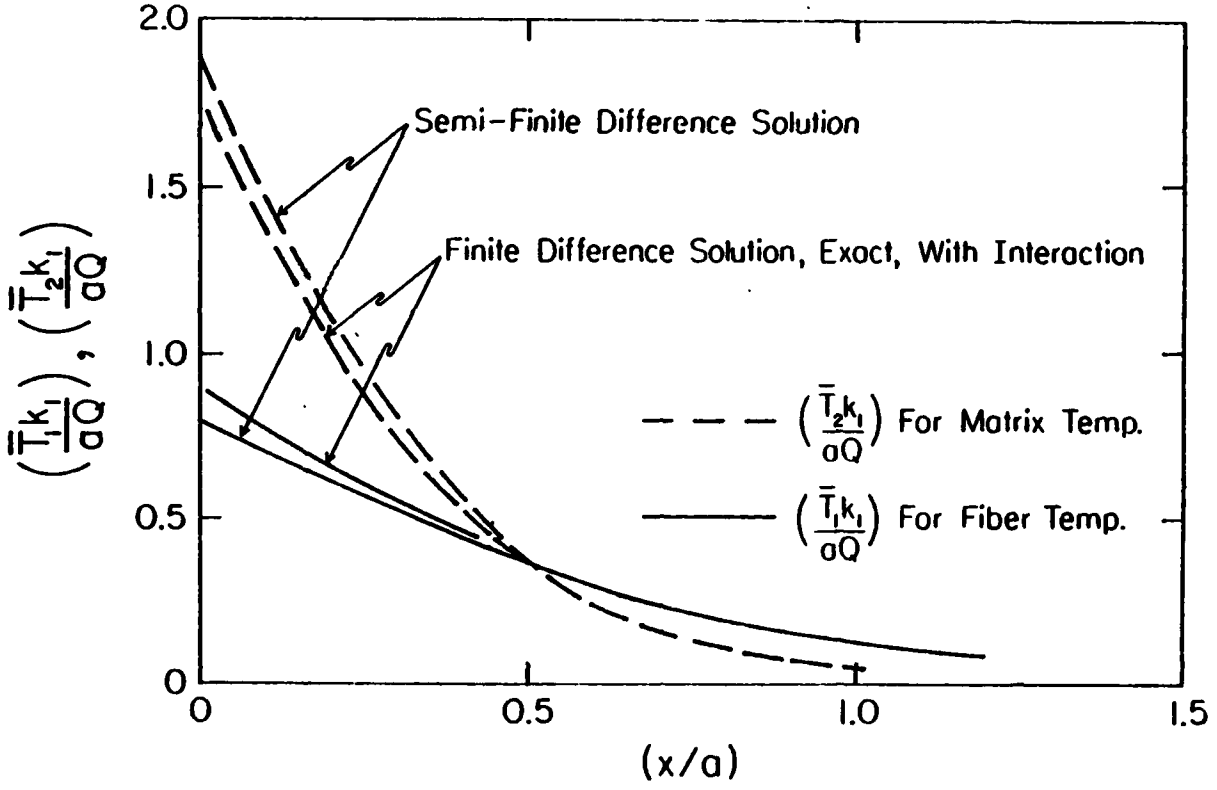

Figure V.3. Temperature Distributions of Fiber and Matrix at $\bar{\theta} = 0.4$ for Constant Heat Flux ($k_1/k_2 = 5$, $\alpha_2/\alpha_1 = 0.3$, $b/a = 2$)

reveals as to why the double heat-balance integral-method fails to yield reasonable results because of the cross-over of the temperature profiles. For larger times, $\bar{\theta} = 1$ and $\bar{\theta} = 2$, the temperature profiles from Method (iii) are compared with those from Method (i), i.e., the no-interaction solutions in Figures V.4 and V.5. A significant observation based on the data in these three figures is the location of the cross-over point at $(x/a) \simeq 1.0$; its precise position varies not appreciably from the value of $(x/a) = 1$ in these figures. The near constancy of the cross-over location is in consonance with the diffusion of $\bar{\theta} = 1$ or a diffusion distance of one fiber radius a. Hence in problems involving constant surface heat flux, large temperature disparity in two different media in thermal contact is expected to be confined to a surface layer of no more than a few fiber or tow radii deep. Temperature differentiation outside this layer is substantially reduced by mutual transverse conduction. From a thermal stress viewpoint, it is in this surface layer where high stress values would be found.

As a further confirmation of the semi-finite-difference approach, the case of a step-rise in surface temperature is also investigated. Figure V.6 contains a typical record of the calculated distributions and those of the exact solutions. It becomes apparent that the semi-finite-difference method gives excellent agreement with the exact solutions. Comparing the results shown in Figure V.3 with those in Figure V.6, it should be noted that the larger difference exists in Figure V.3 than in Figure V.6. For the former, the boundary condition is that of constant heat flux; for the latter it is that of a constant

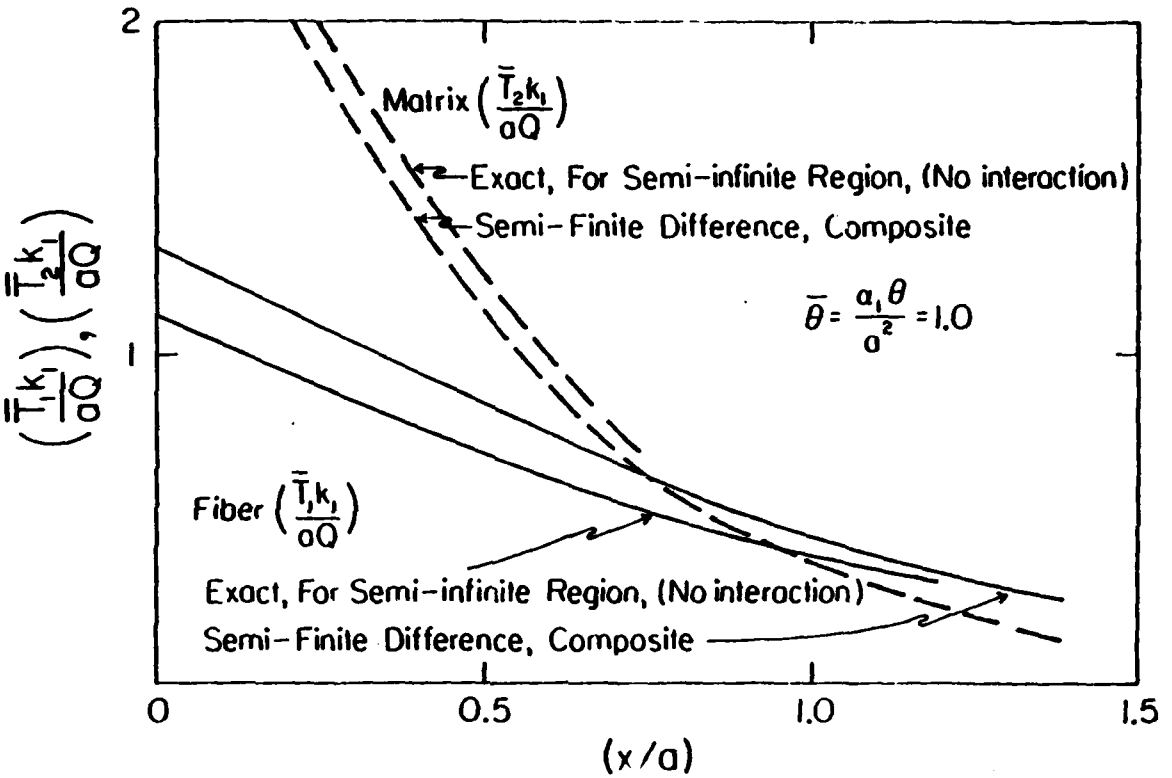

Figure V.4. Comparison of Axial Temperature Distributions in Fiber and Matrix $\bar{\theta} = 1$. For Constant Heat Flux ($k_1/k_2 = 5$, $\alpha_2/\alpha_1 = 0.3$, $b/a = 2$).

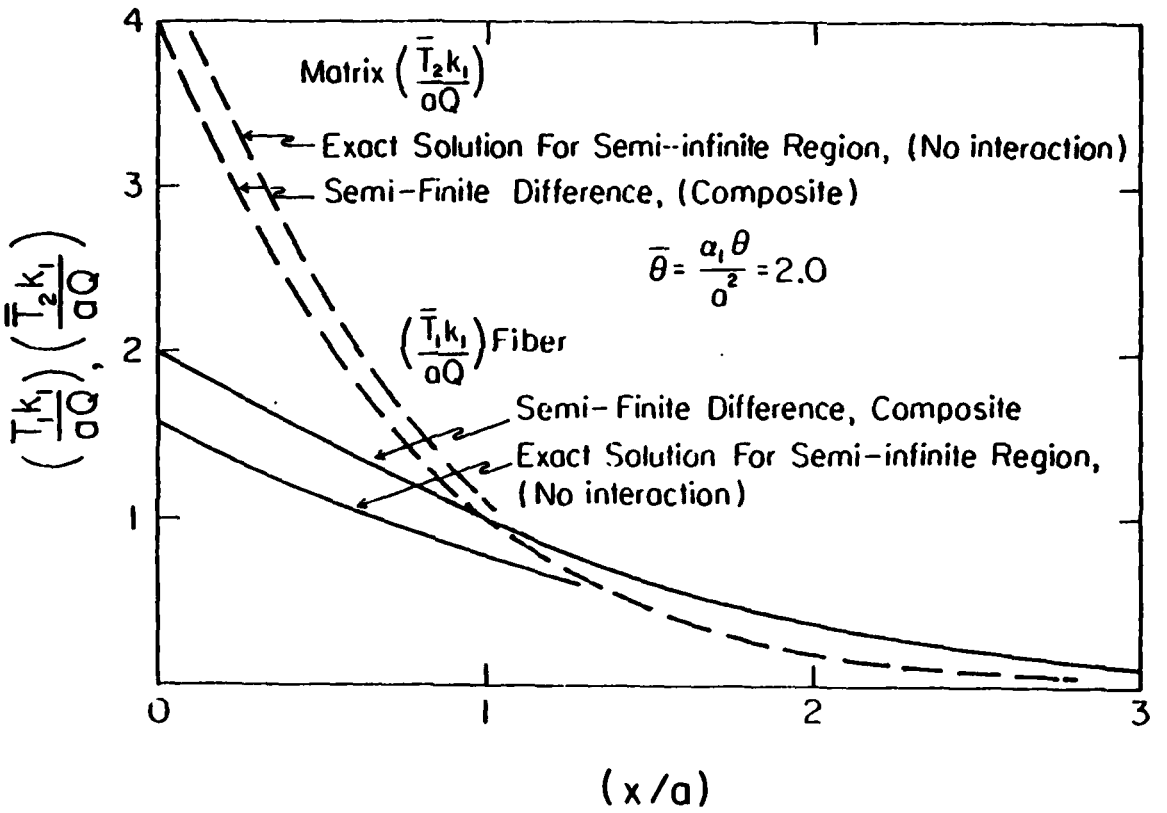

Figure V.5. Comparison of Axial L Temperature Distribution of Fiber and Matrix at $\bar{\theta} = 2$ for Constant Heat Flux. ($R_1/R_2 = 5$, $\alpha_2/\alpha_1 = 0.3$, $b/a = 2$).

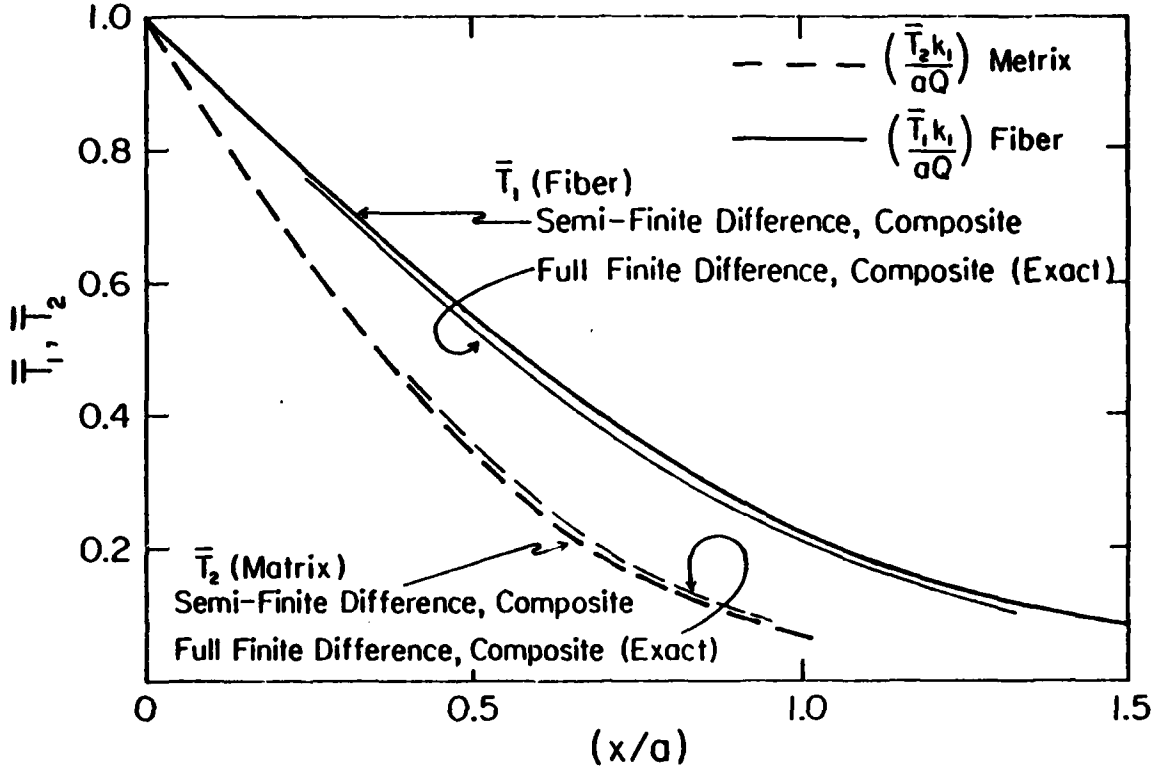

Figure V.6. Axial Temperature Distributions of Fiber and Matrix at $\bar{\theta} = 0.4$ for Constant Surface Temperature. ($k_1/k_2 = 5$, $\alpha_2/\alpha_1 = 0.3$, $b/a = 2$)

surface temperature. It becomes understandable if it is re-called that the solution to a constant surface-heat boundary condition can be synthesized to consist of an infinite number of small surface temperature rises. In this fashion, the minute errors as shown in Figure V.6 are accumulated to the error exhibited in Figure V.3.

V.3 TEMPERATURE DISTRIBUTIONS FOR SPECIFICATION (B)

The physical parameters in Specification (B) were selected with metal matrixes in mind in which the fibers have lower conductivities than the matrix materials. A thermal diffusivity ratio of 0.2 was assumed so that cross-over of the axial temperature profiles for the two media would occur for constant surface-heating boundary condition. As a large number of composites in aero-space applications have a volume ratio of 0.6, a diameter ratio of 1.3 was considered for (b/a) which yields a volume ratio of 0.69. The preceding parameters result in a heat capacity ratio of R = 1.45 which assures that the axial temperature distributions are substantially modified from their independent (no transverse conduction) solutions.

Shown in Figure V.7 are the variations of the transverse time-parameter $\overline{\beta}_1$ and the transverse conductance L. The latter reaches an asymptotic value of L_∞ = 10.4, a value substantially higher than that for Specification (A), but in a much shorter time. Consequently, the surface temperature variations (with time) for the two materials show

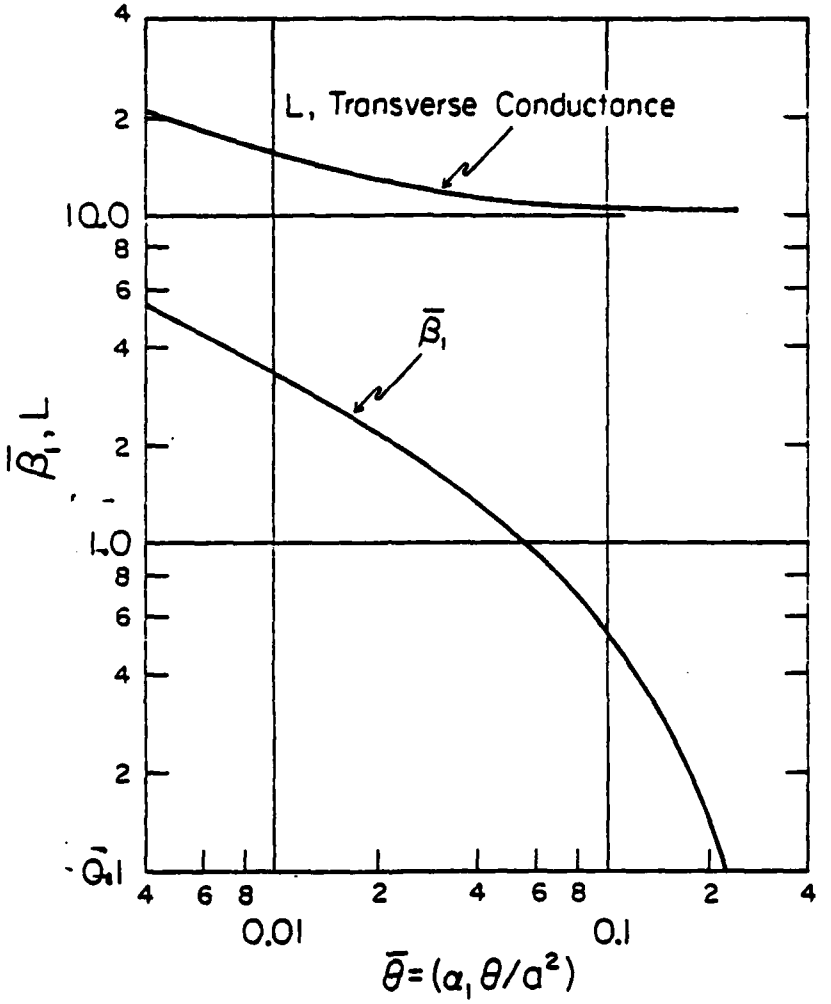

Figure V.7. Variations of Transverse Time-Parameter $\bar{\beta}_1$ and Transverse Conductance L with Time $\bar{\theta}$, Fiber-Composite. (k_1/k_2 = 0.2, α_1/α_2 = 0.2, b/a = 1.3).

a much narrower spread as indicated by the data in Figure V.8 than those based on Specification (A), wherein the asymptotic transverse conductance L_∞ is only 0.75. Hence, it can be concluded that a governing parameter is the transverse conductance L. A larger value of L signifies effective transverse conductance which brings about equalization of the temperature in the two regions in a much shorter distance from the end where heating starts. Consistent with the arguments set forth in the preceding are the temperature responses shown in Figure V.9 where the cross-over of the temperatures in the two regions takes place near $(x/a) \simeq 0.5$ to 0.6 for $\overline{\theta} = 0.4$ and 1.0 respectively. Beyond the cross-over point, the axial temperature distributions are nearly parallel to each other with a much smaller differential between those shown in Figures V.3 and V.4, for which a distinguishing feature is a lower transverse conductance of $L_\infty = 0.75$.

Examination of the formula which defines the asymptotic value of the transverse conductance, L_∞, indicates that the make-up parameter is the fiber/matrix conductivity ratio modified by the volume ratio of the two materials. As a further indication of the significant role of this ratio, the transverse temperature distributions across the fiber and the matrix regions are shown in Fgiure V.10 based on the data for Specification (B). The fiber has much less conduction than the matrix ($k_1/k_2 = 0.2$), resulting in a wider temperature variance in the fiber region than in the matrix region. At $(x/a) = 0$, i.e., on the heating surface, and for $\overline{\theta} = 0.4$, the fiber cross-section has a very substantial temperature variation from the center to its

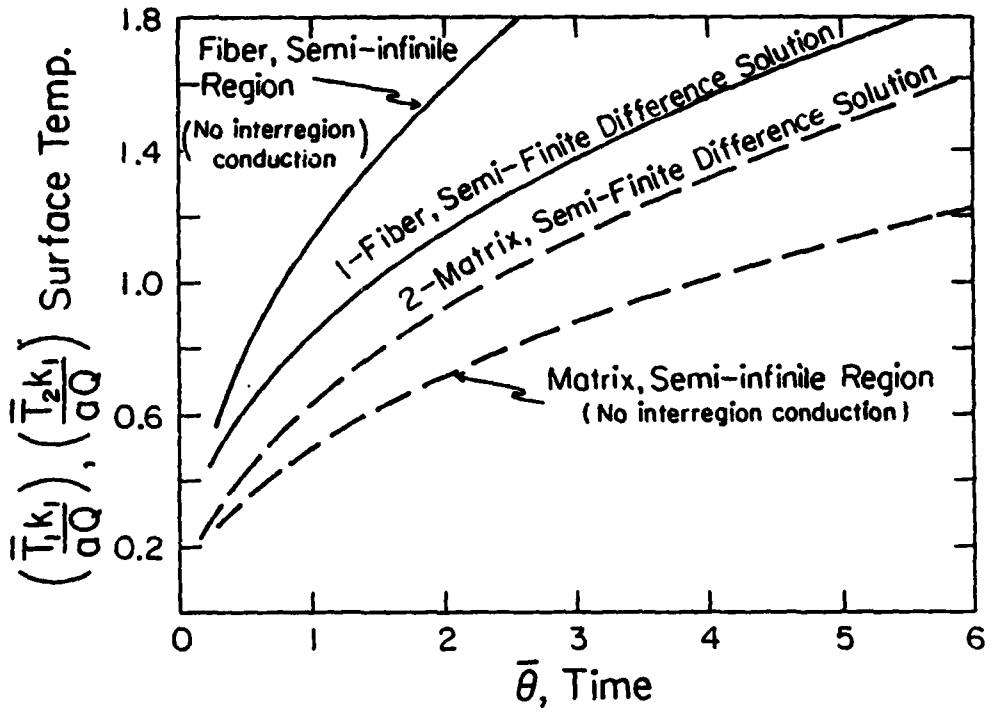

Figure V.8. Surface Temperature Responses to Impulsive Heat Flux, Fiber-Composite (k_1/k_2 = 0.2, α_1/α_2 = 0.2, b/a = 1.3).

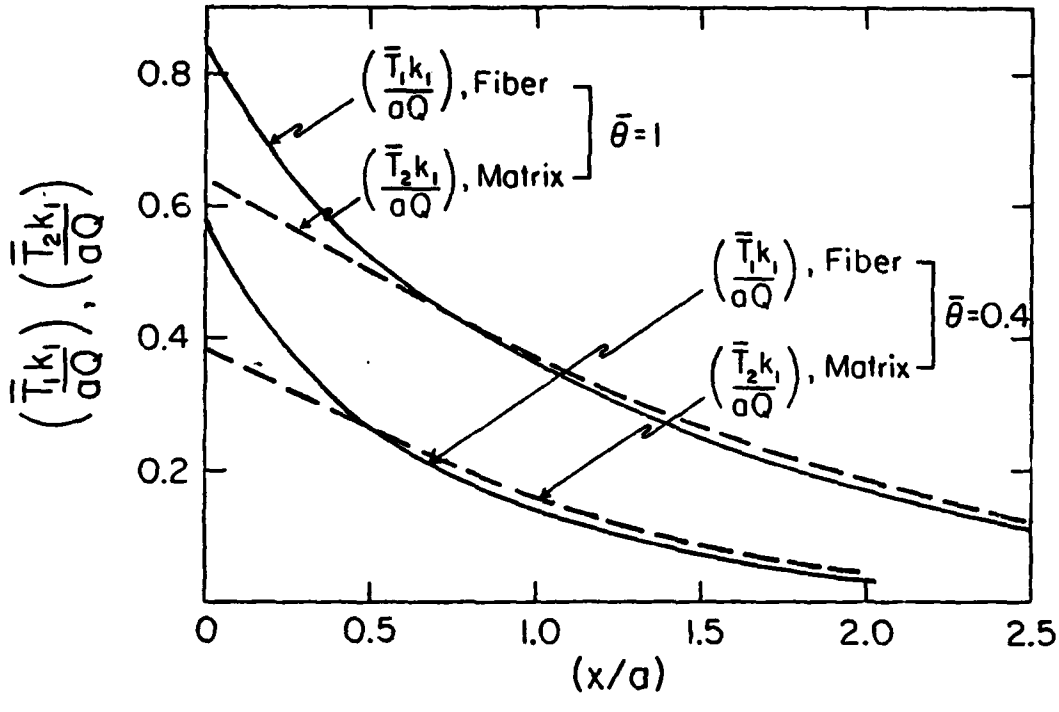

Figure V.9. Axial Temperature Distribution of Fiber and Matrix at $\theta = 0.4$ and $\bar{\theta} = 1$ for Constant Heat Flux. ($k_1/k_2 = 0.2$, $\alpha_1/\alpha_2 = 0.2$, $b/a = 1.3$, $R = 1.45$).

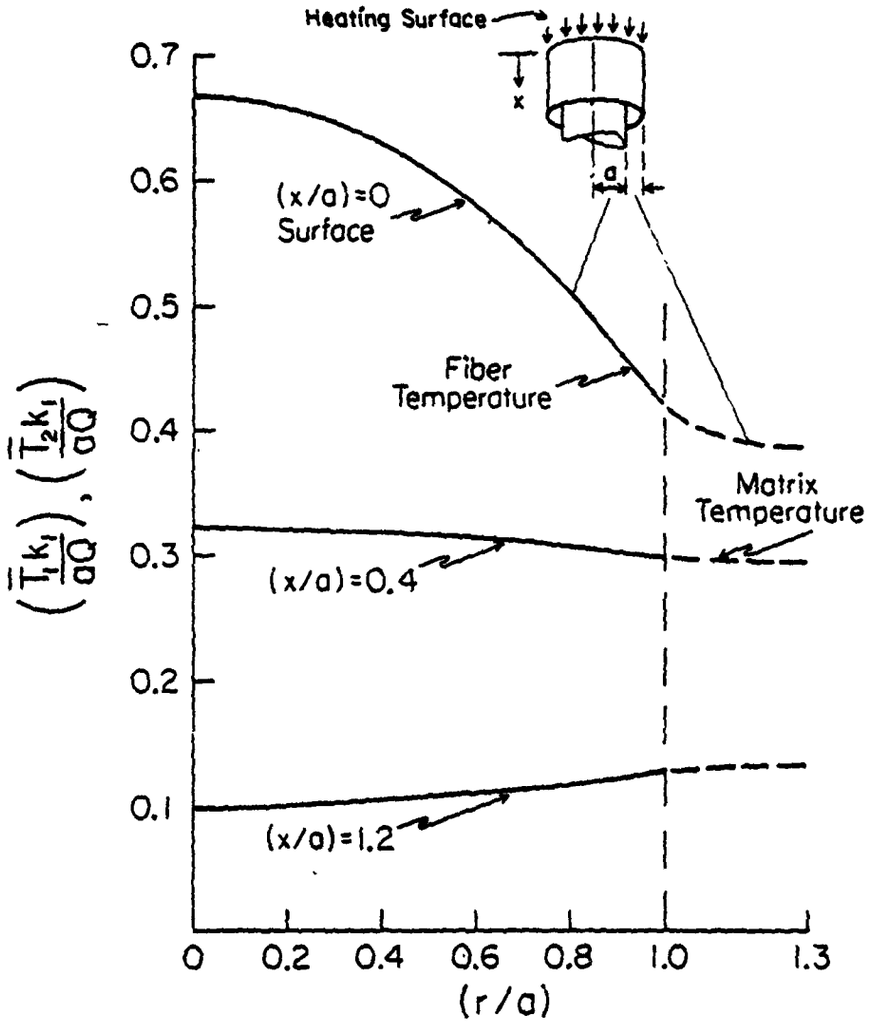

Figure V.10. Transverse Temperature Distributions at Various Axial Positions, $\bar{\theta} = 0.4$ for Impulsive Surface Heat Flux, ($k_1/k_2 = 0.2$, $\alpha_1/\alpha_2 = 0.2$, $b/a = 1.3$).

edge. High Transverse conductance rapidly equalizes the two regions at $(x/a) > 0.4$, even though relative variations in these two materials still exist in the interior of the composite.

V.4 LARGE THERMAL CAPACITY RATIOS

As an additional exploration of relevant parameters in transient flow in composites, several computer runs were made to decipher the effect of the thermal capacity ratio R on the temperature distribution. A typical record is illustrated in Figure V.11 for $k_1/k_2 = 10$. A thermal diffusivity ratio (α_1/α_2) of unity is taken. These parameters and others resulted in a thermal capacity ratio of R = 14.5, which expresses the condition that the fiber has a much larger thermal inertia characterized by the product of (ρc) and the fiber-volume than that of the matrix region. The fact that $\alpha_1/\alpha_2 = 1$ precludes a temperature cross-over, as is evident in preceding combinations. The temperature distribution curves for $\overline{\theta} = 0.4$ and $\overline{\theta} = 1$ show a practical merge of the temperatures in the two different media at $(x/a) = 1$, which would become the cross-over point if $\alpha_1 < \alpha_2$.

As a reference for discussion, the fiber temperature distribution for $\overline{\theta} = 0.4$ by Method (i) is also included in Figure V.11. This reference distribution is of course based on the condition that the fiber-region temperature is independent of that in the matrix region. The corresponding temperature distribution for the matrix region is not present in Figure V.11, for it would be situated above the scope of the

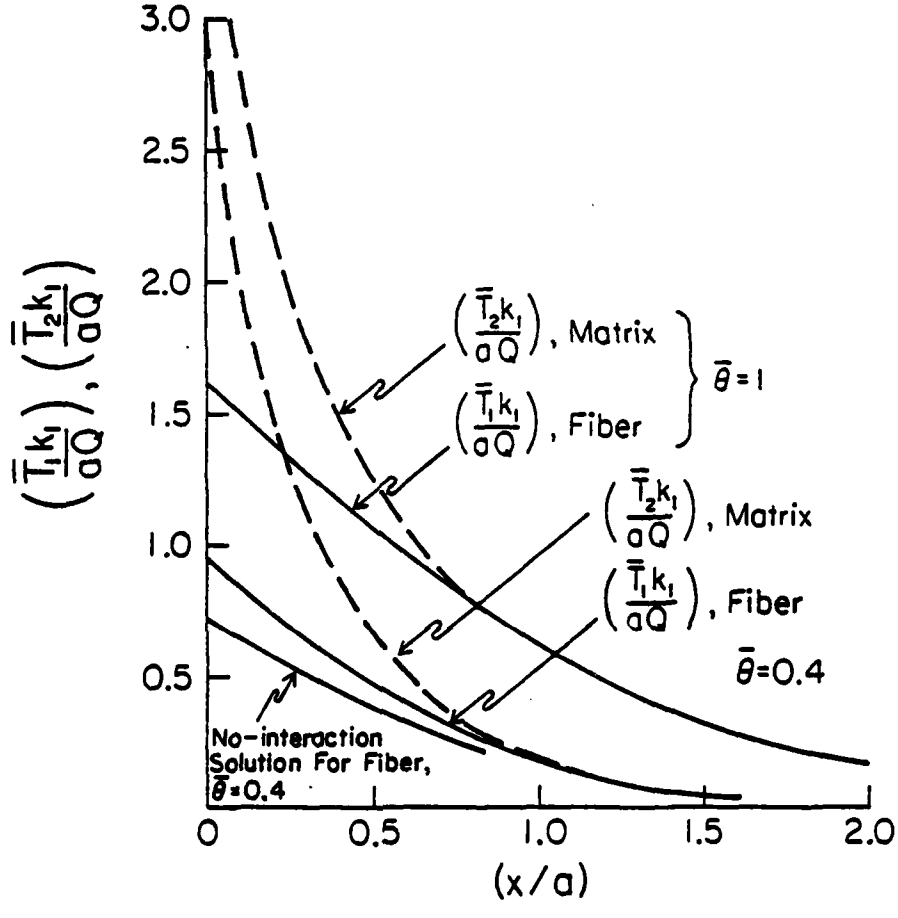

Figure V.11. Temperature Distributions of Fiber and Matrix at $\bar{\theta} = 0.4$ and $\bar{\theta} = 1$ for Impulsive Heat Flux.

ordinate. The influence of the thermal capacity R is accordingly apparent: because of a mutual thermal interaction by virtue of transverse conduction,the fiber temperature is raised and the matrix temperature is lowered from their respective reference distribution curves for zero transverse condition. The deviation from the reference curve is of course more for the matrix region than for the fiber region, but not in exact proportion to the value R. Axial diffusion modifies, to some extent, the transverse shifts of the temperature distribution curves.

VI. CONCLUSIONS

The analyses presented in this report consider the transient heat flow along uni-directional fibers of composites or in the stacking plane of laminated composites. Because of the preponderance of physical and geometrical parameters involved, exact solutions by analytical means are usually not feasible, except for special cases of very much simplified geometries. Furthermore, sorting through a large number of exact numerical solutions in order to extract important parametric groups is prohibitively difficult.

Here in this report, a method has been developed which identifies the parametric combinations and is relatively amenable to numerical solutions. The method has two components: (1) the transverse (to fibers or laminations) temperature profiles are treated by means of two transverse time-dependent parameters which are solutions to heat-balance differential equations, one for each region. (2) The resulting equations for the axial temperature variations in the two materials are much simplified, and their numerical solutions are greatly simpler to implement than the full diffusion equations. The axial diffusion equations contain the governing parametrical groups which are identified to play important roles in the temperature responses to a heat flux at an exposed surface. They are (i) a transverse conductance parameter and (ii) the thermal capacity ratio of the two different materials

comprising a composite. The first governs, for the case of constant surface heating, the extent of a depth near the heating surface wherein a large temperature differential exists between the two materials. The second parameter influences the relative temperature modifications from their respective reference values, the latter being those based on the idealized one-domain no-interaction solution for each region separately.

AD-A122 926 TRANSIENT HEAT FLOW ALONG UNI-DIRECTIONAL FIBERS IN COMPOSITES(U) OHIO STATE UNIV RESEARCH FOUNDATION COLUMBUS L S HAN DEC 82 AFWAL-TR-82-3061 AFOSR-78-3640 2/2

UNCLASSIFIED F/G 11/4 NL

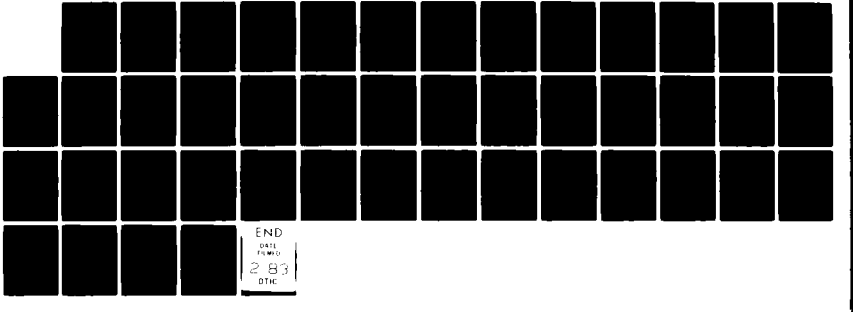

END

DATE FILMED

2 83

DTIC

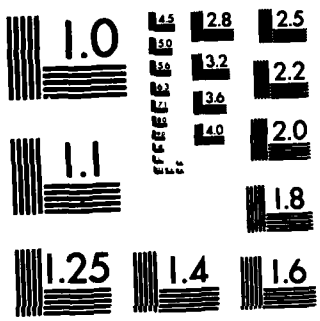

MICROCOPY RESOLUTION TEST CHART
NATIONAL BUREAU OF STANDARDS-1963-A

APPENDIX A

NUMERICAL SOLUTION OF THE TRANSVERSE HEAT-BALANCE-INTEGRAL EQUATION

APPENDIX A. NUMERICAL SOLUTION OF THE TRANSVERSE HEAT-BALANCE-INTEGRAL EQUATION.

In the transverse direction, thermal diffusion time - time required to even out the transverse temperature variations in the two different media in contact - is much smaller than thermal diffusion time in the axial direction. This is due primarily to a difference in the dimensions along these directions in a composite material with thin laminations or fibers of micro-dimensions compared to the length. The transverse heat flow can therefore be treated independently of the overall heat conduction process and this is accomplished by a heat-balance integral method as outlined in Sections II and III for two-dimensional heat flow (laminated composites) and uni-directional fibrous-composites.

The resulting Equations III-8 and IV-9 are grouped together as:

$$\frac{d}{d\bar{\theta}}\left[\frac{\lambda}{1+\lambda}\frac{\tanh\bar{\beta}_1}{\bar{\beta}_1}\right] = \frac{n\lambda}{1+\lambda}\bar{\beta}_1\tanh\bar{\beta}_1 \qquad \text{(A-1)}$$

$$\lambda = \sqrt{\frac{k_2\rho_2c_2}{k_1\rho_1c_1}}\,\frac{\tanh\bar{\beta}_1\left[\left(\frac{b}{a}\right)^r - 1\right]\sqrt{\alpha_1/\alpha_2}}{\tanh\bar{\beta}_1} \qquad \text{(A-2)}$$

where the factors n and r assume the following values:

$n = 4,$	$r = 2$	for	axis-symmetrical heat flow.
$n = 1,$	$r = 1$	for	two-dimensional heat flow.

The boundary condition on $\bar{\beta}_1$ is $\bar{\beta}_1 \to \infty$, as $\bar{\theta} \to 0$.

As $\bar{\theta} \to 0$, $\bar{\beta}_1 \to \infty$, the parameter λ assumes the following value:

$$\lambda = \lambda_0 = \sqrt{(k_2\rho_2c_2)/(k_1\rho_1c_1)} \tag{A-3}$$

Equation A-1 is reduced, for small vaues of $\bar{\theta}$, to:

$$\frac{d}{d\bar{\theta}}\left(\frac{1}{\bar{\beta}_1}\right) = n\bar{\beta}_1 \tag{A-4}$$

for which the solution is clearly:

$$\bar{\beta}_1 = \frac{1}{\sqrt{2n\bar{\theta}}} \tag{A-5}$$

For large values of $\bar{\theta}$, the asymptotic solution A-5 breaks down and the full Equation A-1 must be used to obtain the solution. To do this, the equation is cast in the form:

$$d\bar{\theta} = \frac{(1+\lambda)}{n\lambda\bar{\beta}_1 \tanh\bar{\beta}_1} d\left[\frac{\lambda}{1+\lambda}\frac{\tanh\bar{\beta}_1}{\bar{\beta}_1}\right]$$

Or, in terms of the parameter H defined in Section III, the above equation is put as:

$$d\bar{\theta} = Vd(H) \tag{A-6}$$

The parameters V and H are reproduced here for clarity:

$$V = \frac{1+\lambda}{n\lambda\bar{\beta}_1 \tanh\bar{\beta}_1} \tag{A-7}$$

$$H = \frac{\lambda}{1+\lambda}\frac{\tanh\bar{\beta}_1}{\bar{\beta}_1} \tag{A-8}$$

By assigning a series of values to $\bar{\beta}_1$, starting from a large value and down to, say, $\bar{\beta}_1 = 0.1$, a curve in the H-V plane is obtained.

From Equation A-6, it is clear that $\bar{\theta}$ represents the area underneath the H-V curve as sketched in Figure A.1.

As $\bar{\beta}_1 \to 0$, H and λ approach their limits as follows:

$$\lambda = \lambda_\infty = (\rho_2 c_2/\rho_1 c_1)[(b/a)^r - 1] = 1/R \tag{A-9}$$

$$H = H_\infty = \lambda_\infty/(1+\lambda_\infty)$$

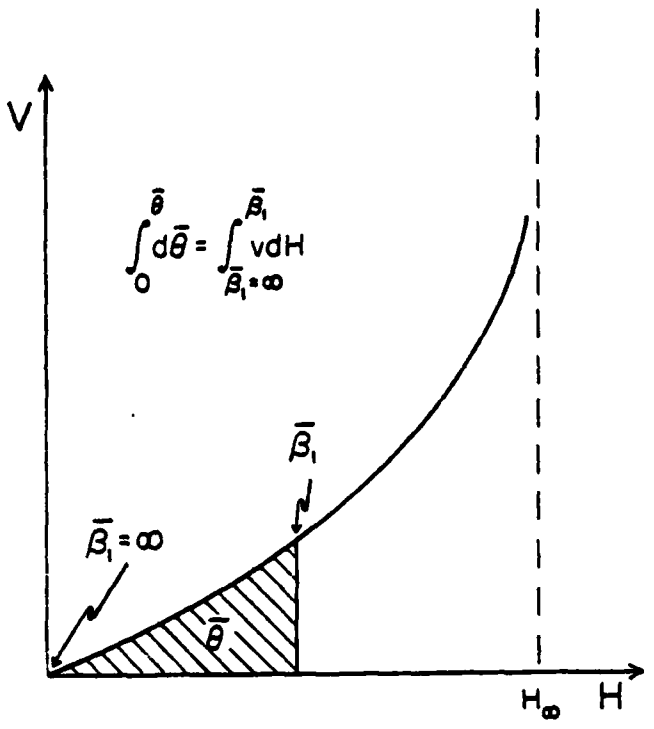

Figure A.1. Graphic Illustration of Integrating Equation A-1.

Hence for very large values of $\bar{\theta}$, the numerical procedure is inherently inaccurate as $H \to H_\infty$ and V increases without limit. For this range, i.e., $\bar{\beta}_1 \to 0$, the parameters H and V are expressed in their asymptotic forms as:

$$H = \frac{\lambda_\infty}{1 + \lambda_\infty} \left[1 - s\bar{\beta}_1^2 + \ldots \right] \tag{A-10}$$

$$(1/V) = \frac{n\lambda_\infty}{1 + \lambda_\infty} \left[\bar{\beta}_1^2 + \ldots \right] \tag{A-11}$$

where $s = [1 + (k_1/k_2)((b/a)^r - 1)]/3[1 + 1/\lambda_\infty]$.

Substitution of these asymptotic forms into Equation A-6 yields:

$$\bar{\beta}_1^2 = g_1 \exp [- (n/s)\bar{\theta}] \tag{A-12}$$

The constant of integration g_1 can be determined by fitting the above equation to the last point of $\bar{\theta}_1 \sim \bar{\beta}_1$ curve obtained from the numerical procedure.

APPENDIX B

FINITE-DIFFERENCE SOLUTION OF THE AXIAL HEAT DIFFUSION EQUATIONS

APPENDIX B. FINITE-DIFFERENCE SOLUTION OF THE AXIAL HEAT DIFFUSION EQUATIONS.

With temperature variations in the transverse direction approximated by two form functions with two transverse time-parameters $\bar{\beta}_1$ and $\bar{\beta}_2$, the reduced heat conduction equations in the axial direction are those of Equations III-19 and III-20 for the two-dimensional case (laminated composites) and Equations IV-19 and IV-20 for the axis-symmetrical case (fibrous composites). These two sets of equations can be jointly represented by the following:

$$\frac{\partial \bar{T}_1}{\partial \bar{\theta}} = \frac{o^2 \bar{T}_1}{\partial \bar{x}^2} + L(\bar{T}_2 - \bar{T}_1) \tag{B-1}$$

$$\frac{\partial \bar{T}_2}{\partial \bar{\theta}} = \frac{\alpha_2}{\alpha_1} \frac{o^2 \bar{T}_2}{\partial \bar{x}^2} - RL(\bar{T}_2 - \bar{T}_1) \tag{B-2}$$

The interaction parameter L denotes the inter-region heat conduction effects based on their respective average temperatures over each cross-section and is defined by:

$$L = \frac{nH\bar{\beta}_1^2}{1 - H(1 + R)} \tag{B-3}$$

The thermal capacity ratio R is defined by:

$$R = (\rho_1 c_1/\rho_2 c_2)/[(b/a)^j - 1] \qquad \text{(B-4)}$$

Equation B-3 for L and Equation B-4 for R cover the two cases through the coefficients n and j in these two equations. They have the following numerical values:

(i) For two-dimensional heat flow (laminated composites)

$$n = 1, \qquad j = 1$$

(ii) For axis-symmetrical heat flow (fiber-composites)

$$n = 4, \qquad j = 2$$

ASYMPTOTIC ANALYSIS FOR SMALL TIMES, $\bar{\theta} \to 0$

It is of interest to note that at very small times, the transverse conduction parameter exhibits a singularity for an impulsive type of thermal loading, either an impulsive temperature rise or an impulsive heat flux at x = 0. The analysis in Appendix A shows that $\bar{\beta}_1 \sim 1/\sqrt{\bar{\theta}}$, which is consistant with more rigorous theoretical results. As the intermediate parameters, H and λ, are defined by:

$$H = \frac{\lambda}{1+\lambda}\,[\tanh\bar{\beta}_1]/\bar{\beta}_1 \qquad \text{(B-5)}$$

$$\lambda = \sqrt{\frac{k_2\rho_2 c_2}{k_1\rho_1 c_1}}\;\frac{\tanh\bar{\beta}_1\left[\left(\frac{b}{a}\right)^j - 1\right]\sqrt{\frac{\alpha_1}{\alpha_2}}}{\tanh\bar{\beta}_1} \qquad \text{(B-6)}$$

the small-time variation of L can be deteremined as follows:

$$\bar{\theta} \to 0, \qquad \bar{\beta}_1 = 1/\sqrt{2n\bar{\theta}}, \qquad \lambda \to \lambda_0$$

where $\lambda_0 = \sqrt{(k_2\rho_2 c_2)/(k_1\rho_1 c_1)} = (k_2/k_1)\sqrt{\alpha_1/\alpha_2}$. Hence, the intermediate parameter H becomes:

$$H \to [\lambda_0/(1+\lambda_0)]\sqrt{2n\bar{\theta}}$$

and the inter-region conduction parameter L is of the form:

$$L \to \left(\frac{\lambda_0}{1+\lambda_0}\sqrt{\frac{n}{2\bar{\theta}}}\right) \qquad \text{(B-7)}$$

ASYMPTOTIC ANALYSIS FOR LARGE TIMES, $\bar{\theta} \to \infty$

As the inter-region conduction proceeds, the interaction parameter L reaches a "steady-state" value, while the temperature profile in each

region establishes itself in a steady-state pattern in the transverse direction. Under this condition, $\bar{\theta} \to \infty$, $\bar{\beta}_1 \to 0$, and the intermediate parameters H and λ are analyzed below:

$$\bar{\theta}_1 \to \infty, \qquad \bar{\beta}_1^2 = g_1 \exp[-(n/s)\bar{\theta}] \tag{B-8}$$

which is obtained in Appendix A [Equation A-12], where:

$$s = \{1 + (k_1/k_2)[(b/a)^j - 1]\}/3[1 + R] \tag{B-9}$$

Other relevant parameters can be expressed as:

$$\lambda = \lambda_\infty \left\{ 1 - \frac{\bar{\beta}_1^2}{3} \left[\frac{\alpha_1}{\alpha_2} \left(\left(\frac{b}{a}\right)^j - 1 \right)^2 - 1 \right] + \ldots \right\} \tag{B-10}$$

$$H = H_\infty [1 - s\bar{\beta}_1^2 + \ldots] \tag{B-11}$$

$$L = L_\infty [1 - s\bar{\beta}_1^2 + \ldots] \tag{B-12}$$

$$\lambda\infty = (1/R) = [\rho_2 c_2/\rho_1 c_1][(b/a)^j - 1] \tag{B-13}$$

$$H_\infty = 1/(1 + R) \tag{B-14}$$

$$L_\infty = 3n/\{1 + (k_1/k_2)[(b/a)^j - 1]\} \tag{B-15}$$

The last quantity L_∞ is of particular interest, for it represents the "steady-state" inter-region conductance, which was analyzed by Maewal, Gurtman and Hegemeir (J. of Heat Transfer, vol. 100, p.128, Feb. 1978). In their analysis, the variation of L at small $\bar{\theta}$-values was not taken into account for a first-order estimate. Figure B-1 illustrates the variation of L as a function of time $\bar{\theta}$ for a combination of $k_2/k_1 = 10$, $\alpha_2/\alpha_1 = 3$ and $b/a = 2$ and for the axis-symmetrical case (fibrous composites).

FINITE-DIFFERENCE EQUATIONS

Let the $\bar{x}$-axis be divided into a number of equi-distant nodes; starting from $\bar{x} = 0$, these nodes are numbered by an index $j = 1, 2, 3, \ldots$. The distance between two adjacent nodes is $\Delta\bar{x}$ and the time advance is represented by $\Delta\bar{\theta}$. A three-point explicit marching (in time) scheme is used, with the following diagram illustrating a three-point cluster of nodes $(j - 1)$, j, and $(j + 1)$:

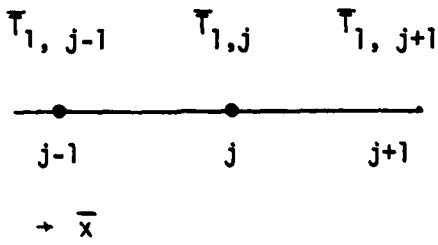

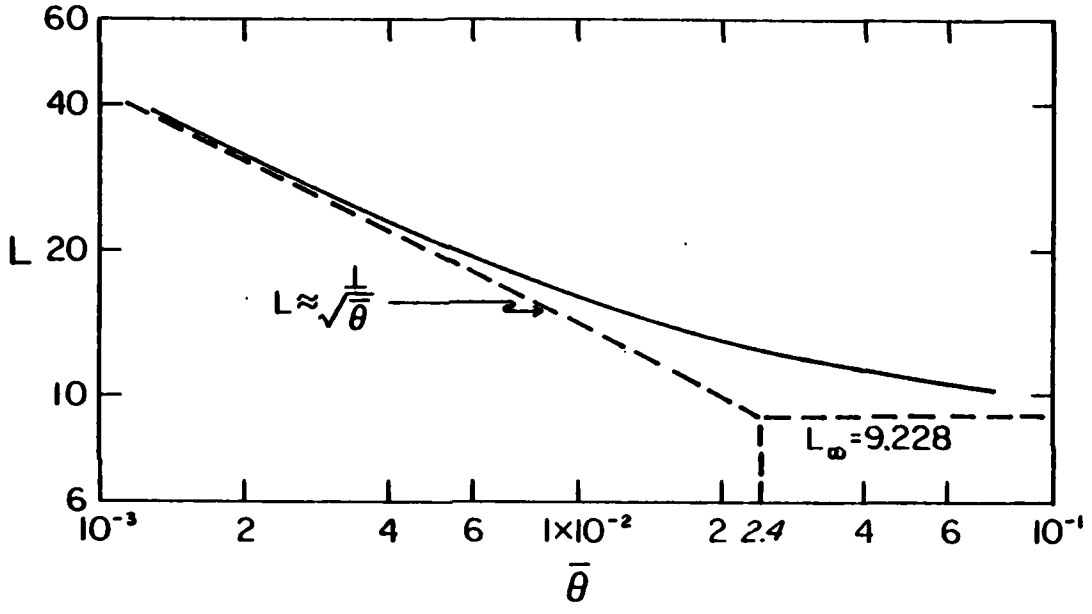

Figure B.1. Variation of Transverse Conduction Parameter, L, with Time $\bar{\theta}$. ($k_2/k_1 = 10$, $\alpha_2/\alpha_1 = 3$, $b/a = 2$, axis symmetry)

Equation B-1 is reduced to:

$$\frac{\bar{T}'_{1,j} - T_{1,j}}{\Delta\bar{\theta}} = \frac{1}{(\Delta\bar{X})^2}\left[\bar{T}_{1,\,j+1} + \bar{T}_{1,\,j-1} - 2\bar{T}_{1,j}\right]$$

$$+ L[\bar{T}_{2,j} - \bar{T}_{1,j}] \qquad \text{(B-16)}$$

where the unprimed quantities are current values and the primed quantity $\bar{T}'_{1,j}$ is the future temperature. Casting B-16 as:

$$\bar{T}'_{1,j} = \frac{\Delta\bar{\theta}}{(\Delta\bar{X})^2}\left[\bar{T}_{1,\,j+1} + \bar{T}_{1,\,j-1}\right] + \bar{T}_{1,j}\left[1 - 2\frac{\Delta\bar{\theta}}{(\Delta\bar{X}^2)} - L\Delta\bar{\theta}\right]$$

$$+ L\Delta\bar{\theta}[\bar{T}_{2,j}] \qquad \text{(B-17)}$$

A similar procedure on Equation B-2 yields:

$$\bar{T}'_{2,j} = \frac{\alpha_2}{\alpha_1}\frac{\Delta\bar{\theta}}{(\Delta\bar{X})^2}\left[\bar{T}_{2,\,j+1} + \bar{T}_{2,\,j-1}\right]$$

$$+ \bar{T}_{2,j}\left[1 - 2\frac{\Delta\bar{\theta}}{(\Delta\bar{X})^2}\left(\frac{\alpha_2}{\alpha_1}\right) - RL\Delta\bar{\theta}\right] + RL\Delta\bar{\theta}[\bar{T}_{1,j}] \qquad \text{(B-18)}$$

Stability of the explicit marching scheme is assured by chosing $\Delta\bar{\theta}$ such that the coefficients of $T_{1,j}$ and $T_{2,j}$ on the right-hand sides of B-17 and B-18 remain positive.

APPENDIX C

EXACT SOLUTIONS FOR LAMINATED COMPOSITES OF FINITE LENGTH

APPENDIX C. EXACT SOLUTIONS FOR LAMINATED COMPOSITES OF FINITE LENGTH

C-I. DEVELOPMENT OF SOLUTIONS

Consider the configuration depicted in Figure C.1 which shows a repeating section of a laminated composite stacked by alternate layers of two different materials 1, and 2. The extent in the x-direction is finite.

At x = L, where heating occurs, two boundary conditions are considered: one is for an impulsive temperature rise from an initial temperature distribution - taken to be zero; the other is for an impulsive heat input - equal in both regions. These two boundary conditions are the basic ingredients with which solutions of more practical interest can be built by a superposition principle. Designating these two boundary conditions as the T-case and Q-case respectively, these can be expressed by:

$$\text{T-case} \qquad T_1 = 1,\ T_2 = 1, \quad \text{at } X = L \tag{C-1}$$

$$\text{Q-case} \qquad k_{1x}\partial T_1/\partial X = k_{2x}\partial T_2/\partial X = Q, \quad \text{at } X = L \tag{C-2}$$

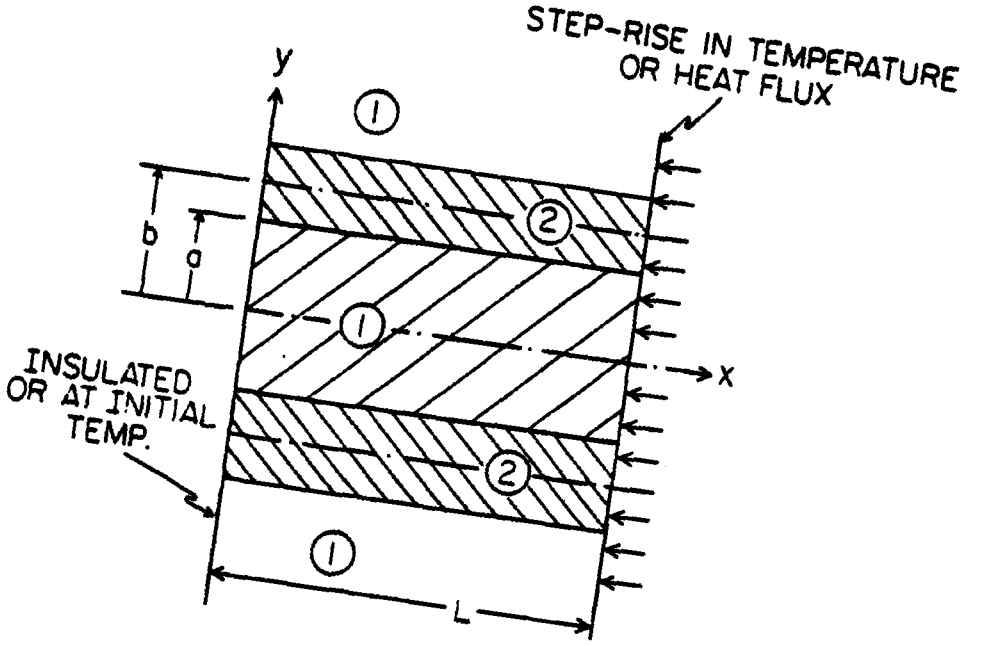

Figure C.1. Schematic of a Laminated Composite of Finite Length.

At the other end $x = 0$, two types of boundary conditions are considered; they are:

$$\text{(i)}\quad T_1 = T_2 = 0 \qquad \text{at } x = 0 \quad \text{(Fixed Temperature)} \tag{C-3a}$$

$$\text{(ii)}\quad \partial T_1/\partial x = \partial T_2/\partial x = 0 \quad \text{at } x = 0 \text{ (Insulated)} \tag{C-3b}$$

The initial condition is of course a uniform (taken to be zero) temperature distribution. At different y-positions, the following conditions apply:

$$\partial T_1/\partial y = \partial T_2/\partial y = 0 \qquad \text{at } y = 0, \text{ and } y = b \tag{C-4}$$

$$T_1 = T_2 \text{ and } k_{1y}\partial T_1/\partial y = k_{2y}\partial T_2/\partial y \quad \text{at } y = a \tag{C-5}$$

All told therefore, four cases are treated in this report; they are:

Case (1): $T_1(y,L,\theta) = 1, \quad T_2(y,L,\theta) = 1$ (C-6a)

$$\partial T_1(y,0,\theta)/\partial x = 0, \quad \partial T_2(y,0,\theta)/\partial x = 0 \tag{C-6b}$$

Case (2): $T_1(y,L,\theta) = 1, \quad T_2(y,L,\theta) = 1$ (C-7a)

$$T_1(y,0,\theta) = 0, \quad T_2(y,0,\theta) = 0 \tag{C-7b}$$

Case (3): $k_{1x}[\partial T_1(y,\theta)/\partial x] = Q, \quad k_{2x}[\partial T_2(y,\theta)/\partial x] = Q$ (C-8a)

$$\partial T_1(y,0,\theta)/\partial x = 0, \qquad \partial T_2(y,0,\theta)/\partial x = 0 \tag{C-8b}$$

Case (4): $k_{1x}[\partial T_1(y,L,\theta)/\partial x] = Q, \quad k_{2x}[\partial T_2(y,L,\theta)/\partial x] = Q$ (C-9a)

$$T_1(y,0,\theta) = 0, \qquad T_2(y,0,\theta) = 0 \tag{C-9b}$$

All these cases are subjected to the interface boundary conditions specified by Equations C-4 and C-5 plus the initial conditions of:

$$T_1(y,x,0) = T_2(y,x,0) = 0 \tag{C-10}$$

Before proceding with the individual cases, the governing differential equations are first non-dimensionalized. Let the characteristic length be L and the characteristic time be (L^2/α_{1x}), the following definitions and variable transformations are obtained:

$$\left.\begin{aligned} &\alpha_{1x} = k_{1x}/(\rho C)_1, \quad \alpha_{2x} = k_{2x}/(\rho C)_2, \quad \bar{y} = y/L, \ \bar{x} = x/L \\ &\lambda_1 = (k_{1y}/k_{1x}), \quad \lambda_2 = (k_{2y}/k_{2x}) \end{aligned}\right\} \tag{C-11}$$

$$\bar{\theta} = (\alpha_{1x}\theta/L^2), \quad \bar{a} = a/L, \quad \bar{b} = b/L$$

The non-dimensional equations governing the temperature distributions T_1, and T_2 for these two regions are:

$$(\partial^2 T_1/\partial \bar{x}^2) + \lambda_1(\partial^2 T_1/\partial \bar{y}^2) = (\partial T_1/\partial \bar{\theta}) \qquad \text{(C-12)}$$

$$(\partial^2 T_2/\partial \bar{x}^2) + \lambda_2(\partial^2 T_2/\partial \bar{y}^2) = (\alpha_1/\alpha_2)(\partial T_2/\partial \bar{\theta}) \qquad \text{(C-13)}$$

CASE (1). Constant Temperature Rise at One End and Insulated Surface at the Other

The complete solutions for T_1 and T_2 can be immediately written as:

$$T_1 = 1 + \sum_{j=1,2..}^{\infty} \sum_{m=1,3,5..}^{\infty} E_{mj}\, e^{-\beta_{mj}^2 \bar{\theta}} [\cos(m\pi\bar{x}/2)]\bar{Y}_1(\bar{y}) \qquad \text{(C-14)}$$

$$T_2 = 1 + \sum_{j=1,2,..}^{\infty} \sum_{m=1,3,5..}^{\infty} E_{mj}\, e^{-\beta_{mj}^2 \bar{\theta}} [\cos(m\pi\bar{x}/2)]\bar{Y}_2(\bar{y}) \qquad \text{(C-15)}$$

where the appearance of $\cos(m\pi\bar{x}/2)$ with m as any odd integer is necessitated by Equations C-6a and C-6b at $\bar{x} = 1$ and $\bar{x} = 0$ respectively.

Direct substitutions of Equations C-14 and C-15 into Equations C-12 and C-13 give the following which govern $\bar{Y}_1$ and $\bar{Y}_2$.

$$\lambda_1 \bar{Y}_1'' + [\beta^2 - (m\pi/2)^2]\bar{Y}_1 = 0 \qquad \text{(C-16)}$$

$$\lambda_2 \bar{Y}_2'' + [(\alpha_1/\alpha_2)\beta^2 - (m\pi/2)^2]\bar{Y}_2 = 0 \qquad \text{(C-17)}$$

Equations C-16 and C-17 are subjected to the boundary conditions $(d\bar{Y}_1/d\bar{y}) = 0$ at $\bar{y} = 0$, $(d\bar{Y}_2/d\bar{y}) = 0$ at $\bar{y} = \bar{b}$. Furthermore, because of the forms of Equations C-14 and C-15 and the equal heat flux requirement, two additional boundary conditions appear:

$$\bar{Y}_1(\bar{a}) = \bar{Y}_2(\bar{a}) \qquad \text{(C-18)}$$

$$k_{1y}\bar{Y}_1'(a) = k_{2y}\bar{Y}_2'(a) \qquad \text{(C-19)}$$

The fact that there are two homogeneous differential equations to comply with four homogeneous boundary conditions results in an eigen-value problem for β. Specifically, one first solves for $\bar{Y}_1$ and $\bar{Y}_2$ from Equations (C-16) and (C-17) giving the following.

$$\bar{Y}_{1,mj} = \frac{\cos\bar{y}\sqrt{[\beta_{mj}^2 - (m\pi/2)^2]/\lambda_1}}{\cos\bar{a}\sqrt{[\beta_{mj}^2 - (m\pi/2)^2]/\lambda_1}} \qquad \text{(C-20a)}$$

$$\bar{Y}_{2,mj} = \frac{\cos(\bar{y} - \bar{b})\sqrt{[(\alpha_1/\alpha_2)\beta_{mj}^2 - (m\pi/2)^2]/\lambda_2}}{\cos(\bar{a} - \bar{b})\sqrt{[(\alpha_1/\alpha_2)\beta_m^2 - (m\pi/2)^2]/\lambda_2}} \qquad \text{(C-20b)}$$

The forms of Equations C-20a and C-20b have been adjusted to comply with all boundary conditions at various y's, except at the interface

$\bar{y} = \bar{a}$ which supplies the eigen-value equation for β_{mj}. Performing the operation indicated in Equation C-5 gives rise to:

$$\sqrt{[\beta_{mj}^2 - (m\pi/2)^2]/\lambda_1}\ \tan\bar{a}\sqrt{[\beta_{mj}^2 - (m\pi/2)^2]/\lambda_1}$$

$$+ (k_{2y}/k_{1y})\sqrt{[(\alpha_1/\alpha_2)\beta_{mj}^2 - (m\pi/2)^2]/\lambda_2}\ \tan(\bar{b} - \bar{a})\sqrt{[(\alpha_1/\alpha_2)\beta_{mj}^2 - (m\pi/2)^2]/\lambda_2} = 0 \qquad \text{(C-21)}$$

Equation C-21 determines, for each odd integer of m, a series of β_{mj}-values, with the running indexes j = 1, 2, 3, ... to denote successive roots. The eigen-value Equation C-21 is discussed in Section C-IV.

For each eigen-value β_{mj} thus obtained, an eigen function $\bar{Y}_{mj}$ is therefore defined for the entire domain from $\bar{y} = 0$ to $\bar{y} = \bar{b}$. The function $\bar{Y}_{mj}$ is, however, defined by two sub-region functions $\bar{Y}_{1,mj}$, for $\bar{y} = 0$ to $\bar{a}$, given by Equation C-19, and $\bar{Y}_{2,mj}$, for $\bar{y} = \bar{a}$ to $\bar{b}$, given by Equation C-20. The eigen-functions $\bar{Y}_{mj}$ and $\bar{Y}_{mi}(i \neq j)$ are orthogonal to each other in the entire domain with respect to a weight function w_f as follows:

$$\begin{aligned} &\bar{y} = 0 \text{ to } \bar{a} && w_f = 1 \\ &\bar{y} = \bar{a} \text{ to } \bar{b} && w_f = (\rho c)_2/(\rho c)_1 \end{aligned} \qquad \text{(C-22)}$$

The development of the preceding steps is contained in Section C-II and parallels with the original derivation by Title and Johnson (ASME paper No. 65-WA/HT-52).

To determine the coefficients E_{mj}, Equations C-14 and C-15 are combined to read:

$$T = 1 + \sum_{j=1,2,..}^{\infty} \sum_{m=1,3,5,..}^{\infty} E_{mj} e^{-\beta_{mj}^2 \bar{\theta}} \cos(m\pi\bar{x}/2)\bar{Y}_{mj} \qquad \text{(C-23)}$$

At $\bar{\theta} = 0$, the initial temperature distribution is zero everywhere. Setting T to zero on the left and $\bar{\theta}$ to zero on the right, Equation C-23 is multiplied by $[\cos(n\pi\bar{x}/2)\bar{Y}_{ni}w_f]$ and is integrated from $\bar{y} = 0$ to $\bar{y} = \bar{b}$ and from $\bar{x} = 0$ to $\bar{x} = 1$. The resulting expression for E_{mj} turns out to be (see Section C-III for details):

$$E_{mj} = -(8/m\pi)(-1)^{\frac{m-1}{2}} \left[f_t/(f_a + f_t)\right] \qquad \text{(C-24)}$$

CASE (2). Constant Temperature Rise at One End and Initial Temperature Maintained at the Other End

The solutions in regions (1) and (2) can be shown as follows:

$$T_1 = \bar{x} + \sum_{n=1,2,3,..}^{\infty} \sum_{j=1,2,..}^{\infty} F_{nj} e^{-\beta_{nj}^2 \bar{\theta}} \sin(n\pi\bar{x}) \bar{Y}_1 \qquad \text{(C-25)}$$

$$T_2 = \bar{x} + \sum_{n=1,2,3,..}^{\infty} \sum_{j=1,2,..}^{\infty} F_{nj} e^{-\beta_{nj}^2 \bar{\theta}} \sin(n\pi\bar{x}) \bar{Y}_2 \qquad \text{(C-26)}$$

$$\bar{Y}_1 = \bar{Y}_{1,nj} = \frac{\cos\bar{y}\sqrt{[\beta_{nj}^2 - (n\pi)^2]/\lambda_1}}{\cos\bar{a}\sqrt{[\beta_{nj}^2 - (n\pi)^2]/\lambda_1}} \qquad \text{(C-27)}$$

for $\bar{y} = 0$ to $\bar{a}$, and

$$\bar{Y}_2 = \bar{Y}_{2,nj} = \frac{\cos(\bar{y} - \bar{b})\sqrt{[(\alpha_1/\alpha_2)\beta_{nj}^2 - (n\pi)^2]/\lambda_2}}{\cos(\bar{a} - \bar{b})\sqrt{[(\alpha_1/\alpha_2)\beta_{nj}^2 - (n\pi)^2]/\lambda_2}} \qquad \text{(C-28)}$$

for $\bar{y} = \bar{a}$ to $\bar{b}$.

Equality of the interface temperatures at $\bar{y} = \bar{a}$ is assured by the forms of Equations C-27 and C-28 and that the same coefficient F_{nj} appears in Equations C-25 and C-26. The condition of equal heat flux on both sides of the interface yields an eigen-equation for β_{nj}:

$$\sqrt{[\beta_{nj}^2 - (n\pi)^2]/\lambda_1}\ \tan\bar{a}\sqrt{[\beta_{nj}^2 - (n\pi)^2]/\lambda_1}$$

$$+ (k_{2y}/k_{1y})\sqrt{[(\alpha_1/\alpha_2)\beta_{nj}^2 - (n\pi)^2]/\lambda_2}\ \tan(\bar{b} - \bar{a})\sqrt{[(\alpha_1/\alpha_2)\beta_{nj}^2 - (n\pi)^2]/\lambda_2} = 0$$

$$(n = 1, 2, 3, \ldots) \qquad \text{(C-29)}$$

Equation C-29 serves to determine, for each integer n, a series of β_{nj}-values for j = 1, 2, 3, ... to denote the successive roots.

The coefficients F_{nj} are given, following the same procedure as for E_{mj}, by:

$$F_{nj} = (4/n\pi)(-1)^n[f_t/(f_a + f_t)] \qquad \text{(C-30)}$$

where f_a and f_t are given by Equations C-59 and C-60, in which m is replaced by n(= 1, 2, 3, ...) and $p = \pi^2$, instead of $P = (\pi/2)^2$ shown after Equation C-60.

CASE (3). Constant Heat Input at One End and Insulated at the Other

The problem of a constant heat input at one surface while the other is perfectly insulated, is of fundamental importance in assessing different rates of the surface temperature rises in the two different regions. Additionaly, the rates of heat propagation are inter-mingled with transverse conduction between the two regions. To analyze the temperature response, an equivalent thermal capacity $(\rho c)_e$ is defined on a prorata basis as:

$$(\rho c)_e = [(\rho c)_1 a + (\rho c)_2 (b - a)]/b \qquad \text{(C-31)}$$

which can be expressed in terms of the non-dimensional quantities as:

$$(\rho c)_e = [(\rho c)_1 \bar{a} + (\rho c)_2 (\bar{b} - \bar{a})]/\bar{b} \qquad \text{(C-31a)}$$

Partial Solutions. Without regard to the interfacial heat conduction, a "steady-state" temperature response for both regions can be envisioned: the temperatures will be linearly (in time) increasing. Writing the partial solutions as:

$$T_1 = [Q/(2k_{1x})][2/L] + [Q\theta/(\rho c)_e L] + \bar{Y}_1 \qquad \text{(C-32a)}$$

$$T_2 = [Q/(2k_{2x})][2/L] + [Q\theta/(\rho c)_e L] + \bar{Y}_2 \qquad \text{(C-32b)}$$

The first terms of the preceding equations are to comply with the constant heat flux Q at X = L, and the second terms indicate that both regions show a linear temperature rise (equal in both regions) in time as a consequence of the heat input.

The functions $\bar{Y}_1$ and $\bar{Y}_2$ are to satisfy their respective governing equations. Thus, by direct substitutions into Equations C-12 and C-13, the forms of Y_1 and Y_2 can be determined, and Equations C-32a and C-33b can be re-cast as:

$$\bar{T}_1 = (\bar{x}^2/2) + [(\rho c)_1/(\rho c)_e]\bar{\theta} + [(\rho c)_1/(\rho c)_e - 1](\bar{y}^2/2)/\lambda_1 \qquad \text{(C-33a)}$$

$$\bar{T}_2 = (k_{1x}/k_{2x})(\bar{x}^2/2) + [(\rho c)_1/(\rho c)_e]\bar{\theta}$$

$$+(k_{1x}/k_{2x})[(\rho c)_2/(\rho c)_e - 1][(\bar{y} - \bar{b})^2/2]/\lambda_2 \qquad \text{(C-33b)}$$

where $\bar{T}_1 = (k_{1x}T_1/QL)$ and $\bar{T}_2 = (k_{1x}T_2/QL)$. (C-34)

To each of Equations C-33a and C-33b, a constant term and a general solution of the Laplace equation can be added. The potential solutions from their respective Laplace equations are:

$$\cos(n\pi\bar{x})\ \cosh(n\pi\bar{y}/\sqrt{\lambda_1})$$

and $\cos(n\pi\bar{x})\ \cosh[n\pi(\bar{y} - \bar{b})/\sqrt{\lambda_2}]$ respectively.

The expanded versions of the partial solutions then assume the forms:

$$\bar{T}_1 = \frac{1}{2}(\bar{x}^2 - \frac{1}{3}) + \frac{1}{2\lambda_1}\left[\frac{(\rho c)_1}{(\rho c)_e} - 1\right][\bar{y}^2 - \bar{a}^2] + [(\rho c)_1/(\rho c)_e]\bar{\theta}$$

$$+ \sum_{n=1,2,3,..}^{\infty} G_{1n} \cos(n\pi\bar{x})[\cosh(n\pi\bar{y}/\sqrt{\lambda_1})/\cosh(n\pi\bar{a}/\sqrt{\lambda_1})] \qquad \text{(C-35a)}$$

$$\bar{T}_2 = (k_{1x}/k_{2x})\left\{\frac{1}{2}(\bar{x}^2 - \frac{1}{3}) + \frac{1}{2\lambda_2}\left[\frac{(\rho c)_2}{(\rho c)_e} - 1\right][(\bar{y} - \bar{b})^2 - (\bar{a} - \bar{b})^2]\right\}$$

$$+[(\rho c)_1/(\rho c)_e]\bar{\theta} + \sum_{n=1,2,3,..}^{\infty} C_{2n} \cos(n\pi x)\ \frac{\cosh[n\pi(\bar{y} - \bar{b})/\sqrt{\lambda_2}]}{\cosh[n\pi(\bar{a} - \bar{b})/\sqrt{\lambda_2}]} \qquad \text{(C-35b)}$$

The coefficients G_{1n} and G_{2n} are connected by the condition of equal heat flux at the interface $\bar{y} = \bar{a}$ through the relation:

$$G_{1n} = (k_{2y}/k_{1y})[\tan(n\pi(\bar{a} - \bar{b})/\sqrt{\lambda_2})/\tan(n\pi\bar{a}/\sqrt{\lambda_1})]G_{2n} \qquad \text{(C-36)}$$

Next, the requirement of equal temperature at $\bar{y} = \bar{a}$ is imposed. Setting $\bar{y} = \bar{a}$ in Equations C-35a and C-35b, and $\bar{T}_1 = \bar{T}_2$, there results:

$$(1/2)[1-(k_{1x}/k_{2x})][\bar{x}^2 - 1/3] + \sum_{n=1,2,..}^{\infty} (G_{1n} - G_{2n})\cos(n\pi x) = 0 \tag{C-37}$$

Through a regular Fourier series technique, the coefficients are obtained as follows:

$$G_{2n} = \frac{2[1 - (k_{1y}/k_{2y})](-1)^n}{n^2\pi^2\left[1 - (k_{1y}/k_{2y})\dfrac{\tan(n\pi(\bar{a} - \bar{b})/\sqrt{\lambda_2})}{\tan(n\pi\bar{a}/\sqrt{\lambda_1})}\right]} \tag{C-38}$$

The partial solutions representing the steady-state behaviors are now defined by Equations C-35a, C-35b, C-36 and C-38

Transient Part. Since the initial conditions of $\bar{T}_1 = \bar{T}_2 = 0$ are yet unfulfilled, transient solutions of the following forms are needed:

$$\bar{T}_1 = \sum_{n=0,1,2,..}^{\infty} \sum_{j=1,2,..}^{\infty} H_{nj} e^{-\beta_{nj}^2 \bar{\theta}} \cos(n\pi\bar{x})\bar{Y}_{1,nj} \tag{C-39a}$$

$$\bar{T}_2 = \sum_{n=0,1,2,..}^{\infty} \sum_{j=1,2,..}^{\infty} H_{nj} e^{-\beta_{nj}^2 \bar{\theta}} \cos(n\pi\bar{x})\bar{Y}_{2,nj} \tag{C-39b}$$

where,

$$\bar{Y}_{1,nj} = \frac{\cos\bar{y}\sqrt{[\beta_{nj}^2 - (n\pi)^2]/\lambda_1}}{\cos\bar{a}\sqrt{[\beta_{nj}^2 - (n\pi)^2]/\lambda_1}} \qquad \text{(C-40a)}$$

and

$$\bar{Y}_{2,nj} = \frac{\cos(\bar{y} - \bar{b})\sqrt{[(\alpha_1/\alpha_2)\beta_{nj}^2 - (n\pi)^2]/\lambda_2}}{\cos(\bar{a} - \bar{b})\sqrt{[(\alpha_1/\alpha_2)\beta_{nj}^2 - (n\pi)^2]/\lambda_2}} \qquad \text{(C-40b)}$$

Again, the forms of Equations C-39 and C-40 assure equality of temperatures $\bar{T}_1$ and $\bar{T}_2$ at $\bar{y} = \bar{a}$. The requirement of equal heat flux results in the following eigen-value equation for $\beta_{nj}(j = 1,2,..)$ for each n-value:

$$\sqrt{[\beta_{nj}^2 - (n\pi)^2]/\lambda_1}\ \tan\bar{a}\sqrt{[\beta_{nj}^2 - (n\pi)^2]/\lambda_1}$$

$$+ (k_{2y}/k_{1y})\sqrt{[(\alpha_1/\alpha_2)\beta_{nj}^2 - (n\pi)^2]/\lambda_2}\ \tan(\bar{b} - \bar{a})\sqrt{[(\alpha_1/\alpha_2)\beta_{nj}^2 - (n\pi)^2]/\lambda_2} = 0$$

(C-41)

for n = 0,1,2, ... Note that Equation C-41 is identical to Equation C-29.

The complete solutions for these two regions are therefore:

$$\bar{T}_1 = \text{Equation C-35a} + \text{Equation C-39a} \qquad \text{(C-42a)}$$

$$\bar{T}_2 = \text{Equation C-35b} + \text{Equation C-39b} \qquad \text{(C-42b)}$$

together with Equations C-36, C-38, C-40a, C-40b and Equation C-41 as auxiliary equations defining the various parameters. The coefficients H_{nj} are evaluated in Section C-III.

CASE (4). Constant Heat Flux at One End and Initial Temperature Maintained at the Other End

The temperature distributions in the two regions are expressed by:

$$\bar{T}_1 = \bar{x} + \sum_{m=1,3,5,..}^{\infty} A_m \sin(m\pi\bar{x}/2)\left[\cosh(m\pi y/2\sqrt{\lambda_1})/\cosh(m\pi\bar{a}/2\sqrt{\lambda_1})\right]$$

$$+ \sum_{m=1,3,5,..}^{\infty} \sum_{j=1,2,..}^{\infty} S_{mj} e^{-\beta_{mj}^2 \bar{\theta}} \sin(m\pi\bar{x}/2)\bar{T}_{1-mj} \qquad \text{(C-43a)}$$

$$\bar{T}_2 = (k_{1x}/k_{2x})\bar{x}$$

$$+ \sum_{m=1,3,5,..}^{\infty} B_m \sin(m\pi\bar{x}/2)[\cosh(m\pi(\bar{y} - \bar{b})/2\sqrt{\lambda_2})/\cosh(m\pi(\bar{a} - \bar{b})/2\sqrt{\lambda_2})]$$

$$+ \sum_{m=1,3,5,..}^{\infty} \sum_{j=1,2,..}^{\infty} S_{mj} e^{-\beta_{mj}^2 \bar{\theta}} \sin(m\pi\bar{x}/2)\bar{Y}_{2-mj} \qquad \text{(C-43b)}$$

The eigen-functions $\bar{Y}_{1,mj}$ and $\bar{Y}_{2,mj}$ are as follows:

$$\bar{Y}_{1-mj} = \left[\cos\bar{y}\sqrt{[\beta_{mj}^2 - (m\pi/2)^2]/\lambda_1} \Big/ \cos\bar{a}\sqrt{[\beta_{mj}^2 - (m\pi/2)^2]/\lambda_1}\right] \qquad \text{(C-44a)}$$

$$Y_{2-mj} = \text{Top/Bottom} \qquad \text{(C-44b)}$$

where Top = $\cos(\bar{y} - \bar{b})\sqrt{[(\alpha_1/\alpha_2)\beta_{mj}^2 - (m\pi/2)^2]/\lambda_2}$

and Bottom = $\cos(\bar{a} - \bar{b})\sqrt{[(\alpha_1/\alpha_2)\beta_{mj}^2 - (m\pi/2)^2]/\lambda_2}$

The eigen-values β_{mj} are defined by the roots of Equation C-21. In equations C-43a and C-43b, the coefficients A_m and B_m are obtained by temperature and heat flux equalities at $\bar{y} = \bar{a}$. Heat flux equality yields:

$$A_m = -B_m(k_{2y}/k_{1y})\sqrt{\lambda_1/\lambda_2}[\tanh(m\pi(\bar{b} - \bar{a})/2\sqrt{\lambda_2})/\tanh(m\pi\bar{a}/2\sqrt{\lambda_1})] \qquad \text{(C-45)}$$

By setting $T_1(\bar{y} = \bar{a}) = T_2(\bar{y} = \bar{a})$, there ensues from Equations C-43a and C-43b (for $\bar{x} = 0$ to 1),

$$\bar{x}\left[1 - (k_{1x}/k_{2x})\right] = \sum_{m=1,3,5,..}^{\infty} (B_m - A_m)\sin(m\pi\bar{x}/2) \qquad \text{(C-46)}$$

Since $\bar{x}$ has a Fourier expansion of,

$$\bar{x} = \sum_{m=1,3,5,..}^{\infty} [8/(m\pi)^2](-1)^{\frac{m-1}{2}} \sin(m\pi\bar{x}/2)$$

hence,

$$B_m - A_m = \left[\frac{8}{(m\pi)^2}(-1)^{\frac{m-1}{2}}\right]\left[1 - \frac{k_{1x}}{k_{2x}}\right] \qquad \text{(C-47)}$$

Equations C-45 and C-47 therefore are used to obtain A_m and B_m as follows:

$$B_m = \left[\frac{8}{(m\pi)^2}(-1)^{\frac{m-1}{2}}\right]\left[1 - \frac{k_{1x}}{k_{2x}}\right] \Bigg/ \left[1 + \left(\frac{k_{2y}}{k_{1y}}\right)\sqrt{\frac{\lambda_1}{\lambda_2}}\,\frac{\tanh(m\pi(b - a)/2\sqrt{\lambda_2})}{\tanh(m\pi a/2\sqrt{\lambda_1})}\right]$$

(C-48)

Equations C-45 and C-48 therefore fix the coefficients A_m and B_m. The double Fourier coefficients S_{mj} in Equations C-43a and C-43b are derived in Section C-II.

C-II. SEGMENTAL ORTHOGONALITY OF $\bar{Y}_{mj}$

The function $\bar{Y}_{mj}$ is defined by the following expressions and is governed by two differential equations in two sub-regions.

$$\bar{Y}_{mj} = \bar{Y}_{1,mj} = \frac{\cos\bar{y}\sqrt{[\beta_{mj}^2 - pm^2]/\lambda_1}}{\cos\bar{a}\sqrt{[\beta_{mj}^2 - pm^2]/\lambda_1}} \tag{C-49}$$

from $\bar{y} = 0$ to $\bar{a}$, and

$$\bar{Y}_{mj} = \bar{Y}_{2,mj} = \frac{\cos(\bar{y} - \bar{b})\sqrt{[(\alpha_1/\alpha_2)\beta_{mj}^2 - pm^2]/\lambda_2}}{\cos(\bar{a} - \bar{b})\sqrt{[(\alpha_1/\alpha_2)\beta_{mj}^2 - pm^2]/\lambda_2}} \tag{C-50}$$

from $\bar{y} = \bar{a}$ to $\bar{b}$. In both expressions, p is simply a parameter. Thus, to bring about Equations C-20a and C-20b, p is set to $\pi^2/4$. In what follows, m does not need to be an integer.

Equations C-49 and C-50 are solutions to their respective differential equations given on the next page.

$$\lambda_1 \bar{Y}''_{1,mj} + [\beta^2_{mj} - pm^2]\bar{Y}_{1,mj} = 0 \qquad (\text{for } \bar{y} = 0 \text{ to } \bar{a}) \qquad \text{(C-51)}$$

$$\lambda_2 \bar{Y}''_{2,mj} + [(\alpha_1/\alpha_2)\beta^2_{mj} - pm^2]\bar{Y}_{2,mj} = 0 \quad (\text{for } \bar{y} = \bar{a} \text{ to } \bar{b}) \qquad \text{(C-52)}$$

Multiply Equation C-51 by $\bar{Y}_{1,mi}$ and integrate both sides from $\bar{y} = 0$ to $\bar{a}$. Similarly, multiply Equation C-52 by $(k_{2x}/k_{1x})\bar{Y}_{2,mi}$ and integrate both sides from $\bar{y} = \bar{a}$ to $\bar{b}$. The results are (re-calling $\bar{Y}_{1,mj}(\bar{a}) = \bar{Y}_{2,mj}(\bar{a}) = 1$):

$$\lambda_1 \bar{Y}'_{1,mj}(\bar{a}) - \lambda_1 \int_0^{\bar{a}} \bar{Y}'_{1,mj}\bar{Y}'_{1,mi}d\bar{y} = [\beta^2_{mj} - pm^2]\int_0^{\bar{a}} \bar{Y}_{1,mj}\bar{Y}_{1,mi}d\bar{y} \qquad \text{(C-53)}$$

$$-\lambda_2(k_{2x}/k_{1x})\bar{Y}'_{2,mj}(\bar{a}) - \lambda_2(k_{2x}/k_{1x})\int_{\bar{a}}^{\bar{b}} \bar{Y}'_{2,mj}\bar{Y}'_{2,mi}d\bar{y}$$

$$= \left[(\alpha_1/\alpha_2)(k_{2x}/k_{1x})\beta^2_{mj} - (k_{2x}/k_{1x})pm^2\right]\int_{\bar{a}}^{\bar{b}} \bar{Y}_{2,mj}\bar{Y}_{2,mi}d\bar{y} \qquad \text{(C-54)}$$

In obtaining the above expressions, the fact that $\bar{Y}'_{1,mj}(0) = 0$, and $\bar{Y}'_{2,mj}(\bar{b}) = 0$ has been taken into account. Furthermore, it can be shown that:

$$\lambda_1 \bar{Y}_{1,mj}(\bar{a}) = \lambda_2(k_{2x}/k_{1x})\bar{Y}'_{2,mj}(\bar{a})$$

is identical to the eigen-equation of heat flux equality at the interface, $\bar{y} = \bar{a}$. By adding Equations C-53 and C-54, there results:

$$\beta_{mj}^2\left[\int_0^{\bar{a}} \bar{Y}_{1,mj}\bar{Y}_{1,mi}d\bar{y} + \int_{\bar{a}}^{\bar{b}} [(\rho c)_2/(\rho c)_1]\bar{Y}_{2,mj}\bar{Y}_{2,mi}d\bar{y}\right]$$

$$= pm^2\left[\int_0^{\bar{a}} \bar{Y}_{1,mj}\bar{Y}_{1,mi}d\bar{y} + (k_{2x}/k_{1x})\int_{\bar{a}}^{\bar{b}} \bar{Y}_{2,mj}\bar{Y}_{2,mi}d\bar{y}\right]$$

$$- \lambda_1\int_0^{\bar{a}} \bar{Y}'_{1,mj}\bar{Y}'_{1,mi}d\bar{y} - \lambda_2(k_{2x}/k_{1x})\int_{\bar{a}}^{\bar{b}} \bar{Y}'_{2,mj}\bar{Y}'_{2,mi}d\bar{y} \qquad \text{(C-55)}$$

By interchanging the indexes i and j, there ensues another equation which has the right-hand-side identical to that of Equation C-55. On the left-hand-side, however, the only difference is $\beta_{mi}2$ instead of β_{mj}^2. Since these two eigen-values are distinct, hence it follows:

$$\int_0^{\bar{a}} \bar{Y}_{1,mj}\bar{Y}_{1,mi}d\bar{y} + \int_{\bar{a}}^{\bar{b}} [(\rho c)_2/(\rho c)_1]\bar{Y}_{2,mj}\bar{Y}_{2,mi}d\bar{y} = 0 \qquad \text{(C-56)}$$

Thus, the segmental orthogonality of Y_{mj}'s is established with respect to the segmental weight function defined by Equation C-22.

C.III. THE COEFFICIENTS E_{mj} IN EQUATIONS C-14 AND C-15

Combining Equations C-14 and C-15 into a single equation, these results:

$$T = 1 + \sum_{j=1,2,..}^{\infty} \sum_{m=1,3,5,..}^{\infty} E_{mj} e^{-\beta_{mj}^2 \bar{\theta}} \cos(m\pi\bar{x}/2)\bar{Y}_{mj} \qquad \text{(C-57)}$$

where $\bar{Y}_{mj}$ are those defined by Equations C-20a and C-20b in their respective regions. In order to satisfy the initial condition of $T = 0$ at $\bar{\theta} = 0$, Equation C-57 becomes:

$$\sum_{j=1,2,..}^{\infty} \sum_{m=1,3,5,..}^{\infty} E_{mj} \cos(m\pi\bar{x}/2)\bar{Y}_{mj} = -1$$

multiplying both sides by $\cos(m\pi\bar{x}/2)\bar{Y}_{mi}w_f$ and integrate the resulting products on both sides from $\bar{x} = 0$ to 1 and $\bar{y} = 0$ to $\bar{b}$, the result is:

$$E_{ni} = \frac{-4}{(n\pi)} (-1)^{\frac{n-1}{2}} \left[\int_0^{\bar{b}} w_f \bar{Y}_{ni} d\bar{y}\right] \Big/ \left[\int_0^{\bar{b}} w_f \bar{Y}_{ni}^2 d\bar{y}\right]$$

In the procedure above, the orthogonality relations of:

$$\int_0^1 \cos(m\pi\bar{x}/2)\cos(n\pi\bar{x}/2)d\bar{x} = 0$$

for $m \neq n$, and

$$\int_0^{\bar{b}} w_f \bar{Y}_{ni} \bar{Y}_{nj} d\bar{y} = 0$$

for $i \neq j$ have been incorporated. The complete expression for E_{mj} is therefore:

$$E_{mj} = -(8/m\pi)(-1)^{\frac{m-1}{2}} [f_t/(f_a + f_t)] \qquad \text{(C-58)}$$

with

$$f_t = \left\{ \tan\bar{a} \sqrt{[\beta_{mj}{}^2 - (pm^2)]/\lambda_1} \right\} \Big/ \sqrt{[\beta_{mj}{}^2 - (pm^2)]/\lambda_1}$$

$$+[(\rho c)_2/(\rho c)_1] \left\{ \tan(\bar{b} - \bar{a}) \sqrt{[(\alpha_1/\alpha_2)\beta_{mj}{}^2 - pm^2]/\lambda_2} \right\} \Big/ \sqrt{[(\alpha_1/\alpha_2)\beta_{mj}{}^2 - pm^2]/\lambda_2}$$

(C-59)

and,

$$f_a = \bar{a} \Big/ \left\{ \cos\bar{a} \sqrt{[\beta_{mj}{}^2 - pm^2]/\lambda_1} \right\}^2$$

$$+ [(\rho c)_2/(\rho c)_1](\bar{b} - \bar{a}) \Big/ \left\{ \cos(\bar{b} - \bar{a}) \sqrt{[(\alpha_1/\alpha_2)\beta_{mj}{}^2 - pm^2]/\lambda_2} \right\}^2 \ldots$$

(C-60)

where $p = (\pi/2)^2$.

C.IV. ANALYSIS OF EIGEN-VALUE β_{mj} AND β_{nj}

The eigen-value Equation C-21 applies to Case 1 and Case 4, and the eigen-value Equation C-29 applies to Case 2 and Case 3. These two Equations C-21 and C-29 can be lumped together as:

$$\sqrt{[\beta_{ij}^2 - (\tfrac{\ell\pi}{2})^2]/\lambda_1}\ \tan\bar{a}\sqrt{[\beta_{ij}^2 - (\tfrac{\ell\pi}{2})^2]/\lambda_1}$$

$$+ (k_{2y}/k_{1y})\sqrt{[(\alpha_1/\alpha_2)\beta_{ij}^2 - (\tfrac{\ell\pi}{2})^2]/\lambda_2}\ \tan(\bar{b} - \bar{a})\sqrt{[(\alpha_1/\alpha_2)\beta_{ij}^2 - (\tfrac{\ell\pi}{2})^2]/\lambda_2} = 0 \qquad \text{(C-61)}$$

For $i = 1,3,5, \ldots$, then the above equation reverts to Equation C-21; for $i = 0,2,4,6, \ldots$, the above equation reverts to Equation C-29. For all four cases, the eigen-values $\beta_{ij}(j = 1,2, \ldots)$ are, of course, all positive and real.

In order to facilitate a unified numerical procedure in obtaining the roots β_{ij}, two separate cases are considered: (i) $(\alpha_1/\alpha_2) > 1$ and (ii) $(\alpha_1/\alpha_2) < 1$.

(i) $(\alpha_1/\alpha_2) > 1$: Let $\phi_\alpha = (\alpha_1/\alpha_2)$,

together with the following substitutions:

$$\phi_k = (k_{2y}/k_{1y})$$
$$\phi_1 = 1$$
$$\phi_2 = (\bar{b}/\bar{a}) - 1$$
$$(\bar{\beta}_{ij}\bar{a}) = (2/\pi)\beta_{ij}\bar{a}$$
$$g_1 = \lambda_1$$
$$g_2 = \lambda_2$$

then Equation C-61 becomes:

$$\sqrt{[(\bar{\beta}_{ij}\bar{a})^2 - (i\bar{a})^2]/g_1}\ \tan\left(\frac{\pi}{2}\phi_1\sqrt{[(\bar{\beta}_{ij}\bar{a})^2 - (i\bar{a})^2]/g_1}\right)$$

$$+\ \phi_k\sqrt{[\phi_\alpha(\bar{\beta}_{ij}\bar{a})^2 - (\ell\bar{a})^2]/g_2}\ \tan\left(\frac{\pi}{2}\phi_2\sqrt{[\phi_\alpha(\bar{\beta}_{ij}\bar{a})^2 - (i\bar{a})^2]/g_2}\right) = 0 \qquad \text{(C-62)}$$

$$(i = 0, 1, 2, 3, \ldots)$$

(ii) $(\alpha_1/\alpha_2) < 1$: Let $\phi_\alpha = (\alpha_2/\alpha_1)$

together the following substitutions:

$$\phi_k = (k_{1y}/k_{2y})$$

$$\phi_1 = (\bar{b}/\bar{a}) - 1$$

$$\phi_2 = 1$$

$$(\bar{\beta}_{ij}\bar{a}) = (2/\pi)(\beta_{ij}\bar{a})\sqrt{(\alpha_1/\alpha_2)}$$

$$g_1 = \lambda_2$$

$$g_2 = \lambda_1,$$

then Equation C-61 becomes:

$$\phi_k \sqrt{[\phi_\alpha(\bar{\beta}_{ij}\bar{a})^2 - (i\bar{a})^2]/g_2}\ \tan\ \tfrac{\pi}{2}\phi_2\sqrt{[\phi_\alpha(\bar{\beta}_{ij}\bar{a})^2 - (i\bar{a})^2]/g_2}$$

$$+ \sqrt{[(\bar{\beta}_{ij}\bar{a})^2 - (i\bar{a})^2]/g_1}\left(\tan\ \tfrac{\pi}{2}\phi_1\sqrt{[(\bar{\beta}_{ij}\bar{a})^2 - (i\bar{a})^2]/g_1}\right) = 0 \qquad \text{(C-63)}$$

Of course, Equations C-62 and C-63 are identical, which is what the two sets of substitutions are designed for.

To solve for $(\bar{\beta}_{ij}\bar{a})$ from Equation C-63, first consider the case for $i \neq 0$. Since $\phi_\alpha > 1$, hence there could be roots of $(\bar{\beta}_{ij}a)$ such that the arguments of the tangent terms in Equation C-63 become of

opposite signs. The roots of $(\overline{\beta}_{ij}\overline{a})$ then lie between the lower limit of $[i\overline{a}/\sqrt{\phi_\alpha}]$ and the upper limit of $(\ell\overline{a})$. The eigen-value equation, reduced from Equation C-63 becomes:

$$- \sqrt{[(i\overline{a})^2 - (\overline{\beta}_{ij}\overline{a})^2]/g_1}\ \tanh\left(\frac{\pi}{2}\phi_1\sqrt{[(i\overline{a})^2 - (\overline{\beta}_{ij}\overline{a})^2]/g_1}\right)$$

$$+ \phi_k\sqrt{[\phi_\alpha(\overline{\beta}_{ij}\overline{a})^2 - (i\overline{a})^2]/g_2}\ \tan\left(\frac{\pi}{2}\phi_2\sqrt{[\phi_\alpha(\overline{\beta}_{ij}\overline{a})^2 - (i\overline{a})^2]/g_2}\right) = 0 \qquad \text{(C-64)}$$

In Equation C-64, the first term is always negative, therefore the value of $(\overline{\beta}_{ij}\overline{a})$ satisfying Equation C-64 must be such that the angular argument in the second term must be in odd quadrants. Hence, a straightforward search for the roots can be initiated. Of course, when i = 0, Equation C-64 is moot and the full Equation C-62 must be used.

For the succeeding range, i.e., $(\overline{\beta}_{ij}\overline{a}) > (i\overline{a})$, solution for the roots can be simplified by observing that the terms in Equation C-62 must be of opposite signs. Hence, by starting with the argument of the first term in the first quadrant, then the equation is satisfied by the argument of the second term located in the second or fourth quadrant. The procedure is systematized by using a search index K for each range of search for the root.

(i) K = 0. The eigen-values $(\overline{\beta}_{ij}\overline{a})$ are determined from Equation C-64 and are bounded by the following limits:

$$(i\overline{a})^2/\phi_\alpha < (\overline{\beta}_{ij}\overline{a})^2 < (i\overline{a})^2$$

The argument in the second term of Equation C-64 must be in an odd quadrant to satisfy the equation.

Of course, the search described in this range is only valid if $i \neq 0$. Otherwise, the search must start with K = 1.

(ii) K = 1. Here the index K = 1 indicates that search for the roots $(\overline{\beta}_{ij}a)$ such that the argument of the first term of Equation C-62 is in the first quadrant. Accordingly, the argument of the second term of Equation C-62 must be in an even quadrant. The range of $(\overline{\beta}_{ij}a)$ can be expressed by:

$$(K-1)\frac{\pi}{2} < \frac{\pi}{2}\phi_1\sqrt{[(\overline{\beta}_{ij}\overline{a})^2 - (i\overline{a})^2]/g_1} < K\frac{\pi}{2}$$

Or,

$$[g_1(K-1)^2/\phi_1^2 + (i\overline{a})^2] < (\overline{\beta}_{ij}\overline{a})^2 < [g_1(K/\phi_1)^2 + (i\overline{a})^2]$$

Within these two limits of $(\overline{\beta}_{ij}\overline{a})$, possible roots of $(\overline{\beta}_{ij}\overline{a})$ are to be located such that the argument of the second term is in the second or fourth quadrants.

(iii) K = 2. In this range, the argument of the first term is in the second quadrant and the lower and upper limits on $(\overline{\beta}_{\ell j}\overline{a})$ are defined by those shown for K = 1. The roots of $(\overline{\beta}_{\ell j}\overline{a})$ are those for which the argument of the second term Equation C-62 is in an odd quadrant.

• U.S. GOVERNMENT PRINTING OFFICE: 1982-559-062/668